

Enhanced Hanford Low- Activity Waste Glass Property Data Development: Phase 5 and Phase 6

June 2023

V Gervasio	JJ Neeway
CE Lonergan	X Lu
JD Vienna	SM Baird
JB Lang	DA Cutforth
BE Westman	M Peterson
JT Reiser	

DISCLAIMER

This report was prepared as an account of work sponsored by an agency of the United States Government. Neither the United States Government nor any agency thereof, nor Battelle Memorial Institute, nor any of their employees, makes **any warranty, express or implied, or assumes any legal liability or responsibility for the accuracy, completeness, or usefulness of any information, apparatus, product, or process disclosed, or represents that its use would not infringe privately owned rights.** Reference herein to any specific commercial product, process, or service by trade name, trademark, manufacturer, or otherwise does not necessarily constitute or imply its endorsement, recommendation, or favoring by the United States Government or any agency thereof, or Battelle Memorial Institute. The views and opinions of authors expressed herein do not necessarily state or reflect those of the United States Government or any agency thereof.

PACIFIC NORTHWEST NATIONAL LABORATORY
operated by
BATTELLE
for the
UNITED STATES DEPARTMENT OF ENERGY
under Contract DE-AC05-76RL01830

Printed in the United States of America

Available to DOE and DOE contractors from the
Office of Scientific and Technical Information,
P.O. Box 62, Oak Ridge, TN 37831-0062;
ph: (865) 576-8401
fax: (865) 576-5728
email: reports@adonis.osti.gov

Available to the public from the National Technical Information Service
5301 Shawnee Rd., Alexandria, VA 22312
ph: (800) 553-NTIS (6847)
email: orders@ntis.gov <<https://www.ntis.gov/about>>
Online ordering: <http://www.ntis.gov>

Enhanced Hanford Low-Activity Waste Glass Property Data Development: Phase 5 and Phase 6

June 2023

V Gervasio
CE Lonergan
JD Vienna
JB Lang
BE Westman
JT Reiser

JJ Neeway
X Lu
SM Baird
DA Cutforth
M Peterson

Prepared for
the U.S. Department of Energy
under Contract DE-AC05-76RL01830

Pacific Northwest National Laboratory
Richland, Washington 99354

Summary

This report summarizes the data collected on two test matrices of low-activity waste (LAW) glass compositions intended to expand the composition-property database: *Low-Activity Waste (LAW) Phase 5: Expansion of LAW Glass Composition Boundaries* and *LAW Phase 6: High PCT and VHT Response Glass Matrix*.

Both matrix glass compositions were statistically designed to expand the LAW glass composition region. The analyses performed on these glasses include chemical composition (for target compositional verification), density, viscosity, electrical conductivity, crystal fraction, container centerline cooling with crystal identification, the product consistency test (PCT) response, the vapor hydration test (VHT) response, and sulfur solubility. Because of the slightly different scope of the two matrices, not all methods were applied to both. Specifically, the following measurements were taken only on the *LAW Phase 5: Expansion of LAW Glass Composition Boundaries* glasses: crystal fraction as a function of temperature, density (ρ), viscosity (η), and electrical conductivity (EC, ϵ).

Combined, these data contribute a significant amount, 51 glasses, to the database for high LAW loaded enhanced waste glasses. Most of these data are focused near the boundaries of acceptable PCT and VHT responses, where prediction uncertainties are most impactful.

Acknowledgments

The authors gratefully acknowledge the financial support provided by the U.S. Department of Energy Office of River Protection Waste Treatment and Immobilization Plant Project, managed by Tom Fletcher, with technical oversight by Albert Kruger. The authors thank Madison Hsieh of Savannah River National Laboratory for chemical analysis of the glasses and product consistency test and sulfur solubility solutions. The following Pacific Northwest National Laboratory staff members are acknowledged for their contributions: Jaime George, Diana Bellofatto, Eden Rivers, Dong-Sang Kim, Renee Russell, and Jose Marcial for technical help, Tongan Jin for his technical review, Matt Wilburn for his editorial review, David MacPherson for quality assurance, and Chrissy Charron, Cassie Martin, and Veronica Perez for programmatic support during the conduct of this work.

Acronyms, Abbreviations, and Symbols

ASTM	American Society for Testing and Materials
CCC	container centerline cooling (heat treatment)
CF	crystal fraction
C_i	concentration of element i in solution
DFLAW	Direct Feed Low-Activity Waste
DI	deionized
d_i	initial thickness of the specimen
DOE	U.S. Department of Energy
d_r	average thickness of remaining glass layer
DWPF	Defense Waste Processing Facility
EC	electrical conductivity
ϵ	electrical conductivity
ϵ_{1150}	electrical conductivity at 1150 °C
η	viscosity
η_{1150}	viscosity at 1150 °C
f_i	mass fraction of element i in the glass
GFA	glass formulation algorithm
GFC	glass-forming chemical
HLW	high-level waste
IC	ion chromatography
ICP-OES	inductively coupled plasma–optical emission spectroscopy
IHLW	immobilized high-level waste
ILAW	immobilized low-activity waste
KH	potassium hydroxide digestion
LAW	low-activity waste
LM	lithium metaborate fusion
m	mass of glass converted to alteration products per unit surface area
NC	normalized concentration
NL	normalized loss
NQAP	Nuclear Quality Assurance Program
ORP	DOE Office of River Protection
PCT	product consistency test
PF	sodium peroxide fusion
PNNL	Pacific Northwest National Laboratory
r_a	alteration rate (via VHT)
ρ	density
S	glass surface area
SCC	single-component constraint
SRNL	Savannah River National Laboratory

<i>t</i>	time
T _K	temperature expressed in Kelvin
T _L	liquidus temperature
TRL	technology readiness level
V	volume of solution
VHT	vapor hydration test
vol%	volume percent
VFT	Vogel-Fulcher-Tammann
wt%	weight percent
WTP	Waste Treatment and Immobilization Plant
XRD	X-ray diffraction
3TS	3-time remelt saturation method

Contents

Summary	ii
Acknowledgments.....	iii
Acronyms, Abbreviations, and Symbols.....	iv
1.0 Introduction.....	1.1
2.0 Test Methods.....	2.1
2.1 Glass Matrix Design	2.1
2.1.1 LAW Phase 5: Expansion of LAW Glass Composition Boundaries Glass Matrix Design	2.1
2.1.2 LAW Phase 6: High PCT and VHT Response Glass Matrix Design	2.2
2.2 Glass Fabrication	2.4
2.3 Chemical Analysis of Glass Composition	2.7
2.4 Container Centerline Cooling and Crystal Identification	2.8
2.5 Crystal Fraction as a Function of Temperature.....	2.9
2.6 Glass Density	2.9
2.7 Glass Viscosity	2.9
2.8 Electrical Conductivity	2.10
2.9 Product Consistency Test.....	2.10
2.10 Vapor Hydration Test	2.11
2.11 Sulfur Solubility Procedure.....	2.12
2.11.1 Step 1: Saturation	2.12
2.11.2 Step 2: Washing.....	2.12
2.11.3 Step 3: Analysis.....	2.12
3.0 Results and Discussion	3.1
3.1 Chemical Analysis of Glass Composition	3.1
3.2 Crystal Identification in Container Centerline Cooling Glasses	3.2
3.3 Crystal Fraction in Isothermal Heat Treatment.....	3.3
3.4 Density	3.3
3.5 Viscosity	3.4
3.6 Electrical Conductivity	3.6
3.7 Product Consistency Test.....	3.8
3.8 Vapor Hydration Test	3.14
3.9 Sulfur Solubility.....	3.15
4.0 Conclusions.....	4.1
5.0 Bibliography	5.1
Appendix A – LAW Phase 5: Expansion of LAW Glass Composition Boundaries Glass Matrix Target Glass Compositions	A.1

Appendix B – LAW Phase 6: High PCT and VHT Response Glass Matrix Target Glass Compositions	B.1
Appendix C – LAW Phase 5: Expansion of LAW Glass Composition Boundaries Glass Matrix Target Modified Glass Compositions	C.1
Appendix D – Morphology/Color of Each Quenched Glass	D.1
Appendix E – Comparison Measured and Target Chemical Compositions.....	E.1
Appendix F – Morphology/Color of Each CCC Glass and XRD Patterns	F.1
Appendix G – Crystal Fraction of Heat-Treated Glasses Photographs.....	G.1
Appendix H – Viscosity Data	H.1
Appendix I – Electrical Conductivity Data.....	I.1

Figures

Figure 2.1. LP5-06 Glass Fourth Melt at 1350 °C	2.5
Figure 2.2. LP5-16 Glass Fifth Melt at 1350 °C	2.5
Figure 2.3. Plot of Temperature Schedule during CCC Heat Treatment of Hanford LAW Glasses	2.8
Figure 3.1. Normalized N_{L_B} and $N_{L_{Na}}$ Release in Natural Logarithm Scale of Quenched vs. CCC LAW Phase 5 Glasses.....	3.13
Figure 3.2. Normalized N_{L_B} and $N_{L_{Na}}$ Release in Natural Logarithm Scale of Quenched vs. CCC LAW Phase 6 Glasses. Blue and orange rhombus represent glass LAW-HPVR-25, the only glass with measurable (by XRD) crystal fraction after CCC, N_{L_B} and $N_{L_{Na}}$. The triangle represents the $N_{L_{Na}}$ significantly affected by CCC.....	3.14

Tables

Table 2.1. Lower and Upper Bounds of Single-Component Constraints in Mass Fractions and Multiple-Component Constraints for the LAW Phase 5 New Compositions	2.2
Table 2.2. Lower and Upper Bounds of Single-Component Constraints as Mass Fractions and Multiple-Component Constraints for LAW Phase 6.....	2.3
Table 2.3. Melt History for the LAW Phase 5 Glasses (LP5-#) and the LAW Phase 6 Glasses (LAW-HPVR-#). Melt duration was 1 hour if not specified differently in parenthesis.	2.6
Table 2.4. Preparation and Measurement Methods Used in Reporting the Analyte Concentrations of the Study Glasses.....	2.7
Table 2.5. Temperature Schedule during CCC Treatment of Hanford LAW Glasses.....	2.8
Table 2.6. Measurement Methods Used in Reporting Glass and Wash Solutions Analytes Concentrations (Hsieh 2021b, 2022b)	2.13
Table 3.1. Primary and Secondary Crystalline Phases in LAW Phase 5 and LAW Phase 6 Glasses	3.3
Table 3.2. Crystalline Phases Recognized by XRD in LAW Phase 5 Glasses Heat Treated at 950 °C. Phases with wt% < 0.1 are not reported.	3.3

Table 3.3.	Measured Densities in the LAW Phase 5 Glasses	3.4
Table 3.4.	Measured η (Pa·s) Values vs. Target Temperature (in the sequence of measurement) for the LAW Phase 5 Glasses.....	3.5
Table 3.5.	Fitted Coefficients of Arrhenius and VFT Models for Viscosity of the LAW Phase 5 Glasses	3.6
Table 3.6.	Measured Electrical Conductivity (S/m) Values vs. Target Temperatures for the LAW Phase 5 Glasses.....	3.7
Table 3.7.	Fitted Coefficients of Arrhenius Model for ϵ_{1150} of the LAW Phase 5 Glasses.....	3.8
Table 3.8.	Average Normalized PCT Loss (NLs) for the LAW Phase 5 Glasses. Missing values were below the analytical laboratory detection limit.	3.9
Table 3.9.	Average Normalized PCT Loss (NLs) for CCC LAW Phase 5 Glasses.....	3.10
Table 3.10.	Average Normalized PCT Loss (NLs) for Q LAW Phase 6 Glasses.....	3.10
Table 3.11.	Average Normalized PCT Loss (NLs) for CCC LAW Phase 6 Glasses.....	3.12
Table 3.12.	Alteration Depth and Rate for Quenched and CCC of the LAW Phase 6 Q and CCC Glasses after 24 Day VHT	3.15
Table 3.13.	SO ₃ Concentrations in the Sulfur-Saturated Samples of the LAW Phase 5 and LAW Phase 6 Glasses.....	3.16

1.0 Introduction

The U.S. Department of Energy (DOE) Hanford Site in Washington state has roughly 56 million gallons of radioactive waste stored in 155 of the original 177 underground tanks, with waste retrieved from 22 of the tanks. The Waste Treatment and Immobilization Plant (WTP) will provide DOE with a capability to treat the waste by vitrification for subsequent disposal. The tank waste will be partitioned into low-activity waste (LAW) and high-level waste (HLW) fractions, which will then be vitrified, respectively, into immobilized low-activity waste (ILAW) and immobilized high-level waste (IHLW) products. The ILAW product will be disposed of in the Integrated Disposal Facility on the Hanford Site, while the IHLW product will be temporarily stored on-site prior to disposal at a national deep geological disposal facility for high-level nuclear waste.

The ILAW and IHLW products must satisfy a variety of requirements with respect to regulatory compliance and protection of the environment before they can be accepted for disposal. Additionally, to be efficiently processed in the WTP, the LAW melts must satisfy process-related properties. Current plans for the WTP envision vitrifying LAW prior to startup of the WTP HLW and Pretreatment facilities using a Direct Feed Low-Activity Waste (DFLAW) approach (Bernards et al. 2020). The glass composition in the WTP LAW Facility will be controlled using a LAW glass formulation algorithm (GFA), with the objective to computationally formulate LAW glass compositions given a waste composition and specific parameters, while applying all property and measurement uncertainties and maximizing the waste loading, i.e., increasing the ratio of waste to glass-forming chemicals (GFCs) in melter feed batches.

Currently, it is envisioned that the preliminary LAW GFA discussed by Kim and Vienna (2012), the LAW glass property-composition models recommended in Piepel et al. (2007), and formulation correlation developed by Muller et al. (2004) will be used for commissioning and initial radioactive operations of the LAW Facility. After commissioning and initial operations, it is intended that the WTP operations contractor will implement an updated LAW GFA, developed at Pacific Northwest National Laboratory (PNNL), in the WTP LAW Facility using the new models in Vienna et al. (2022). The Preliminary Enhanced GFA has been developed by Lumetta et al. (2022) to implement Vienna et al. (2022) models along with several inputs, including the (1) LAW glass formulation methods and constraints, (2) LAW glass property constraints, (3) plant-related uncertainties and operating data, and (4) model validity constraints.

The present tasks, *Low-Activity Waste (LAW) Phase 5: Expansion of LAW Glass Composition Boundaries* and *LAW Phase 6: High PCT and VHT Response Glass Matrix*, support the DOE Office of River Protection (ORP) LAW glass composition property evaluation and model development by improving glass-property/composition data coverage and supply data for potential GFA and/or model updates.

This report presents the glass compositions and glass property data collected during the *Low-Activity Waste (LAW) Phase 5: Expansion of LAW Glass Composition Boundaries* and *LAW Phase 6: High PCT and VHT Response Glass Matrix* tasks. For simplicity, the two matrices will be called Phase 5 and Phase 6, respectively. Where LAW Phase 5 scope was to measure all main glass properties, Phase 6 scope was focused mainly on glass durability testing and SO₃ solubility; thus, not all properties were measured on the glasses belonging to this matrix.

This work was performed in accordance with the PNNL Nuclear Quality Assurance Program (NQAP). The NQAP complies with DOE Order 414.1D, *Quality Assurance*, and 10 CFR 830, *Nuclear Safety Management*, Subpart A, *Quality Assurance Requirements*. The NQAP uses NQA-1-2012, *Quality Assurance Requirements for Nuclear Facility Application*, as its consensus standard and NQA-1-2012, Subpart 4.2.1, as the basis for its graded approach to quality.

The NQAP works in conjunction with PNNL's laboratory-level Quality Management Program, which is based on the requirements as defined in DOE Order 414.1D and 10 CFR 830 Subpart A.

The work of this report was performed to a technology readiness level (TRL) of 6 for LAW Phase 5 and TRL 8 for LAW Phase 6.

2.0 Test Methods

This section describes how the two test matrices of simulated LAW glasses were generated and data were obtained. The descriptions include the methods for 1) glass matrix generation, 2) glass fabrication, 3) chemical composition analysis, 4) secondary phase identification from container centerline cooling (CCC) treatment, 5) crystal fraction (CF) as a function of temperature, 6) density (ρ) determination, 7) viscosity (η) measurement, 8) electrical conductivity (EC, ϵ) measurement, 9) product consistency test (PCT) measurement, 10) vapor hydration test (VHT) measurements, and 11) sulfur solubility measurement used.

2.1 Glass Matrix Design

The space-filling experimental design capabilities of JMP were used to develop the two matrices in the LAW glass composition region. JMP has a unique approach to space-filling designs that are not available in other software packages and are considered the most appropriate method for developing waste simulated glass matrices (Joseph et al. 2015; Lonergan et al. 2020). Standard software default assumptions were used to design the matrices of glasses with a fixed set of single-component constraints (SCCs) for individual oxide concentration ranges. Multi-component constraints (MCCs) were applied to limit certain predicted properties. The designed glasses were required to 1) fall within pre-defined acceptance ranges defined by the SCCs and MCCs and 2) obtain broad dispersion values of each component across the range compared to those of external vertices.

2.1.1 LAW Phase 5: Expansion of LAW Glass Composition Boundaries Glass Matrix Design

A test matrix of 23 new glass compositions was designed to augment 588 existing LAW compositions compiled in Vienna et al. (2022). SCCs and MCCs, as listed in Table 2.1, were applied to the matrix design to include glasses that cover the range of the glass properties below and above the WTP contract and operating limits. Since the current space-filling technique can use first-order models only, the following models were applied to calculate the MCCs: $1 \leq \eta_{1150} \leq 10 \text{ Pa}\cdot\text{s}$; $\ln[NL_B, \text{g m}^{-2}] \geq 0.5$, with predicted properties based on Vienna et al. (2022).

Table 2.1. Lower and Upper Bounds of Single-Component Constraints in Mass Fractions and Multiple-Component Constraints for the LAW Phase 5 New Compositions

Single-Component Constraint		
Component	Lower Bound	Upper Bound
Al ₂ O ₃	0.035	0.1475
B ₂ O ₃	0.06	0.1383
CaO	0	0.1278
Fe ₂ O ₃	0	0.01
K ₂ O	0	0.0575
MgO	0	0.0502
Na ₂ O	0.22	0.27
SiO ₂	0.3352	0.5226
SnO ₂	0	0.045
V ₂ O ₅	0	0.0571
ZnO	0	0.0582
ZrO ₂	0	0.0675
Others ^(a)	0.0123	0.0493
Multi-Component Constraint		
Property	Lower Bound	Upper Bound
η_{1150} (Pa·s) ^(b)	1	10
NL_B (g·m ⁻²) ^(c)	1.65	-

(a) The Others component was composed of the following mixture of minor components (expressed as mass fractions): Cl, Cr₂O₃, F, P₂O₅, SO₃, TiO₂, PbO, NiO, Cs₂O, and Re₂O₇ in varying concentrations as reported in Appendix A.

(b) Viscosity at 1150 °C (Pa·s)

(c) Normalized loss of boron under PCT-A in (g·m⁻²)

In addition to the 23 new compositions, this report describes two previously tested LAW glass compositions: 1) EWG-LAW-Centroid (Russell et al. 2021), identified in the current task as LP5-24, and 2) LAWC22 (Muller et al. 2003), identified here as LP5-25. These two glasses were selected because they have undergone previous testing. Their inclusion and comparison to previously collected results provides assurance that the laboratory testing in the current effort results in similar values as past testing. The glasses from this task are identified with the prefix LP5- and a number from 1 to 25. The 25 glass target compositions are reported in Appendix A.

2.1.2 LAW Phase 6: High PCT and VHT Response Glass Matrix Design

The LAW compositional region with PCT and VHT responses near their limits was the specific focus of this design. The individual oxide concentration ranges and MCCs used to generate the matrix are reported in Table 2.2. The Vienna et al. (2022) models were applied to calculate the MCCs for η at 1150 °C, EC at 1150 °C, as well as the PCT and VHT responses. A matrix with 26 glasses was generated to expand the compositional space near the PCT and VHT WTP constraints and increase the SO₃ saturation data acquired by the 3-time remelt S method (3TS). The glasses from this task were identified with the prefix LAW-HPVR- and a number from 1 to 26. The 26 glass target compositions are reported in Appendix B.

Table 2.2. Lower and Upper Bounds of Single-Component Constraints as Mass Fractions and Multiple-Component Constraints for LAW Phase 6

Single-Component Constraint		
Components	Lower Bound	Upper Bound
Al ₂ O ₃	3.5	11.5
B ₂ O ₃	6	13.8
CaO	6	12.8
K ₂ O	0	5.9
Li ₂ O	0	4.3
Na ₂ O	15.7	27
SiO ₂	34.6	50.2
SnO ₂	0	4.5
TiO ₂	0	3
V ₂ O ₅	0	4
ZrO ₂	2	6.75
Others	1.11	3.33
N _{Alk} ^(h)	20	27
N _{AlZrSn} ⁽ⁱ⁾	3.5	16.55
Multi-Component Constraint		
MCCs	Lower Bound	Upper Bound
η ₁₁₅₀ (Pa·s) ^(b)	1	10
ε ₁₁₅₀ (S/cm) ^(c)	0.1	0.7
NL _B (g/m ²) ^(d)	0.4870931	17.84
NL _{Na} (g/m ²) ^(e)	0.5548264	13.407
pred VHT (pass/fail probability) ^(f)	0.05	0.95
S/C SO ₃ ^(g)	1.25	n/a

(a) The Others component was composed of the following mixture of minor components (expressed as mass fractions): Cl, Cr₂O₃, F, Fe₂O₃, MgO, P₂O₅, SO₃, and ZnO in varying concentrations as reported in Appendix B.

(b) Viscosity at 1150 °C (Pa·s) (based on reduced linear mixture model in Vienna et al. 2022)

(c) EC at 1150 °C (S/cm) (based on reduced linear mixture model in Vienna et al. 2022)

(d) Predicted PCT_B response (g/m²) (based on reduced linear mixture model in Vienna et al. 2022)

(e) Predicted PCT_{Na} response (g/m²) (based on reduced linear mixture model in Vienna et al. 2022)

(f) Predicted VHT response (pass/fail probability) (based on reduced linear mixture model in Vienna et al. 2022)

(g) Predicted SO₃ solubility/SO₃ concentration in glass > 1.25 (based on partial-Quadratic mixture model in Vienna et al. 2022)

(h) N_{Alk} = Na₂O + 0.66 K₂O + 2.07 Li₂O

(i) N_{AlZrSn} = Al₂O₃ + 0.827 ZrO₂ + 0.677 SnO₂

2.2 Glass Fabrication

The glasses from both matrices were batched using GFCs and a dry waste simulant composed of single-metal oxides, single-metal carbonates, and sodium salts in the appropriate masses to form the target composition for each glass (Appendix A and Appendix B).

After thoroughly mixing all the components in a plastic bag for at least 30 seconds and until uniform color developed, the powders were transferred to an agate milling chamber and milled for 4 minutes in a vibratory mill (Angstrom TE110). The powders were then transferred to a clean platinum (Pt)-10% rhodium (Rh) crucible for melting. Initial melting was performed at 1150 °C for 1 hour ± 10 minutes.

After the first melt was air quenched on a stainless-steel pouring plate, the glass was observed under an optical microscope and the presence of undissolved particles and/or salts was reported. The glass was then ground to a fine powder for 5 minutes in a tungsten carbide vibratory mill (Angstrom TE110) and a second melt was performed. The temperature of the second melt varied depending on the outcome of the first melt. If the first melt was homogeneous or had only a small amount of undissolved particles observed by optical microscope, then the second melt was performed again at 1150 °C ± 10 °C for 1 hour ± 10 minutes. If undissolved particles were particularly abundant after the first melt, then the temperature of the second melt was increased. In some cases, more than two melts were necessary to fully dissolve the particles in the glass matrix and obtain a homogeneous glass.

Detailed lists of the number of melts and temperatures are reported in Table 2.3. All melts were 1 hour long ± 10 minutes unless otherwise specified in the table. Re-batched glasses were given a replicate number starting from the value of “1” after the glass ID (e.g., LP5-12-1 in Table 2.3).

Two of the 25 LAW Phase 5 glasses, LP5-06 and LP5-16, displayed heavy sulfur separation even after multiple melts at high temperatures (Figure 2.1 and Figure 2.2, respectively). Therefore, the target compositions of these two glasses were modified to reduce sulfur content and the glasses were remelted. The modified glasses, LP5-06-mod1 and LP5-16-mod1, have been used for the remainder of the study. Target chemical compositions of both original and modified glasses are reported in Appendix C.

The use of higher melting temperature is deemed an acceptable method of fabricating challenging glass compositions. Laboratory crucible-scale fabrication of glasses is not intended to mimic the actual melter process or feed processability; rather, it is intended to fabricate a glass sample with a controlled composition for property testing.

Photographs of each quenched glass are shown in Appendix D.



Figure 2.1. LP5-06 Glass Fourth Melt at 1350 °C



Figure 2.2. LP5-16 Glass Fifth Melt at 1350 °C

Table 2.3. Melt History for the LAW Phase 5 Glasses (LP5-#) and the LAW Phase 6 Glasses (LAW-HPVR-#). Melt duration was 1 hour if not specified differently in parenthesis.

Glass ID	1st Melt (°C)	2nd Melt (°C)	3rd Melt (°C)	4th Melt (°C)	5th Melt (°C)	Glass ID	1st Melt (°C)	2nd Melt (°C)	3rd Melt (°C)
LP5-01	1150	1150				LAW-HPVR-01-1	1150	1150	
LP5-02	1150	1150				LAW-HPVR-02-1	1150	1150	
LP5-03	1150	1150				LAW-HPVR-03-1	1150	1150	
LP5-04	1150	1150				LAW-HPVR-04-1	1150	1150	
LP5-05	1150	1150				LAW-HPVR-05	1150	1300	
LP5-06	1150	1150	1250	1350	1400 (30 min)	LAW-HPVR-06	1150	1150	
LP5-06-mod1	1150	1250	1350			LAW-HPVR-07	1150	1300	1300
LP5-07	1150	1150	1200			LAW-HPVR -08	1150	1200	
LP5-08	1150	1150				LAW-HPVR -09	1150	1150	
LP5-09	1150	1150				LAW-HPVR -10	1150	1150	
LP5-10	1150	1150				LAW-HPVR -11	1150	1250	
LP5-11	1150	1150	1250			LAW-HPVR-12	1150	1150	
LP5-12-1	1150	1250	1350	1450	1450	LAW-HPVR-13	1150	1250	1300
LP5-13	1150	1150				LAW-HPVR-14	1150	1150	
LP5-14	1150	1150	1200			LAW-HPVR-15	1150	1150	
LP5-15	1150	1150	1200	1300		LAW-HPVR-16	1150	1300	
LP5-16	1150	1150	1270	1150	1350	LAW-HPVR-17	1150	1150	
LP5-16-mod1	1150	1300	1400			LAW-HPVR-18	1150	1150	
LP5-17	1150	1150	1300	1350		LAW-HPVR-19	1150	1150	
LP5-18	1150	1150	1250			LAW-HPVR-20	1150	1150	
LP5-19	1150	1150				LAW-HPVR-21	1150	1150	
LP5-20	1150	1150				LAW-HPVR-22	1150	1300	1350
LP5-21	1150	1150				LAW-HPVR-23	1150	1300	
LP5-22	1150	1150				LAW-HPVR-24	1150	1150	
LP5-23	1150	1150				LAW-HPVR-25	1150	1300	1350
LP5-24	1150	1150	1250			LAW-HPVR-26	1150	1150	
LP5-25	1150	1150	1300	1350					

2.3 Chemical Analysis of Glass Composition

To confirm that the “as-fabricated” glasses corresponded to the specified target compositions, a representative sample of each glass was chemically analyzed at the Savannah River National Laboratory (SRNL) Process Science Analytical Laboratory. All analyte concentrations were measured except for Mn. Three dissolution techniques were used to prepare glass samples, in duplicate, for analysis: sodium peroxide fusion (PF), lithium metaborate fusion (LM), and potassium hydroxide fusion (KH). Descriptions of the dissolution processes can be found in Hsieh (2021a, 2022a).

Duplicate samples (two each for the preparation techniques) were analyzed twice for each element of interest by inductively coupled plasma-optical emission spectroscopy (ICP-OES) or ion chromatography (IC). Glass composition standards also were intermittently prepared and analyzed to assess the performance of the ICP-OES and IC instruments over the course of these analyses. Specifically, several samples of the low-level reference material (Ebert and Wolfe 1999) were included as part of the SRNL Process Science Analytical Laboratory analysis plan. The preparation and measurement methods used for each of the reported glass analytes are listed in Table 2.4.

A detailed data analysis of the chemical composition measurements was published elsewhere (Hsieh 2021a, 2022a). A short summary of these data analyses is included in Section 3.1.

Table 2.4. Preparation and Measurement Methods Used in Reporting the Analyte Concentrations of the Study Glasses

Analyte	Measurement Method	Preparation Method
Al	ICP-OES	PF
B	ICP-OES	PF
Ca	ICP-OES	LM
Cl	IC	KH
Cr	ICP-OES	LM
F	IC	KH
Fe	ICP-OES	LM
K	ICP-OES	LM
Li	ICP-OES	PF
Mg	ICP-OES	LM
Na	ICP-OES	LM
P	ICP-OES	PF
S	ICP-OES	LM
Si	ICP-OES	PF
Sn	ICP-OES	LM
Ti	ICP-OES	LM
V	ICP-OES	LM
Zn	ICP-OES	PF
Zr	ICP-OES	PF

2.4 Container Centerline Cooling and Crystal Identification

A portion (~45 g) of each test glass was subjected to the simulated CCC temperature profile shown in Table 2.5 and Figure 2.3. This profile is the temperature schedule of CCC treatment for Hanford LAW glasses planned for use at WTP.¹ Pieces of quenched glass, < 3 cm in diameter, were placed in a Pt-alloy crucible and covered with a Pt-alloy lid. Each glass sample was placed in a furnace preheated to the glass last melting temperature as per Table 2.3. After 30 minutes at the melting temperature, the furnace temperature was quickly reduced to 1114 °C, and the cooling profile was started. It progressed down to about 400 °C based on seven cooling segments listed in Table 2.5.

Table 2.5. Temperature Schedule during CCC Treatment of Hanford LAW Glasses

Segment	Time (min)	Start Temperature (°C)	Rate (°C/min)
1	30	Melt temperature	0
2	0	1114	-7.125
3	0-16	1000	-1.754
4	16-73	900	-0.615
5	73-195	825	-0.312
6	195-355	775	-0.175
7	355-640	725	-0.130
8	640-1600	600	-0.095
9	1600-3710	Room temperature	NA

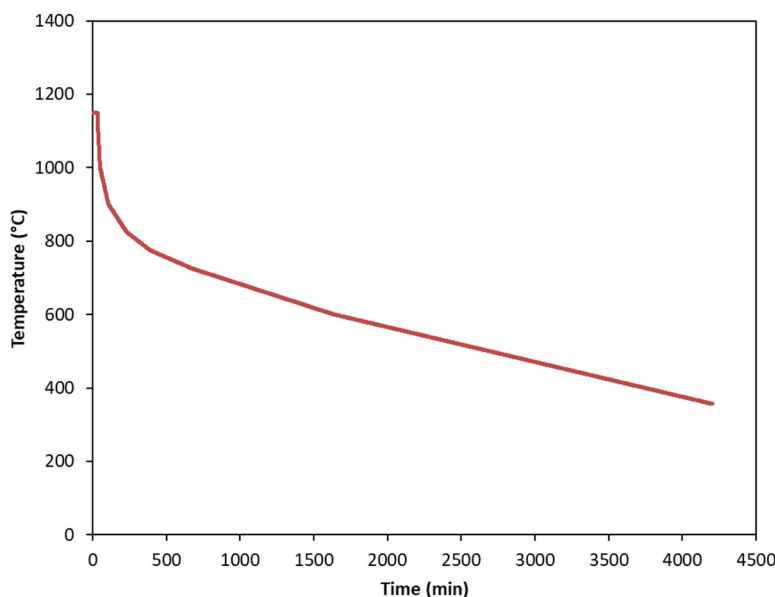


Figure 2.3. Plot of Temperature Schedule during CCC Heat Treatment of Hanford LAW Glasses

¹ Memorandum, “Low Activity Container Centerline Cooling Data,” CCN: 074181, from LL Petkus to CA Musick, RPP-WTP, October 16, 2003.

The amounts and types of crystalline phases that formed during CCC treatment were analyzed using powder X-ray diffraction (XRD) according to Section 12.4.4 of the American Society for Testing and Materials (ASTM) international procedure *Standard Test Method for Determining Liquidus Temperature of Immobilized Waste Glasses and Simulated Waste Glasses* (ASTM C1720). For each crystallized CCC glass, a piece of about 1.5 g of glass, representative of the whole sample, was milled for 1 minute in a 10 cm³ vibratory mill with a tungsten carbide cup and disc. Roughly 5 wt% CeO₂ was added to the powder as an internal standard and milled together with the glass for additional 30 seconds. The powdered glass samples were loaded into XRD sample holders and scanned at a 0.015° 2 θ step size, 1.5-second dwell time, from 5° to 75° 2 θ scan range. XRD spectra were analyzed with DIFFRAC.EVA software (Bruker AXS GmbH, Karlsruhe, Germany) for phase identification. Full-pattern Rietveld refinement using TOPAS 4.2 (Bruker AXS GmbH, Karlsruhe, Germany) was performed to quantify the amounts of crystal phases on samples with crystalline content. These results are discussed in Section 3.2.

2.5 Crystal Fraction as a Function of Temperature

Isothermal CF as a function of temperature was measured in Pt-alloy boats (~2 g of glass per boat) with tight-fitting lids to minimize volatility according to the standard ASTM International procedure *Standard Test Method for Determining Liquidus Temperature of Immobilized Waste Glasses and Simulated Waste Glasses* (ASTM C1720). The heat treatments were performed at 950 °C for 24 hours. Prior to measuring the CF, the accuracy of the furnace temperature was verified using a glass (AmCm2-19) with liquidus temperature (T_L) traceable to a round-robin study, prepared and verified by Gervasio et al. (2019). These results are discussed in Section 3.3.

2.6 Glass Density

The room-temperature density (ρ) of each glass was measured using an AccuPyc II 1340 gas pycnometer (MicroMeritics, Norcross, Georgia) with approximately 1 g of glass pieces. The glass was loaded into a vial and placed within the instrument. The instrument then determined the density by the difference in amount of helium gas needed to fill the vial with glass vs. the amount needed without glass. The pycnometer was calibrated within 6 months of the testing and the calibration was checked before and after measurements for that day using a National Institute of Standards and Technology traceable standard tungsten carbide ball. These results are discussed in Section 3.4.

2.7 Glass Viscosity

The viscosities (η) of the glass melts were measured as functions of temperature with a fully automated Anton Paar FRS 1600 Furnace Rheometer System. Approximately 25 to 30 mL or ~70 g of glass was placed into a Pt-alloy cylindrical cup. It was then heated to ~1150 °C and maintained at that temperature until thermal equilibrium was reached. A Pt-alloy spindle then was lowered into the cup of molten glass. An initial torque reading (at a constant spindle speed) was taken at ~1150 °C, with subsequent measurements at target temperatures of 1050 °C, 950 °C, 1150 °C, 1250 °C, and then 1150 °C using a hysteresis approach. The hysteresis approach allows for the potential impacts of crystallization (at lower temperatures) to be assessed via reproducibility with replicate measurements being taken at approximately the melting temperature. Volatilization (at higher temperatures) is minimized by measuring viscosity at temperatures above the melting temperature as nearly the final viscosity measurement. A 15-minute temperature equilibration time was used. Prior to glass viscosity measurements, halfway through the sample measurements and after sample measurements, the test instrumentation was checked for accuracy using a standard glass (Defense Waste Processing Facility [DWPF] Startup Frit) as discussed in the literature (Crum et al. 2012). These results are discussed in Section 3.5.

2.8 Electrical Conductivity

The EC (ϵ) of glass melts was determined with an Anton Paar FRS 1600 Furnace System using a Solartron impedance analyzer. Platinum plates (1.3 inches long by 0.28 inches wide) were placed parallel to each other with a separation of 0.367 inches. About 30 mL of glass sample was used for EC measurements in a Pt-alloy crucible. Before measuring EC of the test-matrix glasses, calibration was conducted at room temperature with reference solutions of KCl (0.1 M and 1 M) by measuring the resistance values at frequencies ranging from 10^{-1} to 10^6 Hz. Six frequency scans were made for each KCl concentration. The average values of the six readings were then used to calculate the cell constant. The high-temperature EC was validated using DWPF Startup Frit. For glass measurement, the probe was lowered into the molten glass to a depth of 12.7 mm and the sample was first heated at the target temperature of 1200 °C for 30 minutes. After the temperature was stabilized, two scans from 10^{-1} MHz to 10^6 Hz were conducted and the average impedance intercept was used to calculate ϵ for each temperature. The ϵ was measured at four different target temperatures in a range around the melting temperature of the glass (after 25-minute equilibration time): 1200 °C, 1150 °C, 950 °C, and 1150 °C. These results are discussed in Section 3.6.

2.9 Product Consistency Test

PCT responses were measured in triplicate for quenched and CCC samples of each glass using Method A of the standard ASTM International procedure *Standard Test Methods for Determining Chemical Durability of Nuclear, Hazardous, and Mixed Waste Glasses and Multiphase Glass Ceramics: The Product Consistency Test (PCT)* (ASTM C1285). The PCT test matrix also included a reference glass traceable to a round robin study and blanks. Glass samples were ground, sieved to -100+200 mesh, washed, and prepared according to the standard ASTM C1285 procedure, Method A. The prepared glass was added to deionized (DI) water in a 1.5 g:15 mL ratio. The vessels used were desensitized Type 304L stainless steel. The vessels were closed, sealed, and placed into an oven at $90 \text{ °C} \pm 2 \text{ °C}$ for 7 days \pm 3 hours. After 7 days at 90 °C, the vessels were removed from the oven and allowed to cool to room temperature. The final mass of the vessel and the solution pH were recorded on a data sheet. Each test solution was then passed through a 0.45- μm filter and acidified with HNO_3 to maintain the cations in solution. The resulting solutions were analyzed by ICP-OES for Si, Na, and B. Samples of multi-element, standard solutions were also analyzed as a check on the accuracy of the ICP-OES. Normalized concentrations (NC_i , g L^{-1}) were calculated with the following formula:

$$\text{NC}_i = \frac{C_i}{f_i} \quad (2.1)$$

where: NC_i = the normalized concentration of element I in solution (g L^{-1})
 C_i = the concentration of element I in solution ($\text{g}\cdot\text{L}^{-1}$)
 f_i = mass fraction of element I in the glass ($\text{g}_i\cdot\text{g}_{\text{glass}}^{-1}$)

Subsequently, the normalized losses (NL_i , g m^{-2}):

$$\text{NL}_i = \frac{\text{NC}_i}{S/V} \quad (2.2)$$

where: S = glass surface area (m^2)
 V = volume of solution (m^3)

Assuming a spherical particle geometry and a density of $2.65 \text{ g}\cdot\text{cm}^{-3}$, this results in a glass surface area:solution volume ratio of approximately 2000 m^{-1} . The ratio was not adjusted to account for measured glass density.

The calculations of NC_i and NL_i were based on target and measured glass compositions. The target composition was used for data evaluation and analysis. Results are included in Section 3.7.

2.10 Vapor Hydration Test

In the VHT, monolithic glass samples were exposed to water vapor at 200 °C in sealed stainless-steel vessels according to the ASTM International standard procedure *Standard Test Method for Measuring Waste Glass or Glass Ceramic Durability by Vapor Hydration Test* (ASTM C1663). Roughly 1.5-mm × 10-mm × 10-mm samples were cut from annealed or CCC-treated LAW glass bars using a diamond-impregnated saw. All sides of the cut sample were polished to 600-grit surface finishes with silicon carbide paper.

Polished samples were hung from stainless-steel supports with Pt wire within a stainless-steel container. DI water was added to the bottom of the vessel so that enough water was present to react with the specimen, but without enough water to reflux during testing (~0.20 g). The samples were heated and held at 200 °C in a convection oven for either 24 or 7 days. All samples were initially tested for 24 days. Samples found to have fully reacted in 24 days were then tested for shorter times to enable estimation of a numerical alteration rate (as opposed to “greater-than” values).

After removal from the oven, vessels were weighed and then quenched in cold water. The specimens were removed from the vessels and cross-sectioned with or without epoxy (depending on the stability of each sample) for analysis by optical microscopy-image analysis to determine the amount of glass altered during the test. The solution in the vessel was tested for pH to ensure reflux did not occur. Any test with a pH >10 was not used due to reflux.

The remaining glass thickness of the VHT specimen was determined by performing at least 10 measurements distributed (roughly equally) across the crack-free cross section of the sample. Then, the average and standard deviations of the 10 thickness measurements of the remaining glass were calculated. The amount of glass altered per unit surface area of specimen was determined from the average thickness of unaltered glass according to Eq. (2.3):

$$m = \frac{1}{2} \rho (d_i - d_r) \quad (2.3)$$

where: d_i = initial thickness of the specimen (m)
 d_r = average thickness of remaining glass layer (m)
 m = mass of glass converted to alteration products per unit surface area ($g\ m^{-2}$)
 ρ = glass density ($g\ m^{-3}$), assumed to be 2,650,000

The average rate of corrosion was calculated as $r_a = m/t$, where t is the corrosion time. Vienna et al. (2001) showed that if the average rate of corrosion at 200 °C is

$$r_a = m / t < 50\ g\ m^{-2}\ d^{-1} \quad (2.4)$$

then the final rate of corrosion, $r_a < 50\ g\ m^{-2}\ d^{-1}$, meets the current ORP requirement for LAW glass performance. Although the contract limit for VHT response is stated in rates ($50\ g\ m^{-2}\ d^{-1}$), the test directly measures alteration depth (D) in μm at different times. In previous studies (Piepel et al. 2007; Muller et al. 2014), the directly measured parameter of D in μm after 24 days was modeled. This value can be converted to a rate by $D\ (\mu m) \times 10^{-6}\ (m/\mu m) \times \text{density}\ (g/cm^3) \times 10^6\ (cm^3/m^3) / t(d)$. Assuming a density of $2.65\ g\cdot cm^{-3}$, the limit of $50\ g\cdot m^{-2}\cdot d^{-1}$ is equivalent to a D of 453 μm for a 24-day test duration. In the present study, the density was assumed to be $2.65\ g\cdot cm^{-3}$. The results are discussed in Section 3.8.

2.11 Sulfur Solubility Procedure

Sulfur solubility was measured on the quenched glass samples. The procedure was developed by PNNL and is described in Jin et al. (2019). There are three primary steps of testing with each glass: 1) saturation with sodium sulfate, 2) washing with DI water, and 3) analysis of SO₃ in saturated glass. Each step is described below.

2.11.1 Step 1: Saturation

Saturation with sodium sulfate was performed by taking 50 g of each glass, grinding it, and then sieving through a #120 sieve (125 μm). Then, 7.64 g of Na₂SO₄ per 100 g of glass was added to the sieved powdered glass to maintain 4 mass% SO₃ added to the glass/salt system, and the combination was mixed to achieve homogeneity. The mixture of baseline glass and Na₂SO₄ was melted at 1150 °C for 1 hour in a Pt-10%Rh crucible with a tight-fitting lid. After melting, the mixture was poured onto a steel plate to quench. The mixture was again mixed by crushing and sieving through a #120 sieve (125 μm) and placed back into the Pt-10%Rh crucible to melt at 1150 °C for 1 hour the second time. After the second melting, the mixture was quenched by pouring onto a steel plate, mixed by crushing and sieving, and melted under the same conditions for the third time. After three melting cycles, the glass was crushed and sieved through the #120 sieve (125 μm).

2.11.2 Step 2: Washing

After the third melt, a sample of the sieved glass was washed with DI water to remove excess salt prior to further analysis. This was done by adding 2 g of glass/salt mixture to a centrifuge filter in a centrifuge tube and adding 20 g of DI water to the tube. The tube was capped and shaken by hand for 2 minutes. Samples were placed in a balanced centrifuge that was set to 3175 rpm for 5 minutes. The solution was decanted into a bottle through a low-density polyethylene filter.

The filter was removed and then reinserted into the centrifuge tube. A second wash was performed following the same steps, and then the glass was weighed and dried at 80 °C overnight. To assure there was enough sample for analysis, a fresh 2 g of the same glass was obtained, and the procedure described above was repeated. The resulting solutions were combined as well as the dried powders after being homogenized together using a mortar and pestle.

2.11.3 Step 3: Analysis

The washed and filtered glasses and the wash solutions recovered from filtering were then analyzed by ICP-OES and IC by Hsieh (2021b, 2022b). Blanks and standards were used intermittently to assess the performance of each of the instruments and procedures. Methods of measurement are listed in Table 2.6. The results are discussed in Section 3.9.

Table 2.6. Measurement Methods Used in Reporting Glass and Wash Solutions Analytes Concentrations (Hsieh 2021b, 2022b)

Analyte	Measurement Method	Preparation Method	Analyte	Measurement Method	Preparation Method
Al	ICP-OES	LM	Na	ICP-OES	LM
B	ICP-OES	PF	P	ICP-OES	LM
Ca	ICP-OES	LM	S	ICP-OES	LM
Cl	IC	KH	Si	ICP-OES	PF
Cr	ICP-OES	LM	Sn	ICP-OES	LM
F	IC	KH	Ti	ICP-OES	LM
Fe	ICP-OES	LM	V	ICP-OES	LM
K	ICP-OES	LM	Zn	ICP-OES	LM
Li	ICP-OES	PF	Zr	ICP-OES	LM
Mg	ICP-OES	LM			

3.0 Results and Discussion

This section describes the results for the chemical composition, CCC, CF, ρ , η , EC, PCT, VHT, and sulfur solubility.

3.1 Chemical Analysis of Glass Composition

The targeted and average of duplicate measured components in weight percent in the quenched glasses are presented in Appendix E along with the percent differences of components with targeted concentrations of 1 wt% or more. The composition analyses of the glass samples were performed as described in Section 2.3. All the measurements for each oxide in each glass were averaged to determine a representative chemical composition for each glass. Overall, the measured sums of oxides for all glasses fell within the interval of 95 to 102 wt%, indicating acceptable recovery of the glass components. The main observations based on chemical analyses are summarized below. For more details, see Hsieh (2021a, 2022a).

Differences in target vs. measured content close to the 10% threshold were attributed to experimental error. Glass samples LP5-12-1, LP5-15, LP5-17, and LP5-24 were rerun to confirm initial measurements. There were no significant changes in the measurements to indicate errors in preparation or analysis of the samples. Rerun measurements were not used in the averaging of oxides. The measured concentrations of SO₃ were below the targeted values, likely because of volatility during melting. At this point, the source of the Cl differences in samples LP5-15, LP5-17, and LP5-24 was not sought.

The following was observed in the LAW Phase 6 samples:

- Cl relative differences were above 10% for all study glasses except LAW-HPVR-04-1. The Cl relative differences for these glasses ranged from 62% to 3956%. The difference between measured and targeted composition values ranged from 0.03 to 1.42 wt%.
- K₂O relative differences were 10% or greater for LAW-HPVR-03-1, LAW-HPVR-07, LAW-HPVR-11, LAW-HPVR-13, LAW-HPVR-15, LAW-HPVR-21, LAW-HPVR-22, and LAW-HPVR-25.
- Na₂O relative differences were 10% or greater for LAW-HPVR-07, LAW-HPVR-25, and LAW-HPVR-26.
- ZrO₂ relative differences were 10% or greater for LAW-HPVR-02-1, LAW-HPVR-05, LAW-HPVR-09, LAW-HPVR-10, LAW-HPVR-11, LAW-HPVR-12, LAW-HPVR-13, LAW-HPVR-14, LAW-HPVR-15, LAW-HPVR-17, LAW-HPVR-18, LAW-HPVR-19, LAW-HPVR-21, and LAW-HPVR-23.

As for the LAW Phase 5 matrix, differences in target vs. measured content close to the 10% threshold were attributed to experimental error and the measured concentrations of SO₃ below target were attributed to volatility during melting. An investigation of the cause of the high Cl measured concentration in the LAW Phase 6 glasses revealed that the Zr source used for batching had up to 19.27 wt% of unexpected Cl. New target compositions were re-calculated by determining the correction factors for ZrO₂ and Cl based on the chemical composition of pure (desired) ZrO(NO₃)₂·2H₂O and the real composition of the chemical used (analyzed by scanning electron microscopy / energy dispersive X-ray spectroscopy). Then the mass fractions ZrO₂ and Cl in the HPVR glass compositions on the affected glasses (i.e., all except for LAW-HPVR-3 and LAW-HPVR-4) were corrected and renormalized to 1 and are reported in Appendix B. Although there were high levels of Cl in the batched glasses, the results of the matrix were considered still useful as major component distributions still obtained target concentration ranges, including high predicted PCT and VHT responses, and only 25% of the Cl concentrations are above the current model

data set. The three LAW Phase 5 glasses with Cl in excess of target were also batched using the same vendor Zr source, but different lot number. This strongly suggest the same chemical problem with both lots of $ZrO(NO_3)_2 \cdot 2H_2O$ used in this work.

3.2 Crystal Identification in Container Centerline Cooling Glasses

The formation of crystals during the slow cooling of the molten LAW glass in the final containers might adversely affect glass durability by sequestering durability-enhancing chemicals (Kim et al. 1995). Property-composition models were developed by using quenched glass data; therefore, any differences in PCT and VHT responses upon slow cooling need to be evaluated.

Not all crystals affect glass durability the same way; the identification of crystalline phases that form during the CCC process is the first step in predicting glass durability. This section presents and discusses the CF results from the CCC glasses obtained using the methods discussed in Section 2.4. The effects of CCC on PCT and VHT are reported in Sections 3.7 and 3.8, respectively.

Of the 51 total LAW glasses, 10 LAW Phase 5 and 2 LAW Phase 6 HPVR glasses formed some crystals, with content ranging from traces (i.e., crystals were observed by optical microscope, but the quantity was not enough to be detectable by XRD) to ~ 62 wt%. The glasses that had traces of crystals were LP5-03, LP5-06-MOD1, LP5-11, LP5-14, and LAW-HPVR-14. The crystal content and weight percent of crystallinity from XRD scans of CCC glass samples that formed measurable crystals are summarized in Table 3.1.

The main crystalline phases observed were aluminum sodium silicates ($Na_8Al_4Si_4O_{18}$, $Na_{1.55}(Al_{1.55}Si_{0.45}O_4)$, and $Na_{1.52}(Al_{1.45}Si_{0.55}O_4)$), combeite ($Na_2Ca_2Si_3O_9$), zirsinalite ($Na_6(Ca,Mn^{2+},Fe^{2+})Zr(Si_6O_{18})$), potassium magnesium silicate ($K_2Mg(SiO_4)$), $Fe_2(B_2O_5)$, $Na_2(S_2O_5)$, KB_3O_5 , zeolite rho ($(Na,Cs)_{12}(H_2O)_{44}[Al_{12}Si_{36}O_{96}]-RHO$), SiO_2 . Minor phases were detected in quantities too small to be correctly identified by the XRD software. Appendix F provides photographs of each glass after CCC and XRD scans of the CCC glasses that had crystals after the cooling process.

Crystals that sequester GFCs, like Na-Ca-silicates and Na-Al-silicates, have the potential to affect glass durability as the precipitation of components improve chemical durability (e.g., SnO_2 and ZrO_2) (Kim et al. 1995; Lonergan et al. 2021; Riley et al. 2001). The impacts of the other phases are less understood.

Table 3.1. Primary and Secondary Crystalline Phases in LAW Phase 5 and LAW Phase 6 Glasses

Glass ID	LP5-02	LP5-04	LP5-09	LP5-10	LP5-12-1	LP5-16-mod1	LAW-HPVR-25
Phase 1	Combeite	Combeite	Na ₈ Al ₄ Si ₄ O ₁₈	Na ₈ Al ₄ Si ₄ O ₁₈	Na _{1.55} (Al _{1.55} Si _{0.45} O ₄)	Na _{1.75} (Al _{1.75} Si _{0.25} O ₄)	Combeite
wt%	35.7	39.4	46.6	45.1	61.8	32.6	19.4
Phase 2	Na ₈ Al ₄ Si ₄ O ₁₈	Na ₈ Al ₄ Si ₄ O ₁₈	SiO ₂	K ₂ Mg(SiO ₄)	Lazurite	Na _{1.52} (Al _{1.45} Si _{0.55} O ₄)	
wt%	29.7	20	2.3	11	1	18.8	
Phase 3	SiO ₂	Na ₂ (S ₂ O ₅)		Fe ₂ (B ₂ O ₅)		Zirsinalite	
wt%	1	4.1		9.9		18.7	
Phase 4		SiO ₂		Zn _{1.9} (Ti _{0.167} Zr _{0.833}) _{0.9} FeO _{0.2} O ₄		K ₂ Mg(SiO ₄)	
wt%		1.5		4.9		4.4	
Phase 5		Si(P ₂ O ₇)		KB ₃ O ₅			
wt%		0.2		4.2			
Phase 6				zeolite rho			
wt%				3			
Phase 7				(Cs _{0.37} K _{0.63})(B Si ₂ O ₆)			
wt%				2.5			
Phase 8				SiO ₂			
wt%				1.6			

3.3 Crystal Fraction in Isothermal Heat Treatment

The study of crystalline phases and quantities in isothermal heat treatments was investigated in the LAW Phase 5 matrix only. Long idling of glass in the melter at low temperatures might promote crystal formation, impacting glass processability by settling in the melter clogging the pour sprout (Vienna et al. 2001). Also, if components added to glass to improve chemical durability (e.g., SnO₂ and ZrO₂) precipitate from the glass, the durability is likely to be lower than predicted.

CF as a function of temperature was measured as described in Section 2.5 at 950 °C. The following main crystalline phases were identified by XRD analysis: Na_{1.55}(Al_{1.55}Si_{0.45}O₄), Na_{0.558}Ti₂O₄; and akermanite (Ca₂MgSi₂O₇) (Table 3.2). Minor phases were detected and identified as cassiterite (SnO₂), (Cs_{0.37}K_{0.63})(BSi₂O₆), Zn_{1.9}(Ti_{0.167}Zr_{0.833})_{0.9}FeO_{0.2}O₄, and lazurite (Na,Ca)₈[(S,Cl,SO₄,OH)₂](Al₆Si₆O₂₄)] (Table 3.2). However, the concentration was too small to allow an indisputable identification. Photographs of each glass after the 24 hours of heat treatment at 950 °C are provided in Appendix G.

Table 3.2. Crystalline Phases Recognized by XRD in LAW Phase 5 Glasses Heat Treated at 950 °C. Phases with wt% < 0.1 are not reported.

Glass ID	LP5-10	LP5-12-1	LP5-16-MOD1
Phase 1	Na _{0.558} Ti ₂ O ₄	Na _{1.55} (Al _{1.55} Si _{0.45} O ₄)	Cassiterite
wt%	2.7	18.6	0.8
Phase 2	Akermanite	Lazurite	
Wt%	1.2	0.1	
Phase 3	(Cs _{0.37} K _{0.63})(BSi ₂ O ₆)		
wt%	0.6		
Phase 4	Zn _{1.9} (Ti _{0.167} Zr _{0.833}) _{0.9} FeO _{0.2} O ₄		
wt%	0.4		

3.4 Density

This section discusses the results of the LAW Phase 5 glass density measurements obtained using the methods discussed in Section 2.6. The results of the glass density measurements ranged from 2.53 to

2.74 g/cm³ with an average of 2.62 g/cm³ (Table 3.3). All density values are well below the contractual limit of 3.7 g/cm³.

Table 3.3. Measured Densities in the LAW Phase 5 Glasses

Glass ID	Measured Density (g/cm ³)	Glass ID	Measured Density (g/cm ³)
LP5-01	2.64	LP5-14	2.70
LP5-02	2.71	LP5-15	2.58
LP5-03	2.67	LP5-16-MOD1	2.75
LP5-04	2.70	LP5-17	2.79
LP5-05-1	1.68	LP5-18	2.62
LP5-06-MOD1	2.64	LP5-19	2.69
LP5-07	2.53	LP5-20	2.63
LP5-08	2.62	LP5-21	2.60
LP5-09	2.69	LP5-22	2.57
LP5-10	2.74	LP5-23	2.60
LP5-11	2.67	LP5-24	2.65
LP5-12-1	2.64	LP5-25	2.68
LP5-13	2.62		

3.5 Viscosity

This section presents and discusses the viscosity results obtained using the methods discussed in Section 2.7 on the LAW Phase 5 glasses. The results of the viscosity measurements are summarized in Table 3.4. The measured temperatures of LP5-01 to LP5-11 were slightly different from LP5-12 to LP5-25 due to an offset in the furnace set point. However, the range of temperatures from both sets of tests is adequate for viscosity model assessment. Appendix H shows results and plots for the viscosity vs. temperature data obtained.

Table 3.4. Measured η (Pa·s) Values vs. Target Temperature (in the sequence of measurement) for the LAW Phase 5 Glasses

Target Temperature (°C)	1150	1050	950	1150	1250 ^(b)	1150
Glass ID	ln η (Pa·s)					
LP5-01 ^(a)	-0.658	0.065	1.041	-0.610	-0.999	-0.599
LP5-02 ^(a)	-0.575	0.193	1.175	-0.552	-0.946	-0.567
LP5-03 ^(a)	-0.128	0.708	1.755	-0.145	-0.608	-0.161
LP5-04 ^(a)	-0.621	0.079	0.983	-0.662	-1.085	-0.667
LP5-05 ^(a)	-0.292	0.490	1.488	-0.286	-0.703	-0.303
LP5-06-MOD1 ^(a)	1.133	2.040	3.190	1.164	0.662	1.162
LP5-07 ^(a)	1.502	2.318	3.305	1.503	0.995	1.498
LP5-08 ^(a)	1.193	1.994	3.039	1.207	0.773	1.211
LP5-09 ^(a)	0.634	1.471	2.401	0.596	0.118	0.574
LP5-10 ^(a)	0.443	1.323	2.281	0.401	-0.112	0.372
LP5-11 ^(a)	0.450	1.195	2.126	0.485	0.030	0.502
LP5-12-1	1.954	3.063	4.521	1.980	1.327	1.940
LP5-13	0.020	0.808	1.711	0.004	-0.467	0.031
LP5-14	0.873	1.884	3.170	0.885	0.288	0.879
LP5-15	1.620	2.611	3.850	1.626	0.988	1.649
LP5-16-MOD1	0.535	1.565	2.913	0.559	-0.087	0.537
LP5-17	0.404	1.445	2.783	0.403	-0.151	0.378
LP5-18	0.757	1.563	2.688	0.738	0.308	0.745
LP5-19	-0.209	0.639	1.736	-0.188	-0.697	-0.205
LP5-20	0.304	1.196	2.353	0.326	-0.184	0.323
LP5-21	0.017	0.806	1.839	0.025	-0.441	0.010
LP5-22	1.263	2.146	3.326	1.270	0.805	1.258
LP5-23	1.526	2.423	3.554	1.495	1.022	1.486
LP5-24	1.660	2.818	3.995	1.620	1.076	1.617
LP5-25	1.493	2.450	3.708	1.512	1.061	1.478

(a) Viscosity measurements were taken at the following temperatures: 1169 °C, 1074 °C, 979 °C, 1169 °C, 1226^b °C, 1169 °C.
(b) The furnace set point was set at 1250 °C, however the furnace never reached the set point. Measured values range from 1203 °C to 1235 °C, see 5.0Appendix H.

Two model forms are used here to interpolate viscosity-temperature data for each waste glass. The first model form is the Arrhenius equation:

$$\ln(\eta) = A + \frac{B}{T_K} \quad (3.1)$$

where A and B are coefficients independent of temperature expressed in Kelvin ($T_K = T(^{\circ}\text{C}) + 273.15$). The values for the A and B coefficients are reported in Table 3.5 for each glass.

The second model is the Vogel-Fulcher-Tammann (VFT) model:

$$\ln(\eta) = E + \frac{F}{T_k - T_0} \quad (3.2)$$

where E, F, and T_0 are temperature-independent coefficients and T_K is the temperature in Kelvin ($T(^{\circ}\text{C}) + 273.15$). This model can be used to estimate the effect of temperature on viscosity over a wide range of temperatures for silicate-based glasses. Therefore, this model also was applied to the data for each glass; the E, F, and T_0 coefficients for each glass are shown in Table 3.5. Furthermore, Table 3.5 summarizes the viscosity results at 1150 °C (η_{1150}) calculated using both the Arrhenius and the VFT equations for these glasses.

At the melting temperature of 1150 °C, the optimal viscosity of LAW glass melts should be maintained between 2 and 8 Pa-s to avoid processing issues (Vienna et al. 2022). Thirteen out of 25 glasses had measured viscosity at 1150 °C below the optimum viscosity range (see Table 3.5).

Table 3.5. Fitted Coefficients of Arrhenius and VFT Models for Viscosity of the LAW Phase 5 Glasses

Glass ID	Arrhenius Coefficients		VFT Coefficients			Calculate η_{1150} (Pa-s)	
	A (ln Pa-s)	B (ln Pa-s·K)	E (ln Pa-s)	F (ln Pa-s K)	T_0 (K)	Arrhenius	VFT
LP5-01	-11.34	15456	-5.6202	3771.5	685.57	0.618	0.602
LP5-02	-11.80	16203	-6.5623	5057.6	598.38	0.664	0.650
LP5-03	-12.35	17623	-6.9147	5881.2	573.97	1.035	1.011
LP5-04	-11.25	15296	-7.5686	6870.7	448.6	0.603	0.595
LP5-05	-11.87	16694	-7.3493	6629.4	501.79	0.871	0.857
LP5-06-MOD1	-11.94	18893	-5.6586	5612.8	617.76	3.811	3.708
LP5-07	-10.31	17038	-7.9156	11104	262.37	5.248	5.209
LP5-08	-10.72	17190	-5.7208	6245	538.88	3.896	3.825
LP5-09	-11.29	17153	-12.83	21626	-167.27	2.147	2.155
LP5-10	-12.04	17957	-23.358	62846	-1200.9	1.775	1.808
LP5-11	-10.22	15430	-6.2211	6419.5	482.75	1.861	1.832
LP5-12-1	-13.29	21726	-6.157	6759.4	590.13	7.210	7.080
LP5-13	-10.15	14501	-7.4503	8121.1	337.19	1.035	1.028
LP5-14	-12.86	19562	-7.5797	7933.5	485.09	2.433	2.405
LP5-15	-11.63	18893	-6.6194	7788.6	479.26	5.189	5.115
LP5-16-MOD1	-13.40	19888	-6.3413	5387.5	641.07	1.770	1.729
LP5-17	-14.00	20495	-8.9233	9125.6	443.52	1.493	1.480
LP5-18	-10.89	16561	-5.4568	5180.6	586.8	2.112	2.091
LP5-19	-11.79	16502	-7.0046	6135	521.12	0.825	0.816
LP5-20	-11.79	17253	-6.1808	5449.7	584.51	1.393	1.374
LP5-21	-10.85	15484	-6.0932	5318.2	552.6	1.027	1.016
LP5-22	-10.85	17282	-4.1461	3932.9	697.01	3.628	3.561
LP5-23	-10.77	17491	-5.9945	7000.3	490.25	4.569	4.524
LP5-24	-12.87	20660	-19.44	42064	-570.76	5.206	5.240
LP5-25	-11.80	18927	-5.9132	6430.2	554.73	4.481	4.443

3.6 Electrical Conductivity

This section presents and discusses the EC results obtained using the methods discussed in Section 2.8. Table 3.6 lists the ϵ vs. temperature data for each glass, and Appendix I shows plots for the ϵ vs. temperature data obtained from the EC testing. EC of some of the glasses (from LP5-01 to LP5-11, marked with asterisks in Table 3.6) was measured at slightly different temperatures from the target due to an offset in the furnace set point.

The Arrhenius model (Eq (3.2)) was used to describe temperature effects on ϵ . The values for the A and B coefficients obtained by fitting the equation to the ϵ -temperature data for each glass (using least squares regression) are shown in Table 3.7 along with the calculated ϵ at 1150 °C (ϵ_{1150}). At the melting temperature of 1150 °C, the optimal ϵ should be between 0.1 and 0.7 S/cm to make sure that energy is

supplied by the power source without exceeding the current density limits of the power system at nominal throughput (Vienna et al. 2022). Average measured ϵ_{1150} was in the optimum range for 10 glasses, and above it for the remainder, with the maximum value being 1.53 S/cm (Table 3.6).

Table 3.6. Measured Electrical Conductivity (S/m) Values vs. Target Temperatures for the LAW Phase 5 Glasses

Target T , °C	950	950	1050	1050	1150	1150	1200 ^(b)	1200
Glass ID	Electrical Conductivity (S/m)							
LP5-01 ^(a)	35.9	43.2	96.9	84.1	N/A	98.3	135.8	135.7
LP5-02 ^(a)	86.2	86.0	119.8	119.6	152.7	152.6	N/A	166.7
LP5-03 ^(a)	52.7	52.6	72.7	72.6	93.6	93.2	N/A	103.5
LP5-04 ^(a)	63.2	63.0	89.4	89.6	118.7	118.6	133.3	133.7
LP5-05 ^(a)	40.2	32.9	39.9	42.6	50.0	80.2	N/A	85.1
LP5-06-MOD1 ^(a)	59.3	59.2	83.7	83.4	N/A	109.3	N/A	122.0
LP5-07 ^(a)	59.3	59.0	79.0	78.9	97.7	97.7	N/A	106.3
LP5-08 ^(a)	77.7	77.5	104.9	104.8	132.6	132.5	141.2	146.9
LP5-09 ^(a)	66.5	66.4	89.3	89.2	111.1	111.2	121.3	109.3
LP5-10 ^(a)	83.9	82.5	115.6	114.5	146.5	146.9	161.9	139.9
LP5-11 ^(a)	49.4	66.2	83.8	83.2	120.4	108.2	129.2	127.0
LP5-12-1	22.8	23.0	31.1	30.9	46.5	66.6	80.2	74.9
LP5-13	47.1	42.5	91.0	53.8	115.6	111.8	127.2	142.9
LP5-14	30.3	29.7	35.4	42.5	43.2	72.1	96.2	96.8
LP5-15	29.4	29.7	40.9	40.8	62.2	59.0	N/A	110.5
LP5-16-MOD1	44.6	44.3	37.2	43.4	48.6	73.3	82.5	88.8
LP5-17	38.0	37.6	62.8	62.4	87.5	87.7	100.8	101.1
LP5-18	54.6	61.9	72.5	72.8	105.5	105.0	115.1	115.4
LP5-19	51.6	39.6	77.7	75.7	105.8	103.3	120.2	119.2
LP5-20	46.2	40.6	53.2	62.4	49.5	75.0	91.2	90.9
LP5-21	51.3	53.5	79.0	78.7	102.7	103.5	104.2	103.3
LP5-22	53.5	53.2	56.5	54.8	90.8	89.5	114.6	101.6
LP5-23	44.7	44.4	47.8	60.9	85.1	85.2	94.1	94.1
LP5-24	22.9	20.6	64.5	32.8	82.0	86.1	97.9	87.9
LP5-25	12.1	12.0	18.8	21.1	25.7	28.4	N/A	48.3

(a) The temperatures at which EC was measured for this glass were 979 °C, 979 °C, 1074 °C, 1074 °C, 1169 °C, 1169 °C, 1216 °C, 1216 °C. See Appendix I for more details.

(b) Some oscillations were observed around the 1200 °C setpoint. For detailed values at which the EC measurement was taken, see Appendix I.

Table 3.7. Fitted Coefficients of Arrhenius Model for ϵ_{1150} of the LAW Phase 5 Glasses

Glass ID	Arrhenius Coefficients		Calculated
	A, ln[S/m]	B, ln[S/m]-K	ϵ_{1150} (S/m)
LP5-01	11.09	-9156.2	105.24
LP5-02	8.70	-5300	144.89
LP5-03	8.26	-5369.7	88.81
LP5-04	8.87	-5908.1	112.00
LP5-05	8.45	-6181.7	60.67
LP5-06-MOD1	8.67	-5733.7	103.52
LP5-07	7.82	-4670.2	93.49
LP5-08	8.28	-4901.2	125.50
LP5-09	7.77	-4444.5	103.77
LP5-10	8.30	-4822.5	135.29
LP5-11	9.16	-6395.6	106.46
LP5-12-1	10.21	-8772.1	57.35
LP5-13	10.39	-8083.2	111.30
LP5-14	9.62	-7719.6	66.10
LP5-15	9.82	-7965.4	68.52
LP5-16-MOD1	7.35	-4529.7	64.70
LP5-17	9.44	-7071.3	87.25
LP5-18	8.23	-5134.2	101.81
LP5-19	9.55	-6979.1	104.38
LP5-20	7.48	-4562	71.89
LP5-21	8.19	-5124.7	98.04
LP5-22	8.21	-5296	88.73
LP5-23	8.40	-5689.4	81.32
LP5-24	11.93	-10784	77.90
LP5-25	9.41	-8494.4	31.18

3.7 Product Consistency Test

Both LAW Phase 5 and LAW Phase 6 PCTs were performed at PNNL; LAW Phase 5 PCT leachates were analyzed at SRNL (Hsieh 2021c) or at PNNL, whereas LAW Phase 6 leachates were analyzed only at SRNL (Hsieh 2021d).

The average normalized PCT loss (NLs) for B, Na, and Si for Q and CCC glass of the two matrices are reported in Table 3.8 to Table 3.11. Values marked with asterisks were corrected to take into account the Na and/or Si concentration in the blanks. Per the WTP contract (DOE 2000), these values must be below 2.0 g/m². Most of the glasses, both CCC and Q versions, from both matrices exceeded the WTP 2 g/m² constraints. Only 7 of the 23 LAW Phase 5 quenched glasses passed the NL_B and NL_{Na} constraints and only two of the CCC glasses passed the NL_B constraints and five passed the NL_{Na} constraint. Fifteen LAW Phase 5 glasses, both Q and CCC, passed the NL_{Si} constraint. Similarly, 10 Q and 14 CCC LAW Phase 6 glasses passed the NL_B constrain, 8 Q and 11 CCC glasses passed the NL_{Na} constraints. Finally, most Q and CCC LAW Phase 6 passed the NL_{Si} constraint.

Table 3.8. Average Normalized PCT Loss (NLs) for the LAW Phase 5 Glasses. Missing values were below the analytical laboratory detection limit.

Glass ID	NL _B (g/m ²)	NL _{Na} (g/m ²)	NL _{Si} (g/m ²)
LP5-01-Q	46.0	35.3 ^(a)	8.19 ^(a)
LP5-02-Q	0.939	1.92 ^(a)	0.32 ^(a)
LP5-03-Q	10.6	8.83 ^(a)	1.05 ^(a)
LP5-04-Q	0.126	1.23 ^(a)	0.11 ^(a)
LP5-05-Q	8.96	7.38 ^(a)	1.46 ^(a)
LP5-06-mod1-Q	0.862	0.87	0.2 ^(a)
LP5-07-Q	1.96	1.62 ^(a)	0.32 ^(a)
LP5-08-Q	2.34	2.06 ^(a)	0.37 ^(a)
LP5-09-Q	1.01	1.66 ^(a)	0.45 ^(a)
LP5-10-Q	13.6	9.94 ^(a)	2.01 ^(a)
LP5-11-Q	15.1	11.18 ^(a)	2.17 ^(a)
LP5-12-1-Q	0.586	0.69 ^(a)	0.19 ^(a)
LP5-13-Q	43.8	33.5	4.78
LP5-14-Q	8.08	5.69 ^(a)	1.37 ^(a)
LP5-15-Q	2.83	2.08	0.28
LP5-16-mod1-Q	3.92	3.54	0.6 ^(a)
LP5-17-Q	7.70	6.10	1.02
LP5-18-Q	16.7	12.6	2.30
LP5-19-Q	13.2	11.4	2.15
LP5-20-Q	27.9	20.7	3.96
LP5-21-Q	10.5	8.6 ^(a)	1.29 ^(a)
LP5-22-Q	25.2	19.9 ^(a)	5.37 ^(a)
LP5-23-Q	0.538	1.41 ^(a)	0.37 ^(a)
LP5-24-Q	0.51	0.53 ^(a)	0.15 ^(a)
LP5-25-Q	0.38	0.44 ^(a)	0.16 ^(a)

(a) NL after blank correction

Table 3.9. Average Normalized PCT Loss (NLs) for CCC LAW Phase 5 Glasses

Glass ID	NL _B (g/m ²)	NL _{Na} (g/m ²)	NL _{Si} (g/m ²)
LP5-01-CCC	42.8	32.2	7.44
LP5-02-CCC	27.9	17.9	0.99
LP5-03-CCC	10.1	8.73	1.11
LP5-04-CCC	3.12	6.16	0.96
LP5-05-CCC	9.67	8.03	1.58
LP5-06-mod1-CCC	1.11	1.05	0.257
LP5-07-CCC	2.46	1.74	0.383
LP5-08-CCC	2.16	1.98	0.412
LP5-09-CCC	39.5	22.4	4.16
LP5-10-CCC	47.0	24.5	6.56
LP5-11-CCC	15.4	11.2	2.35
LP5-12-1-CCC	4.02	2.12	0.293
LP5-13-CCC	46.1	33.6	4.83
LP5-14-CCC	4.56	3.63	1.01
LP5-15-CCC	2.24	1.76	0.251
LP5-16-mod1-CCC	19.0	10.50	0.561
LP5-17-CCC	6.49	5.46	0.933
LP5-18-CCC	15.9	11.6	2.28
LP5-19-CCC	12.6	10.9	1.87
LP5-20-CCC	29.1	20.4	3.97
LP5-21-CCC	11.6	9.82	1.47
LP5-22-CCC	23.9	18.4	5.26
LP5-23-CCC	0.511	1.37	0.387

Table 3.10. Average Normalized PCT Loss (NLs) for Q LAW Phase 6 Glasses

Glass ID	NL _B (g/m ²)	NL _{Na} (g/m ²)	NL _{Si} (g/m ²)
LAW-HPVR-01-1-Q	7.60	6.15	1.33
LAW-HPVR-02-1-Q	3.95	3.72	0.75
LAW-HPVR-03-1-Q	0.61	0.73	0.17
LAW-HPVR-04-1-Q	6.90	5.50	1.96
LAW-HPVR-05-Q	6.80	5.05	1.62
LAW-HPVR-06-Q	1.79	2.08 ^(a)	0.55 ^(a)
LAW-HPVR-07-Q	2.24	2.60 ^(a)	0.65 ^(a)
LAW-HPVR-08-Q	1.02	1.00 ^(a)	0.19 ^(a)
LAW-HPVR-09-Q	12.85	10.69 ^(a)	2.38 ^(a)
LAW-HPVR-10-Q	9.10	8.76 ^(a)	2.10 ^(a)
LAW-HPVR-11-Q	7.20	5.60	1.07
LAW-HPVR-12-Q	1.06	1.51	0.56
LAW-HPVR-13-Q	2.34	2.10	0.77
LAW-HPVR-14-Q	2.11	2.11	0.52
LAW-HPVR-15-Q	3.25	2.87	1.01
LAW-HPVR-16-Q	1.75	3.01 ^(a)	0.31
LAW-HPVR-17-Q	0.72	1.74 ^(a)	0.20
LAW-HPVR-18-Q	4.62	9.02 ^(a)	0.89
LAW-HPVR-19-Q	0.85	2.46 ^(a)	0.43
LAW-HPVR-20-Q	26.40	46.38 ^(a)	5.15
LAW-HPVR-21-Q	2.02	1.85	0.25
LAW-HPVR-22-Q	0.88	1.10	0.30
LAW-HPVR-23-Q	1.68	1.79	0.55
LAW-HPVR-24-Q	6.65	5.85	1.63
LAW-HPVR-25-Q	2.75	2.87	0.91
LAW-HPVR-26-Q	1.06	1.02	0.20

(a) NL after blank correction

Table 3.11. Average Normalized PCT Loss (NLs) for CCC LAW Phase 6 Glasses

Glass ID	NL _B (g/m ²)	NL _{Na} (g/m ²)	NL _{Si} (g/m ²)
LAW-HPVR-01-1-CCC	7.15	6.04 ^(a)	1.29
LAW-HPVR-02-1-CCC	4.55	4.39 ^(a)	0.81
LAW-HPVR-03-1-CCC	0.57	0.71 ^(a)	0.17
LAW-HPVR-04-1-CCC	5.05	4.59 ^(a)	1.57
LAW-HPVR-05-CCC	4.54	3.54 ^(a)	1.23
LAW-HPVR-06-CCC	1.29	1.45	0.43
LAW-HPVR-07-CCC	1.58	1.68	0.51
LAW-HPVR-08-CCC	0.86	0.80	0.16
LAW-HPVR-09-CCC	10.95	8.60	2.27
LAW-HPVR-10-CCC	6.45	5.80	1.71
LAW-HPVR-11-CCC	5.80	4.69	0.95
LAW-HPVR-12-CCC	0.94	1.38	0.51
LAW-HPVR-13-CCC	1.85	1.75	0.66
LAW-HPVR-14-CCC	1.85	2.03	0.48
LAW-HPVR-15-CCC	2.55	2.33	0.85
LAW-HPVR-16-CCC	1.19	1.10	0.23
LAW-HPVR-17-CCC	0.68	0.80	0.18
LAW-HPVR-18-CCC	3.53	3.39	0.73
LAW-HPVR-19-CCC	0.77	1.12	0.39
LAW-HPVR-20-CCC	18.20	14.83 ^(a)	3.86
LAW-HPVR-21-CCC	1.66	3.05 ^(a)	0.23
LAW-HPVR-22-CCC	0.86	2.10 ^(a)	0.30
LAW-HPVR-23-CCC	1.24	1.39	0.44
LAW-HPVR-24-CCC	4.37	8.07 ^(a)	1.29
LAW-HPVR-25-CCC	6.10	18.31 ^(a)	0.76
LAW-HPVR-26-CCC	1.32	1.11 ^(a)	0.25

(a) NL after blank correction

To determine if the difference between quenched and CCC heat treated glasses was within experimental error, the following hypothesis was tested (Rieck 2018):

$$p_Q - p_C = 0 \quad (3.3)$$

where p_Q and p_C are the true but unknown values of quenched and the CCC $\ln NR_B$ or $\ln NR_{Na}$.

To test this hypothesis, we considered $\hat{p}_C - \hat{p}_Q \pm k \cdot SD(\hat{p}_C - \hat{p}_Q)$ to see if:

$$0 \in (\hat{p}_C - \hat{p}_Q - k \cdot SD(\hat{p}_C - \hat{p}_Q), \hat{p}_C - \hat{p}_Q + k \cdot SD(\hat{p}_C - \hat{p}_Q)) \quad (3.4)$$

where \hat{p}_Q and \hat{p}_C are the measured values of the quenched and the CCC $\ln NR_B$ or $\ln NR_{Na}$, k is a multiplying factor based on the assumed normal distribution of $\hat{p}_C - \hat{p}_Q$ and intended confidence level for the test (in the present study set at 95%), and $SD(\hat{p}_C - \hat{p}_Q)$ is the estimated standard deviation of $\hat{p}_C - \hat{p}_Q$. Assuming $SD(\hat{p}_C) = SD(\hat{p}_Q) = SD$, then:

$$p_c^{\hat{}} - p_Q^{\hat{}} \pm kSD(p_c^{\hat{}} - p_Q^{\hat{}}) = p_c^{\hat{}} - p_Q^{\hat{}} \pm k\sqrt{2}SD \quad (3.5)$$

That is, the measured property of CCC glass is considered the same as that of quenched glass within the experimental error if the following condition is satisfied:

$$p_Q^{\hat{}} \in (p_c^{\hat{}} - k\sqrt{2}SD, p_c^{\hat{}} + k\sqrt{2}SD) \quad (3.6)$$

Most of the LAW Phase 5 glasses satisfied the above condition for NL_B except for six, LP5-02, LP5-04, LP5-09, LP5-10, LP5-12-1, LP5-16mod1, and seven for NL_{Na} (Figure 3.1).

All of the LAW Phase 6 glasses satisfied the above condition for NL_B except for one, LAW-HPVR-25, and the impact of CCC heat treatment appeared to be within the experimental uncertainty in normalized concentration values as shown in Figure 3.2. Seven glasses were significantly impacted in the NL_{Na} after CCC: LAW-HPVR-16, LAW-HPVR-17, LAW-HPVR-18, LAW-HPVR-19, LAW-HPVR-20, LAW-HPVR-22, and LAW-HPVR-25 (Figure 3.2). Glass LAW-HPVR-25 had measurable (by XRD) CF after CCC, represented as a colored rhombus (the color follows the plot legend, blue for NL_{Na} and red for NL_B) in Figure 3.2; the rest of the glasses that resulted in NL_{Na} significantly affected by CCC are represented in blue triangle.

The deterioration of the PCT response in LAW-HPVR-25 is expected since after CCC this glass formed ~19 wt% of combeite (Na₂Ca₂Si₃O₉), a crystal that tends to remove glass-forming constituents from the glass matrix, thus increasing PCT response (Kim et al. 1995; Lonergan et al. 2021; Riley et al. 2001).

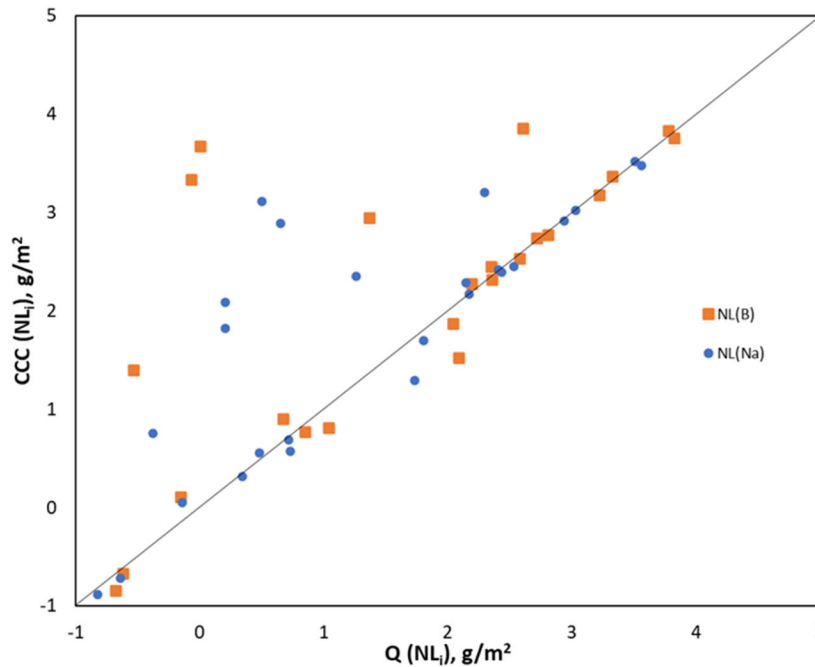


Figure 3.1. Normalized NL_B and NL_{Na} Release in Natural Logarithm Scale of Quenched vs. CCC LAW Phase 5 Glasses

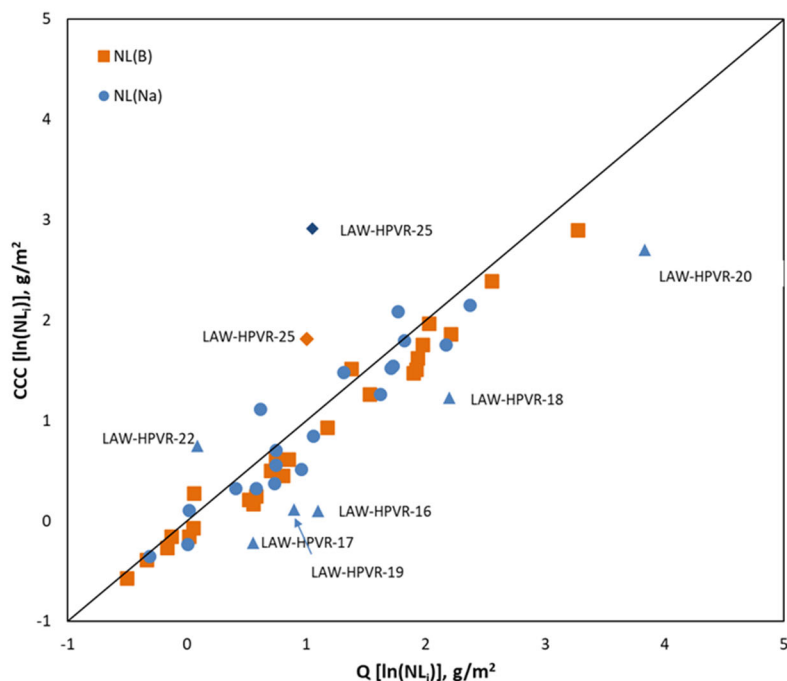


Figure 3.2. Normalized NL_B and NL_{Na} Release in Natural Logarithm Scale of Quenched vs. CCC LAW Phase 6 Glasses. Blue and orange rhombus represent glass LAW-HPVR-25, the only glass with measurable (by XRD) crystal fraction after CCC, NL_B and NL_{Na} . The triangle represents the NL_{Na} significantly affected by CCC.

3.8 Vapor Hydration Test

LAW Phase 5 VHT results reported pH above 10, suggesting that reflux occurred during the test. VHT are currently being rerun and will be presented in future revision of the current report.

VHT alteration rates for the 26 LAW Phase 6 glasses varied from 0.98 to 244.67 $\text{g}\cdot\text{m}^{-2}\cdot\text{d}^{-1}$ for the quenched glasses and from 0.83 to 262.2 $\text{g}\cdot\text{m}^{-2}\cdot\text{d}^{-1}$ for the CCC glasses. Only two quenched glasses (LAWHPVR-11 and -19) and six CCC glasses (LAW-HPVR-06, -10, -12, -17-19, and -20) exceeded the WTP contract limit (Table 3.12). In accordance with the WTP contract, the alteration rates (r_a) of LAW glasses subjected to ≥ 7 -day VHT shall be less than 50 $\text{g}/\text{m}^2/\text{d}$ (DOE 2000).

Table 3.12. Alteration Depth and Rate for Quenched and CCC of the LAW Phase 6 Q and CCC Glasses after 24 Day VHT

Glass ID	Quenched			CCC		
	Alteration depth (μm)	Alteration rate (r_a , $\text{g}\cdot\text{m}^{-2}\cdot\text{d}^{-1}$)	Passed/Failed (0/1)	Alteration depth (μm)	Alteration rate ($\text{g}\cdot\text{m}^{-2}\cdot\text{d}^{-1}$)	Passed/Failed (0/1)
LAW-HPVR-01-1	91.35	10.09	0	70.33	7.77	0
LAW-HPVR-02-1	147.20	16.25	0	92.83	10.25	0
LAW-HPVR-03-1	133.75	14.77	0	107.35	11.85	0
LAW-HPVR-04-1	366.79	40.50	0	296.39	32.73	0
LAW-HPVR-05	120.90	13.35	0	131.35	14.50	0
LAW-HPVR-06	414.20	45.73	0	471.07	52.01	1
LAW-HPVR-07	363.00	40.08	0	7.50	0.83	0
LAW-HPVR-08	113.95	12.58	0	142.21	15.70	0
LAW-HPVR-09	373.15	41.20	0	301.46	33.29	0
LAW-HPVR-10	450.20	49.71	0	463.75 ^(a)	175.56	1
LAW-HPVR-11	697.75	77.04	1	30.71	3.39	0
LAW-HPVR-12	N/A	N/A	N/A	684.17	75.54	1
LAW-HPVR-13	290.15	32.04	0	217.83	24.05	0
LAW-HPVR-14	42.50	4.69	0	151.04	16.68	0
LAW-HPVR-15	312.80	34.54	0	187.20	20.67	0
LAW-HPVR-16	8.85	0.98	0	8.08	0.89	0
LAW-HPVR-17	115.60 ^(a)	43.76 ^(a)	0	532.00	58.74	1
LAW-HPVR-18	33.35	3.68	0	136.13	15.03	0
LAW-HPVR-19	646.30 ^(a)	244.67 ^(a)	1	503.35 ^(a)	190.55	1
LAW-HPVR-20	419.15	46.28	0	692.61 ^(a)	262.20	1
LAW-HPVR-21	341.08	37.66	0	276.70	30.55	0
LAW-HPVR-22	105.65	11.67	0	122.75	13.55	0
LAW-HPVR-23	192.75	21.28	0	398.75	44.03	0
LAW-HPVR-24	413.65	45.67	0	68.80 ^(a)	26.05	0
LAW-HPVR-25	18.00 ^(a)	6.81 ^(a)	0	85.57	9.45	0
LAW-HPVR-26	317.35	35.04	0	270.60	29.88	0

(a) Values of the 24 days test extrapolated by the post 7 days measurements.

3.9 Sulfur Solubility

Melter SO_3 tolerance is the feed SO_3 concentration above which a salt phase accumulates in the melter. The melter SO_3 tolerance at the processing temperature of 1150 °C must exceed the weight percent of SO_3 in the feed to avoid risk of excessive corrosion of melter construction materials and increased radionuclide volatility (Vienna et al. 2014; Muller et al. 2015).

There is a good correlation between the melter SO_3 tolerance and SO_3 solubility (i.e., the saturated SO_3 concentrations) at 1150 °C (Jin et al. 2019; Skidmore et al. 2019). Hence, SO_3 solubility data developed primarily from crucible scale tests can be used to predict the melter SO_3 tolerance that can only be obtained from costly melter tests.

Sulfur solubility of each glass was determined experimentally by measuring SO₃ retention after 3× saturation (see Section 2.11 for procedure). Results are reported in Table 3.13. For more details, see Hsieh (2021b, 2022b). The 3TS values range from 0.862 to 3.13 wt% SO₃.

Table 3.13. SO₃ Concentrations in the Sulfur-Saturated Samples of the LAW Phase 5 and LAW Phase 6 Glasses

Glass ID	SO ₃ (wt%)	Glass ID	SO ₃ (wt%)
LP5-01	3.13	LAW-HPVR-01-1	1.9
LP5-02	1.69	LAW-HPVR-02-1	1.9
LP5-03	1.82	LAW-HPVR-03-1	1.58
LP5-04	2.01	LAW-HPVR-04-1	2.4
LP5-05	1.99	LAW-HPVR-05	1.9
LP5-06-MOD1	1.24	LAW-HPVR-06	1.93
LP5-07	1.29	LAW-HPVR-07	1.87
LP5-08	1.54	LAW-HPVR-08	1.45
LP5-09	1.48	LAW-HPVR-09	2.53
LP5-10	1.58	LAW-HPVR-10	2.51
LP5-11	1.73	LAW-HPVR-11	1.69
LP5-12-1	0.862	LAW-HPVR-12	2.26
LP5-13	2.73	LAW-HPVR-13	1.47
LP5-14	1.56	LAW-HPVR-14	1.77
LP5-15	1.02	LAW-HPVR-15	1.66
LP5-16-MOD1	1.25	LAW-HPVR-16	1.5
LP5-17	1.38	LAW-HPVR-17	1.73
LP5-18	1.52	LAW-HPVR-18	2.18
LP5-19	1.52	LAW-HPVR-19	2.97
LP5-20	1.79	LAW-HPVR-20	2.37
LP5-21	1.96	LAW-HPVR-21	1.67
LP5-22	1.6	LAW-HPVR-22	1.78
LP5-23	2.19	LAW-HPVR-23	1.6
LP5-24	1.03	LAW-HPVR-24	2.02
LP5-25	1.27	LAW-HPVR-25	1.9
--	--	LAW-HPVR-26	1.64

4.0 Conclusions

This report summarizes the data collected and analyzed on 51 LAW glasses, 25 belonging to the *LAW Phase 5: Expansion of LAW Glass Composition Boundaries* and 26 to the *LAW Phase 6: High PCT and VHT Response Glass*. Both matrices were generated using a space-filling experimental design to both fill and expand the existing LAW composition data to higher waste loading and cross glass property constraint boundaries. The conclusions are described below.

Most LAW Phase 5 glasses measured compositions were within experimental error from target compositions. Few glasses reported relative difference above 10% between measured and target compositions for one or more components (Section 3.1). Similarly, most LAW Phase 6 glasses measured composition were within the experimental error except for Cl and ZrO₂. All the LAW Phase 6 glasses except one, LAW-HPVR-04-1, had Cl content above target with the Cl relative differences ranging from 62% to 3956%. Although the high levels of Cl in the batched glasses, the results of the LAW Phase 6 matrix were considered useful as they allow for an expansion of the Cl content in the qualified database to 1.46 wt% compared to the previous range of 1.17 wt%.

After CCC, six LAW Phase 5 and one LAW Phase 6 glass formed some crystals with content ranging from traces (i.e., crystals were observed by optical microscope, but the quantity was not enough to be detectable by XRD) to 61.8 wt% (Table 3.1).

After isothermal heat treatment, several crystalline phases were identified by XRD analysis in LAW Phase 5 glasses, as summarized in Table 3.2.

Measured density of LAW Phase 5 glasses ranged from approximately 1.68 to 2.79 g/cm³ well below the contractual limit of 3.7 g/cm³. (Section 3.4).

Calculated viscosity at 1150 °C using the Arrhenius model of LAW Phase 5 glasses ranged from 0.62 to 7.2 Pa·s within thirteen glasses below the optimum range of 2 to 8 Pa·s (Section 3.5).

Calculated ϵ_{1150} using the Arrhenius model of LAW Phase 5 glasses were between 31.18 and 144.89 S/m with most of the glasses ϵ_{1150} above the optimum range of 0.1 and 0.7 S/cm (Section 3.6).

PCT NL_B and NL_{Na} are described in Section 3.7. Most of the glasses, both CCC and Q versions, from both matrices exceeded the WTP 2 g/m² constraints. Only seven of the 23 LAW Phase 5 quenched glasses passed the NL_B and NL_{Na} constraints and only two of the CCC glasses passed the NL_B constraints and 5 the NL_{Na} constraint. Fifteen LAW Phase 5 glasses, both Q and CCC, passed the NL_{Si} constraint. Similarly, only four Q and six CCC LAW Phase 6 glasses passed the NL_B constraint, two Q and four CCC glasses passed the NL_{Na} constraints, and seventeen glasses, both Q and CCC, passed the NL_{Si} constraint. CCC heat treatment did not appear to significantly increase PCT NL_B responses except when crystals were present and only slightly effected NL_{Na} responses of a few glasses (Figure 3.2).

LAW Phase 6 glasses VHT alteration rates (r_a) varied from ~1 to > 200 g m⁻² d⁻¹ for both the quenched glasses and the CCC (Section 3.8). Only two quenched glasses (LAWHPVR-11 and -19) and six CCC glasses (LAW-HPVR-06, -10, -12, -17-19, and -20) exceeded the WTP contract limit (Table 3.12).

Sulfur solubility (i.e., the saturated SO₃ concentrations) in LAW Phase 5 glasses ranged from ~1 wt% to 3.1 wt% (Section 3.9). In LAW Phase 6 glasses, sulfur solubility ranged from 1.6 wt% to 2.5 wt% (Table 3.13).

Combined, these data have added significantly to the database of LAW glasses available for glass property model development and validation. In particular, they have added valuable data for glasses with properties that exceed processing and product quality constraints. Previously, there has been little of data available to refine models at the property constraint values due to a general lack of data at and above property constraint values. These data are useful to reducing prediction uncertainties where they matter the most.

5.0 Bibliography

10 CFR 830, *Nuclear Safety Management*. Code of Federal Regulations.

ASTM C1285, *Standard Test Methods for Determining Chemical Durability of Nuclear, Hazardous, and Mixed Waste Glasses and Multiphase Glass Ceramics: The Product Consistency Test (PCT)*. ASTM International, West Conshohocken, Pennsylvania.

ASTM C1663, *Standard Test Method for Measuring Waste Glass or Glass Ceramic Durability by Vapor Hydration Test*. ASTM International, West Conshohocken, Pennsylvania.

ASTM C1720. *Standard Test Method for Determining Liquidus Temperature of Immobilized Waste Glasses and Simulated Waste Glasses*. ASTM International, West Conshohocken, Pennsylvania.

Bernards GA, GA Hersi, TM Hohl, RT Jasper, PD Mahoney, NK Pak, SD Reaksecker, AJ Schubick, and EB West. 2020. *River Protection Project System Plan*. ORP-11242, Rev. 9, U.S. Department of Energy, Office of River Protection, Richland, Washington.

Crum JV, TB Edwards, RL Russell, PJ Workman, MJ Schweiger, RF Schumacher, DE Smith, DK Peeler, and JD Vienna. 2012. "DWPF Startup Frit Viscosity Measurement Round Robin Results." *Journal of the American Ceramic Society* 95(7):2196-2205.

DOE Order 414.1D, *Quality Assurance*. U.S. Department of Energy, Washington, D.C.

DOE. 2000. *Design, Construction, and Commissioning of the Hanford Tank Waste Treatment and Immobilization Plant*. Contract DE-AC27-01RV14136, as amended, U.S. Department of Energy, Office of River Protection, Richland, Washington.

Ebert WL and SF Wolfe. 1999. *Round-Robin Testing of a Reference Glass for Low-Activity Waste Forms*. ANL-99/22, Argonne National Laboratory, Argonne, Illinois.

Gervasio V, JV Crum, BJ Riley, JD Vienna, JL George, BA Stanfill, and AA Kruger. 2019. *Liquidus Temperature: Assessing Standard Glasses for Furnace Calibration*. PNNL-29312, Pacific Northwest National Laboratory, Richland, Washington.

Hsieh MC. 2021a. *Composition Measurements of the LAW Phases 5 Glasses*. SRNL-STI-2021-00409, Rev. 0, Savannah River National Laboratory, Aiken, South Carolina.

Hsieh MC. 2021b. *Characterization of the Sulfur-Saturated Melt Versions of the LAW Phase 5 Glasses*. SRNL-STI-2021-00492, Rev. 0, Savannah River National Laboratory, Aiken, South Carolina.

Hsieh MC. 2021c. *Product Consistency Test Results for the LAW Phase 5 Glasses*. SRNL-STI-2021-00446, Rev. 0, Savannah River National Laboratory, Aiken, South Carolina.

Hsieh MC. 2021d. *Product Consistency Test Results for the LAW HPVR Glasses*. SRNL-STI-2021-00658, Rev. 0, Savannah River National Laboratory, Aiken, South Carolina.

Hsieh MC. 2022a. *Composition Measurements of the LAW HPVR Glasses*. SRNL-STI-2021-00265, Rev. 0, Savannah River National Laboratory, Aiken, South Carolina.

Hsieh MC. 2022b. *Characterization of the Sulfur-Saturated Melt Versions of the LAW HPVR Glasses*. SRNL-STI-2022-00553, Rev. 0, Savannah River National Laboratory, Aiken, South Carolina.

Jin T, D Kim, LP Darnell, BL Weese, NL Canfield, M Bliss, MJ Schweiger, JD Vienna, and AA Kruger. 2019. “A crucible salt saturation method for determining sulfur solubility in glass melt.” *International Journal of Applied Glass Science* 10(1):92-102.

Joseph R, E Gui, and S Ba. 2015. “Maximum Projection Designs for Computer Experiments.” *Biometrika* 102(2):371-380

Kim DS, D Peeler, and P Hrma. 1995. “Effect of Crystallization on the Chemical Durability of Simulated Nuclear Waste Glasses.” *Environmental Issues and Waste Management Technologies in the Ceramic and Nuclear Industries* 177-186.

Kim DS and JD Vienna. 2012. *Preliminary ILAW Formulation Algorithm Description*. 24590 LAW-RPT-RT-04-0003, Rev. 1, River Protection Project, Hanford Waste Treatment and Immobilization Plant, Richland, Washington.

Loneragan CE, E Rivers, D Bellofatto, DS Kim, and JD Vienna. 2021. *Crystallization Constraints for WTP LAW Operations: Assessment of CCC Impacts on VHT and PCT*. PNNL-31138, Rev. 0, EWG-RPT-032, Pacific Northwest National Laboratory, Richland, Washington.

Loneragan CE, JL George, D Cutforth, T Jin, P Cholsaipant, SE Sannoh, CH Skidmore, BA Stanfill, SK Cooley, GF Piepel, R Russel, and JD Vienna. 2020. *Enhanced Hanford Low-Activity Waste Glass Property Data Development: Phase 3*. PNNL-29847, Rev. 0, EWG-RPT-026, Pacific Northwest National Laboratory, Richland, Washington.

Lumetta NA, DS Kim, and JD Vienna. 2022. *Preliminary Enhanced LAW Glass Formulation Algorithm*. EWG-RPT-027, PNNL-29475, Rev. 1, Pacific Northwest National Laboratory, Richland, Washington.

Muller IS, G Diener, I Joseph, and IL Pegg. 2004. *Proposed Approach for Development of LAW Glass Formulation Correlation*. VSL-04L4460-1, Rev. 2, ORP-56326, Vitreous State Laboratory, The Catholic University of America, Washington, D.C.

Muller, IS, K Gilbo, I Joseph, and IL Pegg. 2014. *Enhanced LAW Glass Property-Composition Models—Phase 1*. VSL-13R2940-1, Vitreous State Laboratory, The Catholic University of America, Washington, DC.

Muller, I S, E Rielley, IL Pegg, M Chaudhuri, ST Lai, C Mooers, G Bazemore, K Hight, and R Cecil. 2003. *Final Report: LAW Glass Formulation to Support Melter Runs with Simulants*, VSL-03R3460-2, Rev. 0, Vitreous State Laboratory, The Catholic University of America, Washington, D.C.

NQAP-2012. *Nuclear Quality Assurance Program (NQAP) Manual*. PNNL-SA-115260, Pacific Northwest National Laboratory, Richland, Washington.

Piepel GF, SK Cooley, IS Muller, H Gan, I Joseph, and IL Pegg. 2007. *ILAW PCT, VHT, Viscosity, and Electrical Conductivity Model Development*. VSL-07R1230-1, Rev. 0, Vitreous State Laboratory, The Catholic University of America, Washington, D.C.

Rieck BT. 2018. *ILAW Product Qualification Report – Waste Forming Testing*. 24590-LAW-RPT-PENG-17-008-05, Rev. 1, River Protection Project, Hanford Waste Treatment and Immobilization Plant, Richland, Washington.

Riley BJ, JA Rosaria, and P Hrma. 2001. *Impact of HLW Glass Crystallinity on PCT Response*. PNNL-13491, Pacific Northwest National Laboratory, Richland, WA.

Russell RL, RL, BP McCarthy, SK Cooley, EA Cordova, SE Sannoh, V Gervasio, MJ Schweiger, JB Lang, CH Skidmore, CE Lonergan, BA Stanfill, JM Meline, and JD Vienna. 2021. *Enhanced Hanford Low-Activity Waste Glass Property Data Development: Phase 2*. PNNL-28838, Rev. 2, Pacific Northwest Laboratory, Richland, Washington.

Skidmore CH, JD Vienna, T Jin, D Kim, BA Stanfill, KM Fox, and AA Kruger. 2019. “Sulfur solubility in low activity waste glass and its correlation to melter tolerance.” *International Journal of Applied Glass Science* (10):558-68.

Vienna JD, A Heredia-Langner, SK Cooley, AE Holmes, DS Kim, and NA Lumetta. 2020. *Glass Property-Composition Models for Support of Hanford WTP LAW Facility Operation*. PNNL-30932, Rev. 0, Pacific Northwest National Laboratory, Richland, Washington.

Vienna JD, A Heredia-Langner, SK Cooley, AE Holmes, DS Kim, and NA Lumetta. 2022. *Glass Property-Composition Models for Support of Hanford WTP LAW Facility Operation*. PNNL-30932, Rev. 2, Pacific Northwest National Laboratory, Richland, Washington.

Vienna JD, DS Kim, IS Muller, GF Piepel, and AA Kruger. 2014. “Toward Understanding the Effect of Low-Activity Waste Glass Composition on Sulfur Solubility.” *Journal of the American Ceramic Society* 97(10):3135-3142.

Vienna JD, P Hrma, A Jiricka, DE Smith, TH Lorier, IA Reamer, and RL Schultz. 2001. *Hanford Immobilized LAW Product Acceptance Testing: Tanks Focus Area Results*. PNNL-13744, Pacific Northwest National Laboratory, Richland, Washington.

Appendix A – LAW Phase 5: Expansion of LAW Glass Composition Boundaries Glass Matrix Target Glass Compositions

The table in this appendix reports the glass target chemical composition in mass fraction. Numbers 1 to 25 correspond to the experimental IDs of the 25 LAW Phase 5 glasses.

Component	LP5-01	LP5-02	LP5-03	LP5-04	LP5-05	LP5-06	LP5-07	LP5-08	LP5-09	LP5-10
Al ₂ O ₃	0.03745	0.035472	0.048702	0.047982	0.041033	0.118763	0.14538	0.134071	0.093909	0.046306
B ₂ O ₃	0.108172	0.067127	0.103485	0.100414	0.089634	0.069805	0.104233	0.094767	0.067566	0.061491
CaO	0.056662	0.116122	0.06494	0.114542	0.071199	0.037091	0.013509	0.007094	0.043265	0.017111
Fe ₂ O ₃	0.009029	0.008892	0.003199	0.001289	0.009575	0.001711	0.000535	0.005149	0.007432	0.004522
K ₂ O	0.048387	0.012705	0.001159	0.036393	0.025353	0.033173	0.021197	0.046155	0.030688	0.032451
MgO	0.00476	0.047681	0.038721	0.00114	0.049547	0.026444	0.039253	0.000643	0.007588	0.043588
Na ₂ O	0.262921	0.259217	0.24384	0.250201	0.238092	0.220283	0.265044	0.268917	0.265139	0.269339
SiO ₂	0.335846	0.345855	0.339661	0.342999	0.344113	0.336142	0.380499	0.345345	0.34338	0.360817
SnO ₂	0.043516	0.005261	0.005921	0.010995	0.036116	0.02983	0.00206	0.038001	0.024538	0.036847
V ₂ O ₅	0.033414	0.029249	0.048447	0.0013	0.054883	0.05491	0.007305	0.003141	0.010315	0.013599
ZnO	0.011564	0.03546	0.001802	0.057124	0.012916	0.003576	0.002271	0.018173	0.055891	0.055544
ZrO ₂	0.000617	0.003066	0.053283	0.005299	0.005583	0.019041	0.006191	0.015286	0.007733	0.041161
Others	0.047663	0.033895	0.046841	0.030323	0.021956	0.049231	0.012524	0.023257	0.042554	0.017224
Sum	1.0000	1.0000	1.0000	1.0000	1.0000	1.0000	1.0000	1.0000	1.0000	1.0000
Others Composition:										
Cl	0.006535	0.004647	0.006422	0.004157	0.00301	0.00675	0.001717	0.003189	0.005834	0.002361
Cr ₂ O ₃	0.003951	0.00281	0.003883	0.002514	0.00182	0.004081	0.001038	0.001928	0.003528	0.001428
F	0.002607	0.001854	0.002562	0.001659	0.001201	0.002693	0.000685	0.001272	0.002328	0.000942
P ₂ O ₅	0.006268	0.004457	0.00616	0.003988	0.002887	0.006474	0.001647	0.003058	0.005596	0.002265
SO ₃	0.010729	0.00763	0.010544	0.006826	0.004942	0.011082	0.002819	0.005235	0.009579	0.003877
TiO ₂	0.015552	0.01106	0.015284	0.009894	0.007164	0.016064	0.004087	0.007589	0.013885	0.00562
PbO	0.000505	0.000359	0.000497	0.000321	0.000233	0.000522	0.000133	0.000247	0.000451	0.000183
NiO	0.000505	0.000359	0.000497	0.000321	0.000233	0.000522	0.000133	0.000247	0.000451	0.000183
Cs ₂ O	0.000505	0.000359	0.000497	0.000321	0.000233	0.000522	0.000133	0.000247	0.000451	0.000183
Re ₂ O ₇	0.000505	0.000359	0.000497	0.000321	0.000233	0.000522	0.000133	0.000247	0.000451	0.000183

Component	LP5-11	LP5-12	LP5-13	LP5-14	LP5-15	LP5-16	LP5-17	LP5-18	LP5-19	LP5-20
Al ₂ O ₃	0.054993	0.135886	0.044904	0.045144	0.133031	0.079348	0.035601	0.057583	0.038147	0.038772
B ₂ O ₃	0.071367	0.060445	0.128887	0.06675	0.090601	0.062233	0.077387	0.094102	0.104406	0.135126
CaO	0.022851	0.011678	0.000593	0.004388	0.003369	0.087609	0.048121	0.004194	0.064444	0.013672
Fe ₂ O ₃	0.006939	0.005735	0.008518	0.001216	0.009464	0.006312	0.007086	0.005202	0.00042	0.006571
K ₂ O	0.004091	0.022484	0.041909	0.040934	0.048234	0.006391	0.039847	0.018925	0.055781	0.026392
MgO	0.036256	0.049602	0.025996	0.015462	0.019577	0.044639	0.015235	0.050124	0.046216	0.028992
Na ₂ O	0.264513	0.229201	0.264962	0.23661	0.259836	0.251542	0.220208	0.244734	0.22309	0.25484
SiO ₂	0.363057	0.34009	0.340903	0.385743	0.337014	0.335351	0.337497	0.390803	0.345709	0.388061
SnO ₂	0.015936	0.01393	0.007847	0.034321	0.003974	0.041945	0.04211	0.001886	0.015348	0.037299
V ₂ O ₅	0.056681	0.031534	0.045642	0.042491	0.02568	0.007977	0.051505	0.036178	0.013108	0.002114
ZnO	0.042626	0.023055	0.016486	0.044021	0.000171	0.00345	0.056849	0.056825	0.053772	0.004715
ZrO ₂	0.0126	0.027687	0.041798	0.034239	0.055104	0.031763	0.050155	0.001611	0.015482	0.015627
Others	0.048089	0.048673	0.031555	0.048681	0.013945	0.04144	0.0184	0.037832	0.024076	0.047818
Sum	1.0000	1.0000	1.0000	1.0000	1.0000	1.0000	1.0000	1.0000	1.0000	1.0000
Others Composition:										
Cl	0.006593	0.006673	0.004326	0.006674	0.001912	0.005681	0.002523	0.005187	0.003301	0.006556
Cr ₂ O ₃	0.003987	0.004035	0.002616	0.004036	0.001156	0.003435	0.001525	0.003136	0.001996	0.003964
F	0.00263	0.002662	0.001726	0.002663	0.000763	0.002267	0.001006	0.002069	0.001317	0.002616
P ₂ O ₅	0.006324	0.006401	0.00415	0.006402	0.001834	0.005449	0.00242	0.004975	0.003166	0.006288
SO ₃	0.010825	0.010956	0.007103	0.010958	0.003139	0.009328	0.004142	0.008516	0.00542	0.010764
TiO ₂	0.015691	0.015882	0.010296	0.015885	0.00455	0.013522	0.006004	0.012344	0.007856	0.015603
PbO	0.00051	0.000516	0.000334	0.000516	0.000148	0.000439	0.000195	0.000401	0.000255	0.000507
NiO	0.00051	0.000516	0.000334	0.000516	0.000148	0.000439	0.000195	0.000401	0.000255	0.000507
Cs ₂ O	0.00051	0.000516	0.000334	0.000516	0.000148	0.000439	0.000195	0.000401	0.000255	0.000507
Re ₂ O ₇	0.00051	0.000516	0.000334	0.000516	0.000148	0.000439	0.000195	0.000401	0.000255	0.000507

Component	LP5-21	LP5-22	LP5-23	LP5-24	LP5-25
Al ₂ O ₃	0.058621	0.03706	0.038424	0.10000	0.06072
B ₂ O ₃	0.131683	0.126041	0.063678	0.09500	0.1005
CaO	0.047275	0.00314	0.062957	0.05000	0.05107
Fe ₂ O ₃	0.001066	0.007427	0.001562	0.00600	0.05423
K ₂ O	0.046163	0.00325	0.017407	0.01000	0.00083
Li ₂ O	-	-	-	-	0.0251
MgO	0.029667	0.046616	0.023504	0.00650	0.01513
Na ₂ O	0.221365	0.24653	0.2377	0.23000	0.1440
SiO ₂	0.350241	0.479942	0.489759	0.38800	0.46615
SnO ₂	0.012283	0.010561	0.013775	0.01500	-
V ₂ O ₅	0.034014	0.006253	0.027188	0.01000	-
ZnO	0.015128	0.000641	0.004368	0.02800	0.03069
ZrO ₂	0.007656	0.017821	0.003918	0.04000	0.03026
Others	0.044837	0.014719	0.01576	0.02150	0.03026 ^a
Sum	1.0000	1.0000	1.0000	1.0000	0.99999
Others Composition:					
Cl	0.006147	0.002018	0.002161	0.00208	0.00048
Cr ₂ O ₃	0.003717	0.00122	0.001306	0.00450	0.00012
F	0.002453	0.000805	0.000862	0.00316	0.00336
P ₂ O ₅	0.005896	0.001936	0.002072	0.00676	0.00067
SO ₃	0.010093	0.003313	0.003548	0.00500	0.00321
TiO ₂	0.01463	0.004803	0.005142	0.00000	0.01143
PbO	0.000475	0.000156	0.000167	0.00000	0.00000
NiO	0.000475	0.000156	0.000167	0.00000	0.00026
Cs ₂ O	0.000475	0.000156	0.000167	0.00000	0.00000
Re ₂ O ₇	0.000475	0.000156	0.000167	0.00000	0.00100
(a) Others also include (mass fraction): Br = 0.00048, CdO = 0.00003, MoO ₃ = 0.00002, WO ₃ = 0.00009					

Appendix B – LAW Phase 6: High PCT and VHT Response Glass Matrix Target Glass Compositions

The tables in this appendix reports the glass target chemical composition in mass fraction. Numbers 1 to 26 correspond to the experimental IDs of the 26 LAW Phase 6 glasses.

Table B1. Targe glass composition (uncorrected). Note that the compositions in this table are from the original design matrix; however due to the impurities of the Zr source in experiment (details see Section 3.1), correction was made and the re-calculated (corrected) target compositions in Table B2 should be used in future molding work.

Task ID (Matrix ID)	LAW-HPVR-01 (18)	LAW-HPVR-02 (10)	LAW-HPVR-03 (5)	LAW-HPVR-04 (1)	LAW-HPVR-05 (13)	LAW-HPVR-06 (8)	LAW-HPVR-07 (21)	LAW-HPVR-08 (12)	LAW-HPVR-09 (9)	LAW-HPVR-10 (23)
Component										
Al ₂ O ₃	0.03786	0.03857	0.0759	0.03713	0.03845	0.03723	0.04263	0.09303	0.04881	0.03549
B ₂ O ₃	0.12503	0.13623	0.09159	0.08556	0.10714	0.13795	0.07071	0.13114	0.13601	0.1228
CaO	0.065	0.07597	0.06296	0.06691	0.06198	0.12582	0.09877	0.06848	0.06122	0.08878
K ₂ O	0.0256	0.04015	0.05627	0.01609	0.00818	0.05868	0.04307	0.03656	0.01771	0.02272
Li ₂ O	0.02616	0.00167	0.0286	0.0336	0.0414	0.01273	0.01002	0.03502	0.02826	0.00338
Na ₂ O	0.18216	0.17687	0.16109	0.17173	0.17734	0.15865	0.21043	0.16351	0.19105	0.22842
SiO ₂	0.4007	0.41494	0.36152	0.45901	0.439	0.41012	0.37853	0.35175	0.43473	0.40832
SnO ₂	0.02015	0.02826	0.04004	0.01077	0.00842	0.00149	0.01825	0.01486	0.00352	0.03003
TiO ₂	0.01725	0.01155	0.01085	0.02696	0.00452	0.01002	0.00247	0.02574	0.02919	0.00049
V ₂ O ₅	0.03258	0.03567	0.03311	0.03766	0.01822	0.00421	0.03969	0.00731	0.0113	0.0178
ZrO ₂	0.0564	0.02116	0.06291	0.02162	0.06414	0.02927	0.06593	0.05413	0.02266	0.027
Others	0.01111	0.01896	0.01516	0.03296	0.03121	0.01383	0.0195	0.01847	0.01554	0.01477
Sum	1.00000	1.00000	1.00000	1.00000	1.00000	1.00000	1.00000	1.00000	1.00000	1.00000
Others Composition:										
Cl	0.00035	0.0006	0.00048	0.00104	0.00098	0.00044	0.00061	0.00058	0.00049	0.00047
Cr ₂ O ₃	0.0006	0.00102	0.00082	0.00178	0.00169	0.00075	0.00105	0.001	0.00084	0.0008
F	0.0007	0.0012	0.00096	0.00208	0.00197	0.00087	0.00123	0.00116	0.00098	0.00093
Fe ₂ O ₃	0.0008	0.00137	0.00109	0.00238	0.00225	0.001	0.00141	0.00133	0.00112	0.00106
MgO	0.0001	0.00017	0.00014	0.0003	0.00028	0.00012	0.00018	0.00017	0.00014	0.00013
P ₂ O ₅	0.0026	0.00444	0.00355	0.00772	0.00731	0.00324	0.00457	0.00433	0.00364	0.00346
SO ₃	0.00346	0.00589	0.00471	0.01024	0.0097	0.0043	0.00606	0.00574	0.00483	0.00459
ZnO	0.0025	0.00427	0.00341	0.00742	0.00703	0.00311	0.00439	0.00416	0.0035	0.00333

Task ID	LAW-HPVR-11 (11)	LAW-HPVR-12 (7)	LAW-HPVR-13 (6)	LAW-HPVR-14 (16)	LAW-HPVR-15 (3)	LAW-HPVR-16 (22)	LAW-HPVR-17 (14)	LAW-HPVR-18 (4)	LAW-HPVR-19 (24)	LAW-HPVR-20 (17)
Component										
Al ₂ O ₃	0.04017	0.04442	0.03568	0.05769	0.04436	0.06535	0.08223	0.04278	0.05187	0.03507
B ₂ O ₃	0.11038	0.06157	0.06829	0.10965	0.10649	0.12155	0.13566	0.12966	0.09611	0.11885
CaO	0.06063	0.07413	0.06595	0.09116	0.06055	0.06169	0.08737	0.08401	0.08699	0.06246
K ₂ O	0.04225	0.0009	0.03908	0.00138	0.05057	0.02766	0.0509	0.01146	0.00382	0.00006
Li ₂ O	0.00506	0.01811	0.01934	0.0023	0.03107	0.01221	0.01587	0.02799	0.01948	0.00245
Na ₂ O	0.2232	0.23069	0.16905	0.26281	0.15796	0.19938	0.17713	0.1625	0.21445	0.25378
SiO ₂	0.35424	0.48005	0.49033	0.35103	0.45956	0.38232	0.37825	0.39475	0.44127	0.43403
SnO ₂	0.03385	0.02053	0.00591	0.04209	0.0364	0.03935	0.00797	0.04284	0.00392	0.00307
TiO ₂	0.02818	0.01068	0.00085	0.0147	0.00096	0.00945	0.00204	0.00533	0.00888	0.01626
V ₂ O ₅	0.02529	0.01858	0.02228	0.00064	0.0056	0.00925	0.00693	0.03734	0.03999	0.01528
ZrO ₂	0.06548	0.02882	0.06148	0.05159	0.03377	0.04937	0.02636	0.0308	0.02064	0.03098
Others	0.01127	0.01152	0.02176	0.01496	0.01271	0.02242	0.02929	0.03054	0.01258	0.02771
Sum	1.00000	1.00000	1.00000	1.00000	1.00000	1.00000	1.00000	1.00000	1.00000	1.00000
Others Composition:										
Cl	0.00036	0.00036	0.00069	0.00047	0.0004	0.00071	0.00092	0.00096	0.0004	0.00087
Cr ₂ O ₃	0.00061	0.00062	0.00118	0.00081	0.00069	0.00121	0.00158	0.00165	0.00068	0.0015
F	0.00071	0.00073	0.00137	0.00094	0.0008	0.00141	0.00185	0.00193	0.00079	0.00175
Fe ₂ O ₃	0.00081	0.00083	0.00157	0.00108	0.00092	0.00162	0.00211	0.0022	0.00091	0.002
MgO	0.0001	0.0001	0.0002	0.00013	0.00011	0.0002	0.00026	0.00028	0.00011	0.00025
P ₂ O ₅	0.00264	0.0027	0.00509	0.00351	0.00298	0.00525	0.00686	0.00715	0.00295	0.00649
SO ₃	0.0035	0.00358	0.00676	0.00465	0.00395	0.00697	0.00911	0.00949	0.00391	0.00861
ZnO	0.00254	0.0026	0.0049	0.00337	0.00286	0.00505	0.0066	0.00688	0.00283	0.00624

Task ID (Matrix ID)	LAW-HPVR-21 (15)	LAW-HPVR-22 (19)	LAW-HPVR-23 (25)	LAW-HPVR-24 (2)	LAW-HPVR-25 (20)	LAW-HPVR-26 (26)
Component						
Al ₂ O ₃	0.0906	0.05805	0.05394	0.03825	0.0358	0.11447
B ₂ O ₃	0.12932	0.07737	0.0714	0.07042	0.06677	0.13656
CaO	0.06033	0.06952	0.07138	0.08081	0.11388	0.06253
K ₂ O	0.05828	0.03578	0.01484	0.05774	0.0201	0.03095
Li ₂ O	0.00086	0.01598	0.00959	0.02919	0.00437	0.03552
Na ₂ O	0.19759	0.203	0.23339	0.15914	0.24689	0.1756
SiO ₂	0.34677	0.35613	0.41049	0.42645	0.39349	0.35542
SnO ₂	0.00166	0.04454	0.03247	0.02404	0.01729	0.01698
TiO ₂	0.02744	0.02987	0.01451	0.02961	0.01897	0.00884
V ₂ O ₅	0.0342	0.03831	0.01367	0.03064	0.00224	0.0029
ZrO ₂	0.02641	0.04446	0.05374	0.0268	0.04694	0.03572
Others	0.02654	0.02699	0.02058	0.02691	0.03326	0.02451
Sum	1.00000	1.00000	1.00000	1.00000	1.00000	1.00000
Others Composition:						
Cl	0.00084	0.00085	0.00065	0.00085	0.00105	0.00077
Cr ₂ O ₃	0.00143	0.00146	0.00111	0.00145	0.0018	0.00132
F	0.00167	0.0017	0.0013	0.0017	0.0021	0.00155
Fe ₂ O ₃	0.00191	0.00195	0.00148	0.00194	0.0024	0.00177
MgO	0.00024	0.00024	0.00019	0.00024	0.0003	0.00022
P ₂ O ₅	0.00622	0.00632	0.00482	0.0063	0.00779	0.00574
SO ₃	0.00825	0.00839	0.0064	0.00837	0.01033	0.00762
ZnO	0.00598	0.00608	0.00463	0.00606	0.00749	0.00552

Table B2. The re-calculated target chemical composition (in mass fraction) of the LAW Phase 6 glasses that used the Zr source chemical with excess Cl.

Task ID	LAW-HPVR-01	LAW-HPVR-02	LAW-HPVR-05	LAW-HPVR-06	LAW-HPVR-07	LAW-HPVR-08	LAW-HPVR-09
Component							
SiO ₂	0.38788	0.40986	0.42310	0.40320	0.36445	0.34093	0.42903
Al ₂ O ₃	0.03665	0.03810	0.03706	0.03660	0.04104	0.09017	0.04817
B ₂ O ₃	0.12103	0.13456	0.10326	0.13562	0.06808	0.12711	0.13423
CaO	0.06292	0.07504	0.05973	0.12370	0.09510	0.06637	0.06042
Cl	0.02044	0.00829	0.02371	0.01103	0.02396	0.01988	0.00872
Cr ₂ O ₃	0.00058	0.00101	0.00163	0.00074	0.00101	0.00097	0.00083
F	0.00068	0.00119	0.00190	0.00086	0.00118	0.00112	0.00097
Fe ₂ O ₃	0.00077	0.00135	0.00217	0.00098	0.00136	0.00129	0.00111
K ₂ O	0.02478	0.03966	0.00788	0.05769	0.04147	0.03544	0.01748
Li ₂ O	0.02532	0.00165	0.03990	0.01252	0.00965	0.03394	0.02789
MgO	0.00010	0.00017	0.00027	0.00012	0.00017	0.00016	0.00014
Na ₂ O	0.17633	0.17470	0.17092	0.15597	0.20260	0.15848	0.18855
P ₂ O ₅	0.00252	0.00439	0.00705	0.00319	0.00440	0.00420	0.00359
SnO ₂	0.01951	0.02791	0.00811	0.00146	0.01757	0.01440	0.00347
SO ₃	0.00335	0.00582	0.00935	0.00423	0.00583	0.00556	0.00477
TiO ₂	0.01670	0.01141	0.00436	0.00985	0.00238	0.02495	0.02881
V ₂ O ₅	0.03154	0.03523	0.01756	0.00414	0.03821	0.00709	0.01115
ZnO	0.00242	0.00422	0.00678	0.00306	0.00423	0.00403	0.00345
ZrO ₂	0.06649	0.02545	0.07528	0.03505	0.07731	0.06389	0.02723
SUM	1.00000	1.00000	1.00000	1.00000	1.00000	1.00000	1.00000

Task ID	LAW-HPVR-10	LAW-HPVR-11	LAW-HPVR-12	LAW-HPVR-13	LAW-HPVR-14	LAW-HPVR-15	LAW-HPVR-16
Component							
SiO ₂	0.40196	0.34115	0.47208	0.47328	0.34073	0.45064	0.37157
Al ₂ O ₃	0.03494	0.03869	0.04368	0.03444	0.05600	0.04350	0.06351
B ₂ O ₃	0.12089	0.10630	0.06055	0.06591	0.10643	0.10442	0.11813
CaO	0.08740	0.05839	0.07290	0.06366	0.08848	0.05937	0.05996
Cl	0.01025	0.02357	0.01079	0.02252	0.01890	0.01259	0.01836
Cr ₂ O ₃	0.00079	0.00059	0.00061	0.00114	0.00079	0.00068	0.00118
F	0.00092	0.00068	0.00072	0.00132	0.00091	0.00078	0.00137
Fe ₂ O ₃	0.00104	0.00078	0.00082	0.00152	0.00105	0.00090	0.00157
K ₂ O	0.02237	0.04069	0.00089	0.03772	0.00134	0.04959	0.02688
Li ₂ O	0.00333	0.00487	0.01781	0.01867	0.00223	0.03047	0.01187
MgO	0.00013	0.00010	0.00010	0.00019	0.00013	0.00011	0.00019
Na ₂ O	0.22486	0.21495	0.22686	0.16317	0.25510	0.15489	0.19377
P ₂ O ₅	0.00341	0.00254	0.00266	0.00491	0.00341	0.00292	0.00510
SnO ₂	0.02956	0.03260	0.02019	0.00570	0.04085	0.03569	0.03824
SO ₃	0.00452	0.00337	0.00352	0.00652	0.00451	0.00387	0.00677
TiO ₂	0.00048	0.02714	0.01050	0.00082	0.01427	0.00094	0.00918
V ₂ O ₅	0.01752	0.02436	0.01827	0.02151	0.00062	0.00549	0.00899
ZnO	0.00328	0.00245	0.00256	0.00473	0.00327	0.00280	0.00491
ZrO ₂	0.03237	0.07680	0.03452	0.07227	0.06098	0.04033	0.05843
SUM	1.00000	1.00000	1.00000	1.00000	1.00000	1.00000	1.00000

Task ID	LAW-HPVR-17	LAW-HPVR-18	LAW-HPVR-19	LAW-HPVR-20	LAW-HPVR-21	LAW-HPVR-22	LAW-HPVR-23
Component							
SiO ₂	0.37250	0.38775	0.43600	0.42629	0.34148	0.34709	0.39796
Al ₂ O ₃	0.08098	0.04202	0.05125	0.03444	0.08922	0.05658	0.05229
B ₂ O ₃	0.13360	0.12736	0.09496	0.11673	0.12735	0.07541	0.06922
CaO	0.08604	0.08252	0.08595	0.06135	0.05941	0.06775	0.06920
Cl	0.01046	0.01208	0.00790	0.01206	0.01040	0.01678	0.01981
Cr ₂ O ₃	0.00156	0.00162	0.00067	0.00147	0.00141	0.00142	0.00108
F	0.00182	0.00190	0.00078	0.00172	0.00164	0.00166	0.00126
Fe ₂ O ₃	0.00208	0.00216	0.00090	0.00196	0.00188	0.00190	0.00143
K ₂ O	0.05013	0.01126	0.00377	0.00006	0.05739	0.03487	0.01439
Li ₂ O	0.01563	0.02749	0.01925	0.00241	0.00085	0.01557	0.00930
MgO	0.00026	0.00028	0.00011	0.00025	0.00024	0.00023	0.00018
Na ₂ O	0.17444	0.15962	0.21189	0.24925	0.19458	0.19784	0.22626
P ₂ O ₅	0.00676	0.00702	0.00291	0.00637	0.00613	0.00616	0.00467
SnO ₂	0.00785	0.04208	0.00387	0.00302	0.00163	0.04341	0.03148
SO ₃	0.00897	0.00932	0.00386	0.00846	0.00812	0.00818	0.00620
TiO ₂	0.00201	0.00524	0.00877	0.01597	0.02702	0.02911	0.01407
V ₂ O ₅	0.00682	0.03668	0.03951	0.01501	0.03368	0.03734	0.01325
ZnO	0.00650	0.00676	0.00280	0.00613	0.00589	0.00593	0.00449
ZrO ₂	0.03161	0.03684	0.02484	0.03706	0.03167	0.05277	0.06345
SUM	1.000001	1.00000	1.00000	1.00000	1.00000	1.00000	1.00000

Task ID	LAW-HPVR-24	LAW-HPVR-25	LAW-HPVR-26
Component			
SiO ₂	0.41986	0.38295	0.34813
Al ₂ O ₃	0.03766	0.03484	0.11212
B ₂ O ₃	0.06933	0.06498	0.13376
CaO	0.07956	0.11083	0.06125
Cl	0.01055	0.01784	0.01364
Cr ₂ O ₃	0.00143	0.00175	0.00129
F	0.00167	0.00204	0.00152
Fe ₂ O ₃	0.00191	0.00234	0.00173
K ₂ O	0.05685	0.01956	0.03032
Li ₂ O	0.02874	0.00425	0.03479
MgO	0.00024	0.00029	0.00022
Na ₂ O	0.15668	0.24028	0.17200
P ₂ O ₅	0.00620	0.00758	0.00562
SnO ₂	0.02367	0.01683	0.01663
SO ₃	0.00824	0.01005	0.00746
TiO ₂	0.02915	0.01846	0.00866
V ₂ O ₅	0.03017	0.00218	0.00284
ZnO	0.00597	0.00729	0.00541
ZrO ₂	0.03213	0.05564	0.04261
SUM	1.00000	1.00000	1.00000

Appendix C – LAW Phase 5: Expansion of LAW Glass Composition Boundaries Glass Matrix Target Modified Glass Compositions

The table in this appendix reports the glass target chemical composition of glasses LP5-06 and LP5-16 before and after composition modification. The modified samples are identified by the suffix -mod1 added to the original sample ID.

Component	LP5-06	LP5-06-mod1	LP5-16	LP5-16-mod1
Al ₂ O ₃	0.118763	0.118763	0.079348	0.0791348
B ₂ O ₃	0.069805	0.079805	0.062233	0.072233
CaO	0.037091	0.037091	0.087609	0.087609
Fe ₂ O ₃	0.001711	0.001711	0.006312	0.006312
K ₂ O	0.033173	0.033173	0.006391	0.006391
MgO	0.026444	0.026444	0.044639	0.044639
Na ₂ O	0.220283	0.220283	0.251542	0.251542
SiO ₂	0.336142	0.336142	0.335351	0.335351
SnO ₂	0.02983	0.029830	0.041945	0.041945
V ₂ O ₅	0.05491	0.054910	0.007977	0.007977
ZnO	0.003576	0.003576	0.00345	0.003450
ZrO ₂	0.019041	0.019041	0.031763	0.031763
Others	0.049231	0.118711	0.04144	0.031438
Sum	1.0000	1.097948	1.0000	0.9998
Others Composition:				
Cl	0.00675	0.005379	0.005681	0.004310
Cr ₂ O ₃	0.004081	0.003252	0.003435	0.002606
F	0.002693	0.002146	0.002267	0.001720
P ₂ O ₅	0.006474	0.005159	0.005449	0.004134
SO ₃	0.011082	0.08831	0.009328	0.007077
TiO ₂	0.016064	0.012801	0.013522	0.010259
PbO	0.000522	0.000416	0.000439	0.0000333
NiO	0.000522	0.000416	0.000439	0.0000333
Cs ₂ O	0.000522	0.000416	0.000439	0.0000333
Re ₂ O ₇	0.000522	0.000416		0.0000333

Appendix D – Morphology/Color of Each Quenched Glass

The photographs in this appendix show each glass after melting in a platinum/rhodium crucible at the melt temperatures and times specified in Section 2.2 of the main report. The LAW Phase 5 glasses are identified as LP5-# and the LAW Phase 6 glasses as LAW-HPVR-#.

D.1 LAW Phase 5: Expansion of LAW Glass Composition Boundaries Glasses



Figure D.1. Glass LP5-01 Morphology after the Second Melt



Figure D.2. Glass LP5-02 Morphology after the Second Melt



Figure D.3. Glass LP5-03 Morphology after the Second Melt



Figure D.4. Glass LP5-04 Morphology after the Second Melt



Figure D.5. Glass LP5-05 Morphology after the Second Melt



Figure D.6. Glass LP5-06-mod1 Morphology after the Third Melt



Figure D.7. Photo of Glass LP5-07 Morphology of the Third Melt



Figure D.8. Photo of Glass LP5-08 Morphology of the Second Melt



Figure D.9. Photo of Glass LP5-09 Morphology of the Second Melt



Figure D.10. Photo of Glass LP5-10 Morphology of the Second Melt



Figure D.11. Photo of Glass LP5-11 Morphology of the Third Melt



Figure D.12. Photo of Glass LP5-12-1 Morphology of the Fifth Melt



Figure D.13. Photo of Glass LP5-13 Morphology after the Second Melt



Figure D.14. Photo of Glass LP5-14 Morphology after the Third Melt



Figure D.15. Photo of Glass LP5-15 Morphology after the Forth Melt



Figure D.16. Photo of Glass LP5-16-mod1 Morphology after the Third Melt



Figure D.17. Photo of Glass LP5-17 Morphology after the Forth Melt



Figure D.18. Photo of Glass LP5-18 Morphology after the Third Melt



Figure D.19. Photo of Glass LP5-19 Morphology after the Second Melt



Figure D.20. Photo of Glass LP5-20 Morphology after the Second Melt



Figure D.21. Photo of Glass LP5-21 Morphology after the Second Melt



Figure D.22. Photo of Glass LP5-22 Morphology after the Second Melt



Figure D.23. Photo of Glass LP5-23 Morphology after the Second Melt



Figure D.24. Photo of Glass LP5-24 Morphology after the Third Melt



Figure D.25. Photo of Glass LP5-25 Morphology after the Third Melt

D.2 LAW Phase 6: High PCT and VHT Response Glass Matrix Glasses



Figure D.26. Photo of Glass LAW-HPVR-01-1 Morphology after the Second Melt



Figure D.27. Photo of Glass LAW-HPVR-02-1 Morphology after the Second Melt



Figure D.28. Photo of Glass LAW-HPVR-03-1 Morphology after the Third Melt



Figure D.29. Photo of Glass LAW-HPVR-04-1 Morphology after the Second Melt



Figure D.30. Photo of Glass LAW-HPVR-05 Morphology after the Second Melt



Figure D.31. Photo of Glass LAW-HPVR-06 Morphology after the Second Melt



Figure D.32. Photo of Glass LAW-HPVR-07 Morphology after the Third Melt



Figure D.33. Photo of Glass LAW-HPVR-08 Morphology after the Second Melt

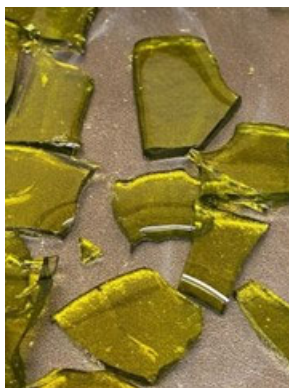


Figure D.34. Photo of Glass LAW-HPVR-09 Morphology after the Second Melt



Figure D.35. Photo of Glass LAW-HPVR-10 Morphology after the Second Melt



Figure D.36. Photo of Glass LAW-HPVR-11 Morphology after the Second Melt



Figure D.37. Photo of Glass LAW-HPVR-12 Morphology after the Second Melt



Figure D.38. Photo of Glass LAW-HPVR-13 Morphology after the Third Melt



Figure D.39. Photo of Glass LAW-HPVR-14 Morphology after the Second Melt



Figure D.40. Photo of Glass LAW-HPVR-15 Morphology after the Second Melt



Figure D.41. Photo of Glass LAW-HPVR-16 Morphology after the Second Melt



Figure D.42. Photo of Glass LAW-HPVR-17 Morphology after the Second Melt



Figure D.43. Photo of Glass LAW-HPVR-18 Morphology after the Second Melt



Figure D.44. Photo of Glass LAW-HPVR-19 Morphology after the Second Melt



Figure D.45. Photo of Glass LAW-HPVR-20 Morphology after the Second Melt



Figure D.46. Photo of Glass LAW-HPVR-21 Morphology after the Second Melt



Figure D.47. Photo of Glass LAW-HPVR-22 Morphology after the Third Melt



Figure D.48. Photo of Glass LAW-HPVR-23 Morphology after the Second Melt



Figure D.49. Photo of Glass LAW-HPVR-24 Morphology after the Second Melt



Figure D.50. Photo of Glass LAW-HPVR-25 Morphology after the Third Melt



Figure D.51. Photo of Glass LAW-HPVR-26 Morphology after the Second Melt

Appendix E – Comparison Measured and Target Chemical Compositions

This section compares the targeted glass compositions with the analyzed glass compositions and their percent differences. Table E.1 reports the data from the LAW Phase 5 (glasses identified as LP5-#) and

Table E.2 reports the data from the LAW Phase 6 (glasses identified as LAW-HPVR-#). The measured sums of oxides for all glasses fall within the interval of 95 to 102 wt %, indicating acceptable recovery of the glass components. Percent differences of components with targeted concentrations of 1 wt% or more are reported.

Table E.1. Targeted vs. Measured Composition (mass fraction) for the LAW Phase 5 Glasses. Only the relative differences between the measured and targeted values for the analytes with measured and targeted values above 1 wt% are reported in the table.

Oxide	LP5-01			LP5-02			LP5-03		
	Measured (wt%)	Target (wt%)	% Difference	Measured (wt%)	Target (wt%)	% Difference	Measured (wt%)	Target (wt%)	% Difference
			Measured vs. Target			Measured vs. Target			Measured vs. Target
Al ₂ O ₃	3.81	3.74	2%	3.45	3.55	-3%	4.78	4.87	-2%
B ₂ O ₃	11.3	10.8	4%	6.76	6.71	1%	10.4	10.4	1%
CaO	5.92	5.67	4%	11.7	11.6	1%	6.59	6.49	2%
Cl	0.555	0.65		0.356	0.46		0.519	0.64	
Cr ₂ O ₃	0.362	0.4		0.253	0.28		0.363	0.39	
F	0.223	0.26		0.148	0.19		0.224	0.26	
Fe ₂ O ₃	0.832	0.9		0.815	0.89		0.345	0.32	
K ₂ O	4.9	4.84	1%	1.29	1.27	1%	0.141	0.12	
Li ₂ O	<0.215	0		<0.215	0		<0.215	0	
MgO	0.493	0.48		4.8	4.77	1%	3.83	3.87	-1%
Na ₂ O	25.5	26.3	-3%	25	25.9	-3%	24.7	24.4	1%
NiO	<0.127	0.05		<0.127	0.04		<0.127	0.05	
P ₂ O ₅	0.58	0.63		0.4	0.45		0.537	0.62	
PbO	<0.108	0.05		<0.108	0.04		<0.108	0.05	
Re ₂ O ₇	<0.0325	0.05		<0.0325	0.04		<0.0325	0.05	
SiO ₂	34.5	33.6	3%	35.1	34.6	1%	34.1	34	0%
SnO ₂	4.25	4.35	-2%	0.475	0.53		0.62	0.59	
SO ₃	1.04	1.07	-3%	0.774	0.76		1.05	1.05	0%
TiO ₂	1.48	1.56	-5%	1.05	1.11	-5%	1.49	1.53	-2%
V ₂ O ₅	3.36	3.34	1%	2.94	2.92	1%	4.78	4.84	-1%
ZnO	1.17	1.16	0%	3.5	3.55	-1%	0.196	0.18	
ZrO ₂	<0.135	0.06		0.296	0.31		5.12	5.33	-4%
Sum of Oxides	101	100	1%	99.6	100	0%	100	100	0%

Table E.1. (continued)

Oxide	LP5-04			LP5-05			LP5-06-MOD1		
	Measured (wt%)	Target (wt%)	% Difference Measured vs. Target	Measured (wt%)	Target (wt%)	% Difference Measured vs. Target	Measured (wt%)	Target (wt%)	% Difference Measured vs. Target
Al ₂ O ₃	4.65	4.8	-3%	4.01	4.1	-2%	11.8	11.9	-1%
B ₂ O ₃	10.3	10	2%	8.99	8.96	0%	8.36	7.98	5%
CaO	11.4	11.5	-1%	7.1	7.12	0%	3.82	3.71	3%
Cl	0.319	0.42		0.25	0.3		0.285	0.538	
Cr ₂ O ₃	0.233	0.25		0.17	0.18		0.3	0.325	
F	0.132	0.17		0.101	0.12		0.176	0.215	
Fe ₂ O ₃	<0.147	0.13		0.903	0.96		0.181	0.17	
K ₂ O	3.54	3.64	-3%	2.47	2.54	-3%	3.29	3.32	-1%
Li ₂ O	<0.215	0		<0.215	0		<0.251	0	
MgO	0.21	0.11		4.93	4.95	0%	2.66	2.64	1%
Na ₂ O	24.6	25	-1%	23.1	23.8	-3%	22.2	22	1%
NiO	<0.127	0.03		<0.127	0.02		<0.127	0.0416	
P ₂ O ₅	0.357	0.4		0.265	0.29		0.415	0.516	
PbO	<0.108	0.03		<0.108	0.02		<0.108	0.0416	
Re ₂ O ₇	<0.0325	0.03		<0.0325	0.02		<0.0325	0.0416	
SiO ₂	35.5	34.3	4%	34.6	34.4	1%	35.4	33.6	5%
SnO ₂	1.05	1.1	-5%	3.54	3.61	-2%	2.89	2.98	-3%
SO ₃	0.669	0.68		0.534	0.49		0.811	0.883	
TiO ₂	0.972	0.99		0.703	0.72		1.24	1.28	-3%
V ₂ O ₅	<0.179	0.13		5.44	5.49	-1%	5.5	5.49	0%
ZnO	5.92	5.71	4%	1.27	1.29	-2%	0.367	0.36	
ZrO ₂	0.5	0.53		0.507	0.56		1.78	1.9	-6%
Sum of Oxides	101	99.9	1%	99.4	99.9	-1%	102	99.9	2%

Table E.1. (continued)

Oxide	LP5-07	LP5-08	LP5-09
-------	--------	--------	--------

	% Difference Measured vs. Target			% Difference Measured vs. Target			% Difference Measured vs. Target		
	Measured (wt%)	Target (wt%)	% Difference	Measured (wt%)	Target (wt%)	% Difference	Measured (wt%)	Target (wt%)	% Difference
Al ₂ O ₃	13.9	14.5	-4%	13.5	13.4	1%	9.11	9.39	-3%
B ₂ O ₃	10.4	10.4	0%	9.84	9.48	4%	6.79	6.76	0%
CaO	1.32	1.35	-2%	0.745	0.71		4.44	4.33	2%
Cl	0.153	0.17		0.282	0.32		0.476	0.58	
Cr ₂ O ₃	0.159	0.1		0.179	0.19		0.323	0.35	
F	0.0565	0.07		0.116	0.13		0.206	0.23	
Fe ₂ O ₃	<0.143	0.05		0.508	0.51		0.689	0.74	
K ₂ O	2.07	2.12	-2%	4.84	4.62	5%	3.1	3.07	1%
Li ₂ O	<0.215	0		<0.215	0		<0.215	0	
MgO	4.16	3.93	6%	<0.166	0.06		0.749	0.76	
Na ₂ O	25.1	26.5	-5%	27.1	26.9	1%	25.8	26.5	-2%
NiO	<0.265	0.01		<0.127	0.02		<0.127	0.05	
P ₂ O ₅	<0.229	0.16		0.268	0.31		0.485	0.56	
PbO	<0.108	0.01		<0.108	0.02		<0.108	0.05	
Re ₂ O ₇	<0.0325	0.01		<0.0325	0.02		<0.0325	0.05	
SiO ₂	38.6	38.1	1%	35.6	34.5	3%	35	34.3	2%
SnO ₂	0.206	0.21		3.85	3.8	1%	2.39	2.45	-2%
SO ₃	0.333	0.28		0.512	0.52		0.93	0.96	
TiO ₂	0.445	0.41		0.769	0.76		1.34	1.39	-3%
V ₂ O ₅	0.744	0.73		0.319	0.31		0.993	1.03	-4%
ZnO	0.222	0.23		1.83	1.82	1%	5.53	5.59	-1%
ZrO ₂	0.574	0.62		1.47	1.53	-4%	0.736	0.77	
Sum of Oxides	99.4	100	-1%	102	99.9	2%	99.6	99.9	0%

Table E.1. (continued)

Oxide	LP5-10			LP5-11			LP5-12-1		
	Measured (wt%)	Target (wt%)	% Difference	Measured (wt%)	% Difference	Measured (wt%)	% Difference		

	Measured vs.			Measured vs.			Measured vs.		
	Measured (wt%)	Target (wt%)	% Difference	Measured (wt%)	Target (wt%)	% Difference	Measured (wt%)	Target (wt%)	% Difference
Al ₂ O ₃	4.64	4.63	0%	5.42	5.5	-1%	13.4	13.6	-2%
B ₂ O ₃	6.29	6.15	2%	7.13	7.14	0%	5.88	6.04	-3%
CaO	1.87	1.71	10%	2.39	2.29	4%	1.34	1.17	15%
Cl	0.176	0.24		0.508	0.66		0.125	0.67	
Cr ₂ O ₃	0.135	0.14		0.387	0.4		0.377	0.4	
F	0.0848	0.09		0.225	0.26		0.211	0.27	
Fe ₂ O ₃	0.453	0.45		0.669	0.69		0.582	0.57	
K ₂ O	3.1	3.25	-5%	0.445	0.41		2	2.25	-11%
Li ₂ O	<0.215	0		<0.215	0		<0.215	0	
MgO	4.52	4.36	4%	3.66	3.63	1%	5.24	4.96	6%
Na ₂ O	26.4	26.9	-2%	25.8	26.5	-3%	23.1	22.9	1%
NiO	<0.127	0.02		<0.127	0.05		<0.127	0.05	
P ₂ O ₅	<0.229	0.23		0.525	0.63		0.579	0.64	
PbO	<0.108	0.02		<0.108	0.05		<0.108	0.05	
Re ₂ O ₇	<0.0325	0.02		<0.0325	0.05		<0.0325	0.05	
SiO ₂	36.4	36.1	1%	36.8	36.3	1%	35.1	34	3%
SnO ₂	3.77	3.68	3%	1.58	1.59	-1%	1.49	1.39	7%
SO ₃	0.443	0.39		1.07	1.08	-1%	0.664	1.1	-40%
TiO ₂	0.581	0.56		1.52	1.57	-3%	1.67	1.59	5%
V ₂ O ₅	1.37	1.36	1%	5.69	5.67	0%	3.28	3.15	4%
ZnO	5.5	5.55	-1%	4.19	4.26	-2%	2.29	2.31	-1%
ZrO ₂	3.71	4.12	-10%	1.18	1.26	-7%	2.63	2.77	-5%
Sum of Oxides	100	100	0%	99.7	100	0%	100	99.9	1%

Table E.1. (continued)

Oxide	LP5-13			LP5-14			LP5-15		
	Measured (wt%)	Target (wt%)	% Difference Measured vs. Target	Measured (wt%)	Target (wt%)	% Difference Measured vs. Target	Measured (wt%)	Target (wt%)	% Difference Measured vs. Target

Al ₂ O ₃	4.54	4.49	1%	4.45	4.51	-1%	12.9	13.3	-3%
B ₂ O ₃	13.1	12.9	1%	6.62	6.68	-1%	9.49	9.06	5%
CaO	0.259	0.06		0.591	0.44		0.357	0.34	
Cl	0.343	0.43		0.483	0.67		1.11	0.19	482%
Cr ₂ O ₃	0.252	0.26		0.389	0.4		0.074	0.12	
F	0.144	0.17		0.223	0.27		0.0649	0.08	
Fe ₂ O ₃	0.83	0.85		<0.143	0.12		0.879	0.95	
K ₂ O	3.94	4.19	-6%	3.75	4.09	-8%	4.4	4.82	-9%
Li ₂ O	<0.215	0		<0.215	0		<0.215	0	
MgO	2.69	2.6	3%	1.63	1.55	5%	1.99	1.96	2%
Na ₂ O	26	26.5	-2%	23.4	23.7	-1%	25.2	26	-3%
NiO	<0.127	0.03		<0.127	0.05		<0.127	0.01	
P ₂ O ₅	0.385	0.41		0.581	0.64		<0.229	0.18	
PbO	<0.108	0.03		<0.108	0.05		<0.108	0.01	
Re ₂ O ₇	<0.0325	0.03		<0.0325	0.05		<0.0325	0.01	
SiO ₂	34.2	34.1	0%	38.9	38.6	1%	35.8	33.7	6%
SnO ₂	0.767	0.78		3.54	3.43	3%	0.377	0.4	
SO ₃	0.744	0.71		1.12	1.1	2%	0.24	0.31	
TiO ₂	1.04	1.03	1%	1.57	1.59	-1%	0.461	0.46	
V ₂ O ₅	4.62	4.56	1%	4.33	4.25	2%	2.56	2.57	0%
ZnO	1.63	1.65	-1%	4.31	4.4	-2%	<0.124	0.02	
ZrO ₂	3.86	4.18	-8%	3.19	3.42	-7%	5.18	5.51	-6%
Sum of Oxides	99.8	100	0%	99.7	100	0%	102	100	2%

Table E.1. (continued)

Oxide	LP5-16-MOD1			LP5-17			LP5-18		
	Measured (wt%)	Target (wt%)	% Difference Measured vs. Target	Measured (wt%)	Target (wt%)	% Difference Measured vs. Target	Measured (wt%)	Target (wt%)	% Difference Measured vs. Target
Al ₂ O ₃	8.09	7.93	2%	3.55	3.56	0%	5.74	5.76	0%
B ₂ O ₃	7.43	7.22	3%	7.74	7.74	0%	9.57	9.41	2%
CaO	8.56	8.76	-2%	4.97	4.81	3%	0.487	0.42	
Cl	0.369	0.431		0.825	0.25	230%	0.395	0.52	
Cr ₂ O ₃	0.275	0.261		0.142	0.15		0.316	0.31	
F	0.129	0.172		0.0845	0.1		0.174	0.21	
Fe ₂ O ₃	0.637	0.63		0.692	0.71		0.592	0.52	
K ₂ O	0.552	0.64		3.44	3.98	-14%	1.8	1.89	-5%
Li ₂ O	<0.215	0		<0.215	0		<0.215	0	
MgO	4.71	4.46	6%	1.53	1.52	1%	5.2	5.01	4%
Na ₂ O	24.1	25.2	-5%	20.9	22	-5%	23.9	24.5	-2%
NiO	0.179	0.0333		<0.127	0.02		<0.127	0.04	
P ₂ O ₅	0.373	0.413		<0.231	0.24		0.483	0.5	
PbO	<0.108	0.0333		<0.108	0.02		<0.108	0.04	
Re ₂ O ₇	<0.0325	0.0333		<0.0325	0.02		<0.0325	0.04	
SiO ₂	34.7	33.5	4%	35	33.8	4%	39.5	39.1	1%
SnO ₂	4.27	4.19	2%	4.27	4.21	1%	0.256	0.19	
SO ₃	0.616	0.708		0.404	0.41		0.903	0.85	
TiO ₂	1.04	1.03	1%	0.595	0.6		1.25	1.23	1%
V ₂ O ₅	0.806	0.8		5.25	5.15	2%	3.69	3.62	2%
ZnO	0.35	0.35		5.72	5.68	1%	5.79	5.68	2%
ZrO ₂	3.01	3.18	-5%	4.73	5.02	-6%	0.167	0.16	
Sum of Oxides	101	100	1%	101	100	1%	101	100	1%

Table E.1. (continued)

Oxide	LP5-19			LP5-20			LP5-21		
	Measured (wt%)	Target (wt%)	% Difference Measured vs. Target	Measured (wt%)	Target (wt%)	% Difference Measured vs. Target	Measured (wt%)	Target (wt%)	% Difference Measured vs. Target
Al ₂ O ₃	3.75	3.81	-2%	4.06	3.88	5%	5.92	5.86	1%
B ₂ O ₃	10.5	10.4	0%	14.2	13.5	5%	13.6	13.2	3%
CaO	6.71	6.44	4%	1.43	1.37	4%	4.87	4.73	3%
Cl	0.246	0.33		0.6	0.66		0.491	0.61	
Cr ₂ O ₃	0.179	0.2		0.389	0.4		0.352	0.37	
F	0.11	0.13		0.227	0.26		0.2	0.25	
Fe ₂ O ₃	<0.143	0.04		0.657	0.66		<0.143	0.11	
K ₂ O	5.65	5.58	1%	2.5	2.64	-5%	4.44	4.62	-4%
Li ₂ O	<0.215	0		<0.215	0		<0.215	0	
MgO	4.6	4.62	0%	3.03	2.9	5%	2.97	2.97	0%
Na ₂ O	22.2	22.3	0%	24.9	25.5	-2%	21.8	22.1	-1%
NiO	<0.127	0.03		<0.127	0.05		<0.127	0.05	
P ₂ O ₅	0.272	0.32		0.572	0.63		0.53	0.59	
PbO	<0.108	0.03		<0.108	0.05		<0.108	0.05	
Re ₂ O ₇	<0.0325	0.03		<0.0325	0.05		<0.0325	0.05	
SiO ₂	35.2	34.6	2%	39.8	38.8	3%	35.6	35	2%
SnO ₂	1.49	1.53	-2%	3.82	3.73	2%	1.17	1.23	-5%
SO ₃	0.578	0.54		1.12	1.08	4%	0.998	1.01	-1%
TiO ₂	0.753	0.79		1.56	1.56	0%	1.43	1.46	-2%
V ₂ O ₅	1.25	1.31	-4%	0.221	0.21		3.39	3.4	0%
ZnO	5.3	5.38	-1%	0.478	0.47		1.52	1.51	1%
ZrO ₂	1.46	1.55	-6%	1.51	1.56	-3%	0.736	0.77	
Sum of Oxides	101	100	1%	102	100	2%	101	99.9	1%

Table E.1. (continued)

Oxide	LP5-22			LP5-23			LP5-24		
	Measured (wt%)	Target (wt%)	% Difference Measured vs. Target	Measured (wt%)	Target (wt%)	% Difference Measured vs. Target	Measured (wt%)	Target (wt%)	% Difference Measured vs. Target
Al ₂ O ₃	3.66	3.71	-1%	3.71	3.84	-3%	9.71	10	-3%
B ₂ O ₃	12.7	12.6	1%	6.41	6.37	1%	9.53	9.5	0%
CaO	0.414	0.31		6.37	6.3	1%	5.14	5	3%
Cl	0.169	0.2		0.19	0.22		1.06	0.21	406%
Cr ₂ O ₃	0.109	0.12		0.119	0.13		0.378	0.45	
F	0.0646	0.08		0.0703	0.09		0.27	0.32	
Fe ₂ O ₃	0.687	0.74		0.174	0.16		0.575	0.6	
K ₂ O	0.401	0.32		1.79	1.74	3%	1.03	1	3%
Li ₂ O	<0.215	0		<0.215	0		<0.215	0	
MgO	4.53	4.66	-3%	2.36	2.35	1%	0.664	0.65	
Na ₂ O	24.5	24.7	-1%	24.1	23.8	1%	22.4	23	-3%
NiO	<0.127	0.02		<0.127	0.02		<0.127	0	
P ₂ O ₅	<0.229	0.19		<0.229	0.21		0.569	0.68	
PbO	<0.108	0.02		<0.108	0.02		<0.108	0	
Re ₂ O ₇	<0.0325	0.02		<0.0325	0.02		<0.0325	0	
SiO ₂	48.7	48	2%	49.1	49	0%	39.3	38.8	1%
SnO ₂	0.973	1.06	-8%	1.36	1.38	-2%	1.48	1.5	-1%
SO ₃	0.365	0.33		0.371	0.35		0.396	0.5	
TiO ₂	0.466	0.48		0.505	0.51		<0.167	0	
V ₂ O ₅	0.608	0.63		2.7	2.72	-1%	0.977	1	-2%
ZnO	<0.124	0.06		0.453	0.44		2.82	2.8	1%
ZrO ₂	1.65	1.78	-7%	0.37	0.39		3.7	4	-8%
Sum of Oxides	101	100	1%	101	100	1%	101	100	1%

Table E.1. (continued)

Oxide	LP5-25		% Difference
	Measured (wt%)	Target (wt%)	Measured vs. Target
Al ₂ O ₃	6.11	6.07	1%
B ₂ O ₃	10.4	10.1	3%
CaO	5.25	5.11	3%
Cl	0.0307	0.05	
Cr ₂ O ₃	<0.0365	0.01	
F	0.241	0.34	
Fe ₂ O ₃	5.13	5.42	-5%
K ₂ O	<0.122	0.08	
Li ₂ O	2.06	2.51	-18%
MgO	1.45	1.51	-4%
Na ₂ O	14.4	14.4	0%
NiO	<0.127	0.026	
P ₂ O ₅	<0.229	0.07	
PbO	<0.108	0.01	
Re ₂ O ₇	<0.0325	0.1	
SiO ₂	47.8	46.6	2%
SnO ₂	<0.127	0	
SO ₃	0.182	0.32	
TiO ₂	1.09	1.14	-4%
V ₂ O ₅	<0.179	0	
ZnO	3.06	3.07	0%
ZrO ₂	2.86	3.03	-6%
Sum of Oxides	101	99.9	1%

Table E.2. Targeted vs. Measured Composition (mass fraction) for the LAW Phase 6 Glasses. Only the relative differences between the measured and targeted values for the analytes with measured and targeted values above 1 wt% are reported in the table. Note that the corrected target wt% of Cl may still have large errors due to relatively low Cl as impurity in the Zr source. Therefore, the target vs. measured Cl wt% should not be used in the future calculation of volatile loss of C.

Oxide	LAW-HPVR-01-1			LAW-HPVR-02-1			LAW-HPVR-03-1		
	Measured (wt%)	Target (wt%)	% Difference	Measured (wt%)	Target (wt%)	% Difference	Measured (wt%)	Target (wt%)	% Difference
			Measured vs. Target			Measured vs. Target			Measured vs. Target
Al ₂ O ₃	3.68	3.66	0%	3.69	3.81	-3%	7.09	7.59	-7%
B ₂ O ₃	12.3	12.10	2%	13	13.46	-3%	8.58	9.16	-6%
CaO	6.66	6.29	6%	7.43	7.50	-1%	6.58	6.3	4%
Cl	1.41	2.04	-31%	0.659	0.83		0.0779	0.048	
Cr ₂ O ₃	0.055	0.0581		0.101	0.1008		0.0742	0.082	
F	0.0502	0.0678		0.0851	0.1185		0.0821	0.096	
Fe ₂ O ₃	0.133	0.0774		0.154	0.1353		0.115	0.109	
K ₂ O	2.52	2.48	2%	3.78	3.97	-5%	5.07	5.63	-10%
Li ₂ O	2.63	2.53		0.154	0.165		2.62	2.86	-8%
MgO	0.0632	0.010		0.0789	0.017		0.0646	0.014	
Na ₂ O	17.4	17.63	-1%	16.4	17.47	-6%	16	16.1	-1%
P ₂ O ₅	<0.247	0.252		0.385	0.439		0.304	0.355	
SiO ₂	39.5	38.79	2%	39.6	40.99	-3%	34.3	36.2	-5%
SnO ₂	2.15	1.95	10%	2.95	2.79	6%	4.27	4	7%
SO ₃	0.312	0.335		0.504	0.582		0.421	0.471	
TiO ₂	1.71	1.67	2%	1.12	1.14	-2%	1	1.09	-8%
V ₂ O ₅	3.28	3.15	4%	3.49	3.52	-1%	3.35	3.31	1%
ZnO	0.257	0.242		0.423	0.422		0.314	0.341	
ZrO ₂	5.21	6.65	-22%	1.86	2.55	-27%	6.08	6.29	-3%
Sum of Oxides	99.6	100	0%	95.8	100	-4%	96.4	100	-4%

Table E.2 (continued)

Oxide	LAW-HPVR-04-1			LAW-HPVR-05			LAW-HPVR-06		
	Measured (wt%)	Target (wt%)	% Difference Measured vs. Target	Measured (wt%)	Target (wt%)	% Difference Measured vs. Target	Measured (wt%)	Target (wt%)	% Difference Measured vs. Target
Al ₂ O ₃	3.58	3.71	-4%	3.64	3.71	-2%	3.65	3.66	0%
B ₂ O ₃	8.4	8.56	-2%	10.2	10.33	-1%	13.8	13.56	2%
CaO	6.54	6.69	-2%	6.55	5.97	10%	11.9	12.37	-4%
Cl	0.101	0.104		1.35	2.37	-43%	0.778	1.10	-29%
Cr ₂ O ₃	0.175	0.178		0.151	0.1629		0.068	0.0737	
F	0.165	0.208		0.158	0.1899		0.0608	0.0855	
Fe ₂ O ₃	0.249	0.238		0.225	0.2168		0.109	0.0983	
K ₂ O	1.67	1.61	4%	0.795	0.79		5.54	5.77	-4%
Li ₂ O	3.35	3.36	0%	3.76	3.99	-6%	1.28	1.25	2%
MgO	0.0873	0.03		0.0789	0.027		0.101	0.012	
Na ₂ O	16.1	17.2	-6%	16.9	17.09	-1%	15.8	15.60	1%
P ₂ O ₅	0.79	0.772		0.681	0.705		0.296	0.319	
SiO ₂	44.9	45.9	-2%	42	42.31	-1%	41	40.32	2%
SnO ₂	1.11	1.08	3%	0.877	0.811		0.169	0.146	
SO ₃	0.954	1.02	-6%	0.696	0.935		0.394	0.423	
TiO ₂	2.64	2.7	-2%	0.432	0.436		0.944	0.985	
V ₂ O ₅	3.66	3.77	-3%	1.84	1.76	5%	0.402	0.414	
ZnO	0.731	0.742		0.664	0.678		0.3	0.306	
ZrO ₂	2.21	2.16	2%	5.58	7.53	-26%	2.66	3.50	-24%
Sum of Oxides	97.4	100	-3%	96.6	100	-3%	99.2	100	-1%

Table E.2 (continued)

Oxide	LAW-HPVR-07			LAW-HPVR-08			LAW-HPVR-09		
	Measured (wt%)	Target (wt%)	% Difference Measured vs. Target	Measured (wt%)	Target (wt%)	% Difference Measured vs. Target	Measured (wt%)	Target (wt%)	% Difference Measured vs. Target
Al ₂ O ₃	4.35	4.10	6%	9.07	9.02	1%	4.84	4.823	0%
B ₂ O ₃	6.95	6.81	2%	13.3	12.71	5%	13.4	13.42	0%
CaO	9.39	9.51	-1%	6.79	6.64	2%	6.09	6.04	1%
Cl	0.753	2.40	-69%	1.27	1.99	-36%	0.701	0.872	
Cr ₂ O ₃	0.103	0.1011		0.09	0.0969		0.0793	0.083	
F	0.0989	0.1184		0.091	0.1124		0.0794	0.097	
Fe ₂ O ₃	0.16	0.1358		0.137	0.1289		0.12	0.111	
K ₂ O	3.58	4.15	-14%	3.42	3.54	-3%	1.79	1.75	2%
Li ₂ O	1.05	0.9647		3.51	3.39	3%	2.81	2.79	1%
MgO	0.0988	0.017		0.0684	0.016		0.0624	0.014	
Na ₂ O	18.6	20.26	-8%	15.5	15.85	-2%	18.4	18.85	-2%
P ₂ O ₅	0.419	0.440		0.396	0.420		0.338	0.359	
SiO ₂	38	36.44	4%	35.9	34.09	5%	42.9	42.90	0%
SnO ₂	1.92	1.76	9%	1.56	1.44	8%	0.375	0.347	
SO ₃	0.524	0.583		0.465	0.556		0.442	0.477	
TiO ₂	0.257	0.238		2.52	2.49	1%	2.81	2.88	-2%
V ₂ O ₅	3.87	3.82	1%	0.699	0.709		1.08	1.12	-3%
ZnO	0.458	0.423		0.396	0.403		0.331	0.345	
ZrO ₂	6.25	7.73	-19%	4.94	6.39	-23%	2.05	2.72	-25%
Sum of Oxides	96.8	100	-3%	100	100	0%	98.8	100	-1%

Table E.2 (continued)

Oxide	LAW-HPVR-10			LAW-HPVR-11			LAW-HPVR-12		
	Measured (wt%)	Target (wt%)	% Difference Measured vs. Target	Measured (wt%)	Target (wt%)	% Difference Measured vs. Target	Measured (wt%)	Target (wt%)	% Difference Measured vs. Target
Al ₂ O ₃	3.56	3.49	2%	3.82	3.87	-1%	4.22	4.37	-3%
B ₂ O ₃	12.3	12.09	2%	10.5	10.63	-1%	6.07	6.05	0%
CaO	8.62	8.74	-1%	6.37	5.84	9%	7.66	7.29	5%
Cl	0.805	1.02	-21%	1.46	2.36	-38%	0.84	1.08	-22%
Cr ₂ O ₃	0.0767	0.0788		0.0569	0.0587		0.0601	0.0610	
F	0.0712	0.0916		0.0569	0.0684		0.0566	0.0718	
Fe ₂ O ₃	0.118	0.1043		0.0885	0.0780		0.112	0.0816	
K ₂ O	2.29	2.24	2%	3.59	4.07	-12%	0.266	0.09	
Li ₂ O	0.349	0.333		0.474	0.487		1.79	1.78	1%
MgO	0.0785	0.013		0.058	0.010		0.0682	0.010	
Na ₂ O	22.5	22.49	0%	21.7	21.50	1%	22.5	22.69	-1%
P ₂ O ₅	0.324	0.341		<0.233	0.254		<0.258	0.266	
SiO ₂	40.6	40.20	1%	34	34.11	0%	47	47.21	0%
SnO ₂	3.12	2.96	6%	3.69	3.26	13%	2.16	2.02	7%
SO ₃	0.398	0.452		0.345	0.337		0.324	0.352	
TiO ₂	0.0834	0.0482		2.89	2.71	6%	0.989	1.05	-6%
V ₂ O ₅	1.69	1.75	-4%	2.6	2.44	7%	1.87	1.83	2%
ZnO	0.315	0.328		0.239	0.245		0.245	0.256	
ZrO ₂	2.44	3.24	-25%	5.76	7.68	-25%	2.57	3.45	-26%
Sum of Oxides	99.8	100	0%	97.9	100	-2%	99.1	100	-1%

Table E.2 (continued)

Oxide	LAW-HPVR-13			LAW-HPVR-14			LAW-HPVR-15		
	Measured (wt%)	Target (wt%)	% Difference Measured vs. Target	Measured (wt%)	Target (wt%)	% Difference Measured vs. Target	Measured (wt%)	Target (wt%)	% Difference Measured vs. Target
Al ₂ O ₃	3.61	3.57	1%	5.46	5.77	-5%	4.16	4.44	-6%
B ₂ O ₃	6.83	6.83	0%	10.9	11	-1%	10.1	10.6	-5%
CaO	6.91	6.6	5%	9.26	9.12	1%	5.89	6.06	-3%
Cl	1.12	0.069	1527%	1.42	0.047	2911%	0.98	0.04	2350%
Cr ₂ O ₃	0.116	0.118		0.074	0.081		0.07	0.069	
F	0.107	0.137		0.0704	0.094		0.0638	0.08	
Fe ₂ O ₃	0.169	0.157		0.117	0.108		0.11	0.092	
K ₂ O	3.49	3.91	-11%	0.303	0.138		4.57	5.06	-10%
Li ₂ O	1.93	1.93	0%	0.236	0.23		2.9	3.11	-7%
MgO	0.0732	0.02		0.079	0.013		0.062	0.011	
Na ₂ O	16.4	16.9	-3%	25.3	26.3	-4%	14.6	15.8	-8%
P ₂ O ₅	0.485	0.509		0.307	0.351		0.268	0.298	
SiO ₂	48.9	49	0%	34.9	35.1	-1%	43.6	46	-5%
SnO ₂	0.638	0.591		4.43	4.21	5%	3.74	3.64	3%
SO ₃	0.435	0.676		0.414	0.465		0.378	0.395	
TiO ₂	0.0945	0.085		1.34	1.47	-9%	0.108	0.096	
V ₂ O ₅	2.28	2.23	2%	<0.0893	0.064		0.548	0.56	
ZnO	0.471	0.49		0.316	0.337		0.289	0.286	
ZrO ₂	5.54	6.15	-10%	4.53	5.16	-12%	2.95	3.38	-13%
Sum of Oxides	99.6	100	0%	99.5	100	-1%	95.4	100	-5%

Table E.2 (continued)

Oxide	LAW-HPVR-16			LAW-HPVR-17			LAW-HPVR-18		
	Measured (wt%)	Target (wt%)	% Difference Measured vs. Target	Measured (wt%)	Target (wt%)	% Difference Measured vs. Target	Measured (wt%)	Target (wt%)	% Difference Measured vs. Target
Al ₂ O ₃	6.44	6.35	1%	7.7	8.10	-5%	4.03	4.20	-4%
B ₂ O ₃	12	11.81	2%	12.9	13.36	-3%	12.3	12.74	-3%
CaO	6.06	6.00	1%	8.24	8.60	-4%	7.84	8.25	-5%
Cl	1.16	1.84	-37%	0.784	1.05	-25%	0.906	1.21	-25%
Cr ₂ O ₃	0.116	0.1176		0.16	0.1556		0.153	0.1621	
F	0.112	0.1370		0.145	0.1822		0.142	0.1896	
Fe ₂ O ₃	0.182	0.1574		0.222	0.2078		0.215	0.2161	
K ₂ O	2.55	2.69	-5%	4.65	5.01	-7%	1.17	1.13	4%
Li ₂ O	1.25	1.19	5%	1.48	1.56	-5%	2.6	2.75	-5%
MgO	0.0724	0.019		0.0945	0.026		0.0876	0.028	
Na ₂ O	18.4	19.38	-5%	16.2	17.44	-7%	15.3	15.96	-4%
P ₂ O ₅	0.532	0.510		0.597	0.676		0.638	0.702	
SiO ₂	38.3	37.16	3%	36.2	37.25	-3%	37.5	38.78	-3%
SnO ₂	4.11	3.82	7%	0.848	0.785		4.22	4.21	0%
SO ₃	0.557	0.677		0.861	0.897		0.741	0.932	
TiO ₂	0.919	0.918		0.218	0.201		0.495	0.524	
V ₂ O ₅	0.902	0.899		0.684	0.682		3.48	3.67	-5%
ZnO	0.516	0.491		0.661	0.650		0.628	0.676	
ZrO ₂	4.58	5.84	-22%	2.3	3.16	-27%	2.68	3.68	-27%
Sum of Oxides	98.7	100	-1%	95	100	-5%	95.1	100	-5%

Table E.2 (continued)

Oxide	LAW-HPVR-19			LAW-HPVR-20			LAW-HPVR-21		
	Measured (wt%)	Target (wt%)	% Difference Measured vs. Target	Measured (wt%)	Target (wt%)	% Difference Measured vs. Target	Measured (wt%)	Target (wt%)	% Difference Measured vs. Target
Al ₂ O ₃	5.07	5.13	-1%	3.43	3.44	0%	8.4	8.92	-6%
B ₂ O ₃	9.47	9.50	0%	11.8	11.67	1%	12.1	12.73	-5%
CaO	8.43	8.60	-2%	6.12	6.13	0%	5.99	5.94	1%
Cl	0.662	0.79	-16%	1.02	1.21	-15%	0.815	1.04	-22%
Cr ₂ O ₃	0.0623	0.0672		0.14	0.1473		0.143	0.1408	
F	0.0573	0.0781		0.136	0.1719		0.14	0.1645	
Fe ₂ O ₃	0.1	0.0899		0.202	0.1964		0.211	0.1881	
K ₂ O	0.557	0.38		0.151	0.01		5.27	5.74	-8%
Li ₂ O	1.93	1.92	0%	0.249	0.241		0.108	0.085	
MgO	0.0762	0.011		0.075	0.025		0.0721	0.024	
Na ₂ O	21.2	21.19	0%	24.3	24.93	-3%	19.3	19.46	-1%
P ₂ O ₅	0.269	0.291		0.606	0.637		0.537	0.613	
SiO ₂	43.2	43.60	-1%	43.1	42.63	1%	32.9	34.15	-4%
SnO ₂	0.417	0.387		0.325	0.302		0.189	0.163	
SO ₃	0.351	0.386		0.797	0.846		0.753	0.812	
TiO ₂	0.823	0.877		1.54	1.60	-4%	2.67	2.70	-1%
V ₂ O ₅	3.9	3.95	-1%	1.45	1.50	-3%	3.33	3.37	-1%
ZnO	0.268	0.280		0.59	0.613		0.565	0.589	
ZrO ₂	1.82	2.48	-27%	2.81	3.71	-24%	2.27	3.17	-28%
Sum of Oxides	98.6	100	-1%	98.8	100	-1%	95.9	100	-4%

Table E.2 (continued)

Oxide	LAW-HPVR-22			LAW-HPVR-23			LAW-HPVR-24		
	Measured (wt%)	Target (wt%)	% Difference Measured vs. Target	Measured (wt%)	Target (wt%)	% Difference Measured vs. Target	Measured (wt%)	Target (wt%)	% Difference Measured vs. Target
Al ₂ O ₃	5.65	5.66	0%	5.13	5.23	-2%	3.78	3.77	0%
B ₂ O ₃	7.49	7.54	-1%	6.85	6.92	-1%	6.78	6.93	-2%
CaO	7.32	6.78	8%	7.35	6.92	6%	7.77	7.96	-2%
Cl	0.801	1.68	-52%	1.26	1.98	-36%	0.788	1.06	-25%
Cr ₂ O ₃	0.148	0.1423		0.104	0.1076		0.136	0.1428	
F	0.134	0.1657		0.107	0.1260		0.131	0.1674	
Fe ₂ O ₃	0.199	0.1900		0.154	0.1435		0.199	0.1910	
K ₂ O	3.2	3.49	-8%	1.36	1.44	-5%	5.59	5.68	-2%
Li ₂ O	1.61	1.56	3%	0.908	0.930		2.87	2.87	0%
MgO	0.0783	0.023		0.0763	0.018		0.0849	0.024	
Na ₂ O	20.1	19.78	2%	22.1	22.63	-2%	15.4	15.67	-2%
P ₂ O ₅	0.596	0.616		0.442	0.467		0.608	0.620	
SiO ₂	35.1	34.71	1%	39.7	39.80	0%	41.9	41.99	0%
SnO ₂	4.83	4.34	11%	3.48	3.15	11%	2.48	2.37	5%
SO ₃	0.695	0.818		0.571	0.620		0.748	0.824	
TiO ₂	3.1	2.91	6%	1.36	1.41	-3%	2.84	2.92	-3%
V ₂ O ₅	3.99	3.73	7%	1.29	1.33	-3%	2.95	3.02	-2%
ZnO	0.572	0.593		0.441	0.449		0.571	0.597	
ZrO ₂	4.08	5.28	-23%	4.71	6.34	-26%	2.46	3.21	-23%
Sum of Oxides	99.7	100	0%	97.5	100	-3%	98.1	100	-2%

Table E.2 (continued)

Oxide	LAW-HPVR-25			LAW-HPVR-26		
	Measured (wt%)	Target (wt%)	% Difference Measured vs. Target	Measured (wt%)	Target (wt%)	% Difference Measured vs. Target
Al ₂ O ₃	3.6	3.48	3%	11.7	11.21	4%
B ₂ O ₃	6.47	6.50	0%	13.5	13.38	1%
CaO	10.7	11.08	-3%	6.06	6.12	-1%
Cl	0.708	1.78	-60%	0.983	1.36	-28%
Cr ₂ O ₃	0.175	0.1752		0.129	0.1293	
F	0.168	0.2044		0.118	0.1518	
Fe ₂ O ₃	0.262	0.2336		0.195	0.1734	
K ₂ O	1.76	1.96	-10%	3.09	3.03	2%
Li ₂ O	0.458	0.425		3.59	3.48	3%
MgO	0.119	0.029		0.0747	0.022	
Na ₂ O	21.9	24.03	-9%	15.9	17.20	-8%
P ₂ O ₅	0.764	0.758		0.591	0.562	
SiO ₂	39.6	38.30	3%	35.9	34.81	3%
SnO ₂	1.78	1.68	6%	1.7	1.66	2%
SO ₃	0.947	1.01	-6%	0.725	0.746	
TiO ₂	1.86	1.85	1%	0.867	0.866	
V ₂ O ₅	0.229	0.218		0.291	0.284	
ZnO	0.764	0.729		0.558	0.541	
ZrO ₂	4.42	5.56	-21%	3.29	4.26	-23%
Sum of Oxides	96.8	100	-3%	99.2	100	-1%

Appendix F – Morphology/Color of Each CCC Glass and XRD Patterns

The photographs in this appendix show the morphology of the LAW Phase 5 and the LAW Phase 6 glasses after container centerline cooling (CCC) as described in Section 2.4 of the main report. X-ray diffraction (XRD) patterns are reported for the CCC glasses that crystallized. The LAW Phase 5 glasses are identified as LP5-# and the LAW Phase 6 glasses are identified as LAW-HPVR-#.



Figure F.1. Glass LP5-01 Morphology after CCC



Figure F.2. Glass LP5-02 Morphology after CCC

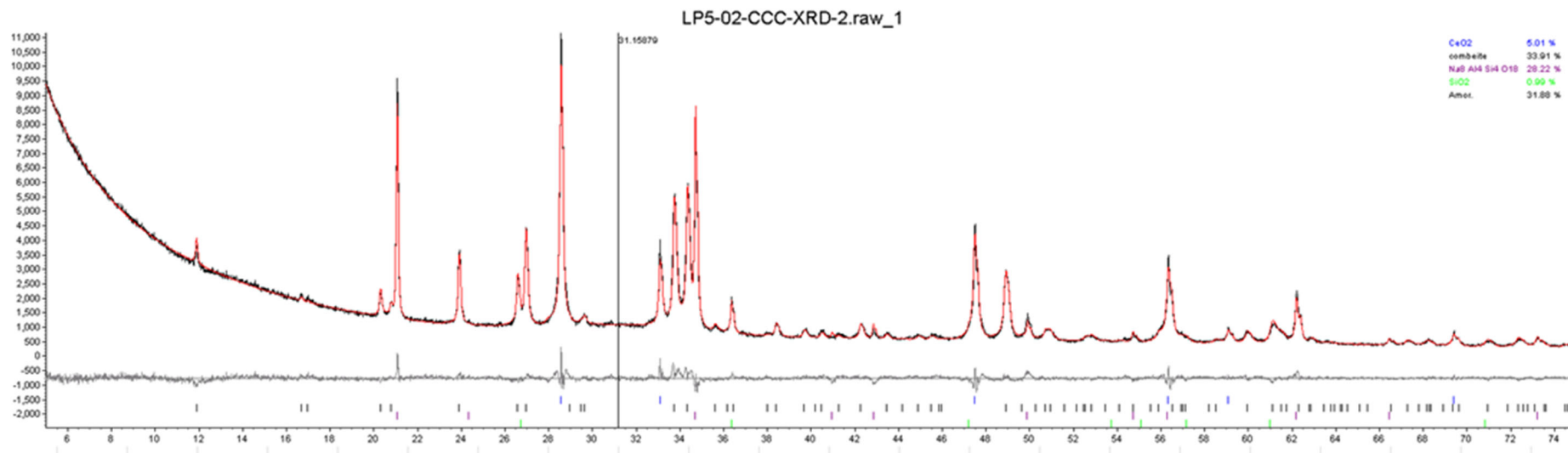


Figure F.3. XRD Pattern for Glass LP5-02 after CCC



Figure F.4. Glass LP5-03 Morphology after CCC. The quantity of the crystals was too low to be identified by XRD.



Figure F.5. Glass LP5-04 Morphology after CCC

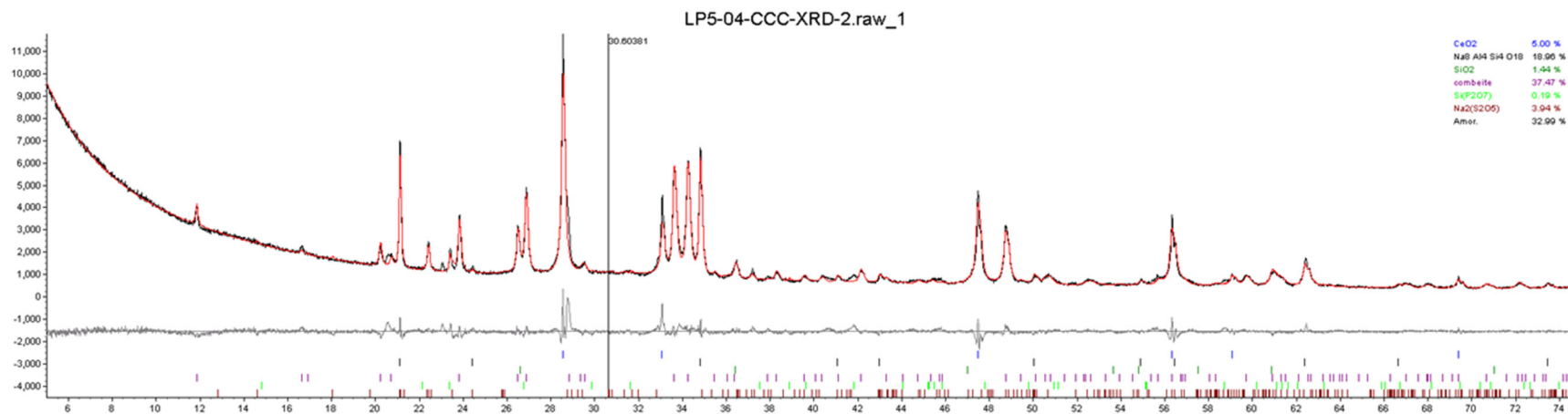


Figure F.6. XRD Pattern for Glass LP5-04 after CCC



Figure F.7. Glass LP5-05 Morphology after CCC



Figure F.8. Glass LP5-06-MOD1 Morphology after CCC. The quantity of the crystals was too low to be identified by XRD.



Figure F.9. Glass LP5-07 Morphology after CCC



Figure F.10. Glass LP5-08 Morphology after CCC



Figure F.11. Glass LP5-09 Morphology after CCC

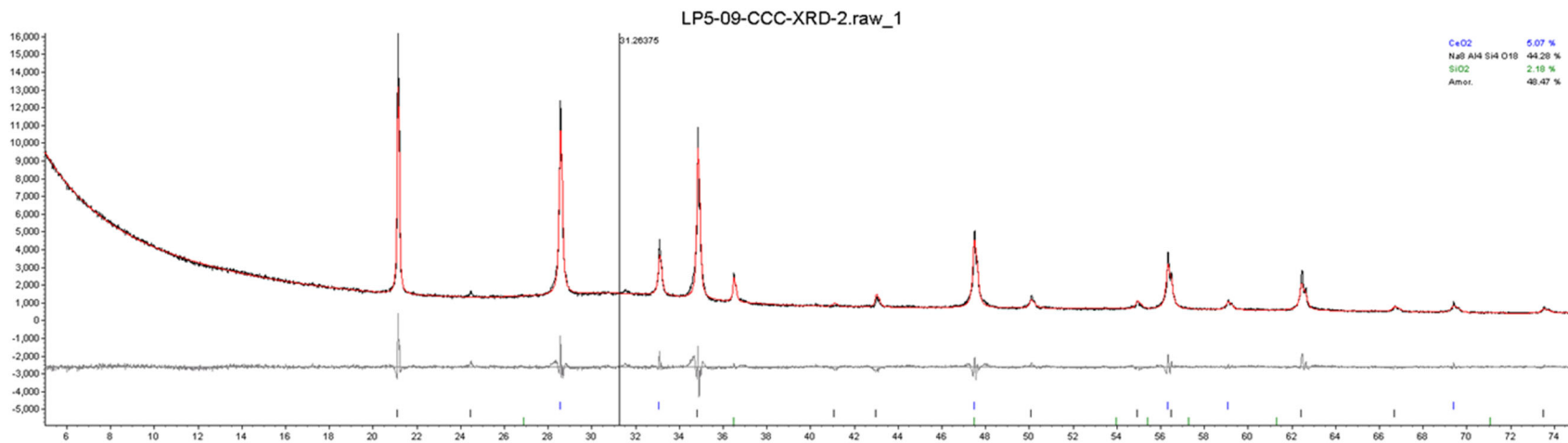


Figure F.12. XRD Pattern for Glass LP5-09 after CCC



Figure F.13. Glass LP5-10 Morphology after CCC

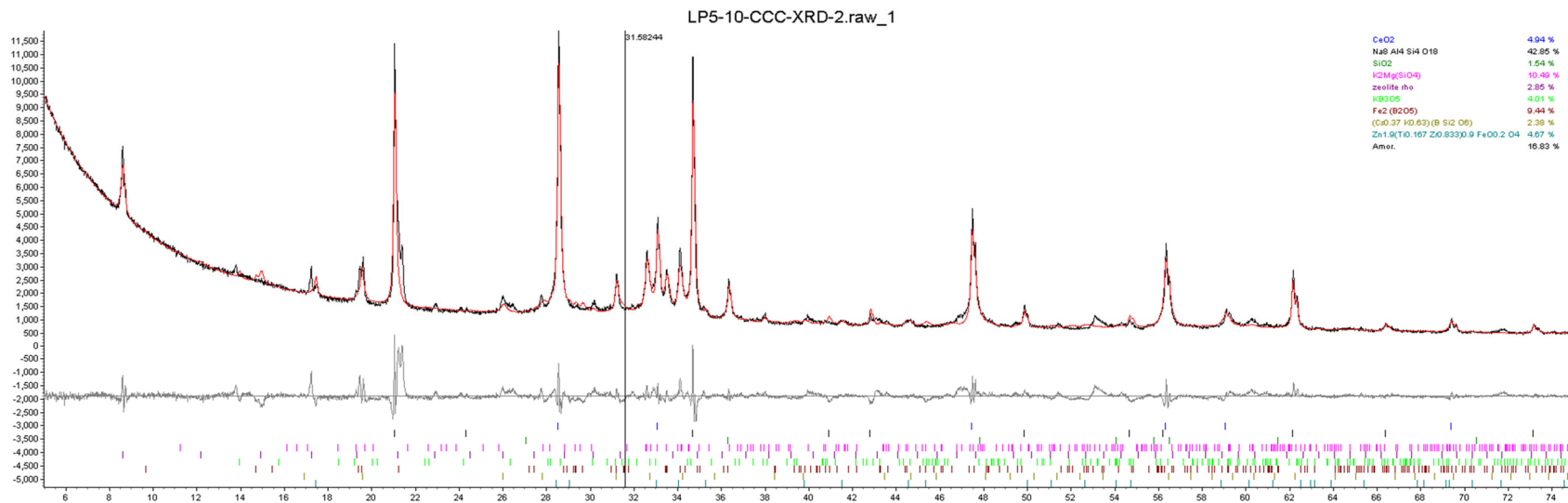


Figure F.14. XRD Pattern for Glass LP5-10 after CCC



Figure F.15. Glass LP5-11 Morphology after CCC. The quantity of the crystals was too low to be identified by XRD.



Figure F.16. Glass LP5-12-1 Morphology after CCC

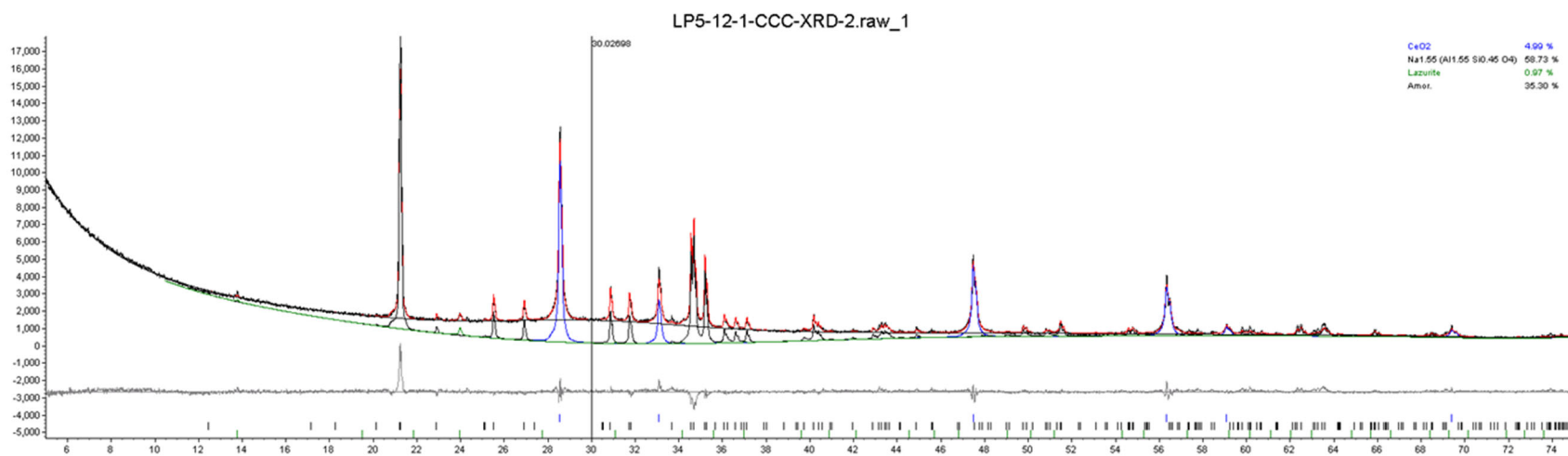


Figure F.17. XRD Pattern for Glass LP5-12-1 after CCC



Figure F.18. Glass LP5-13 Morphology after CCC



Figure F.19. Glass LP5-14 Morphology after CCC. The quantity of the crystals was too low to be identified by XRD.



Figure F.20. Glass LP5-15 Morphology after CCC



Figure F.21. Glass LP5-16-MOD1 Morphology after CCC

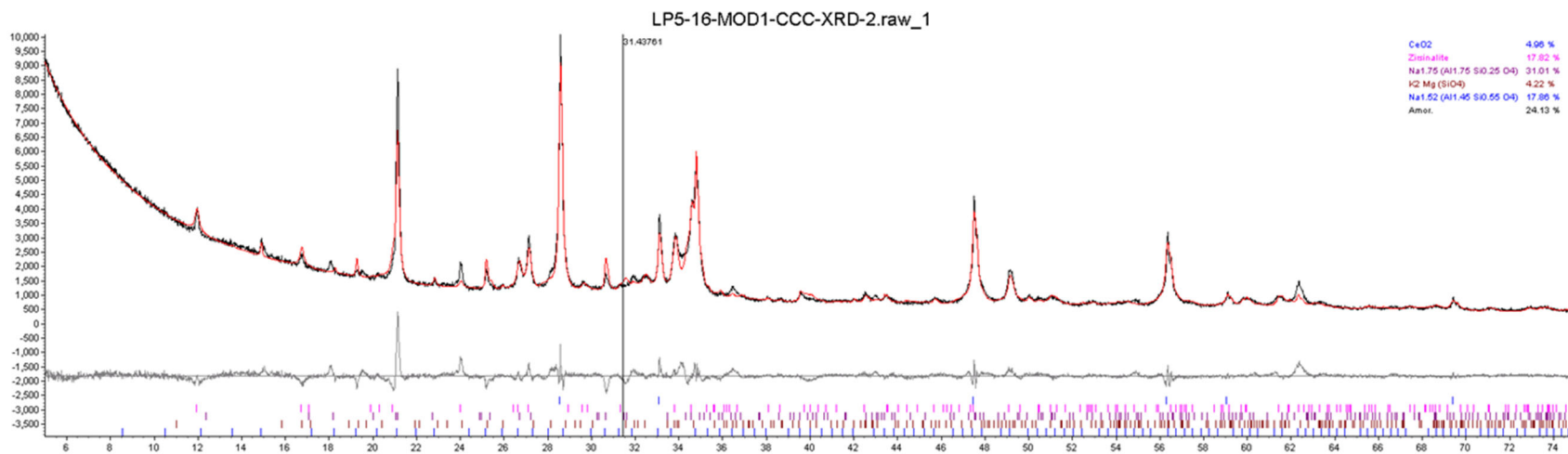


Figure F.22. XRD Pattern for Glass LP5-16-MOD1 after CCC



Figure F.23. Glass LP5-17 Morphology after CCC



Figure F.24. Glass LP5-18 Morphology after CCC



Figure F.25. Glass LP5-19 Morphology after CCC



Figure F.26. Glass LP5-20 Morphology after CCC



Figure F.27. Glass LP5-21 Morphology after CCC



Figure F.28. Glass LP5-22 Morphology after CCC



Figure F.29. Glass LP5-23 Morphology after CCC



Figure F.30. Glass LP5-24 Morphology after CCC



Figure F.31. Glass LP5-25 Morphology after CCC



Figure F.32. Glass LAW-HPVR-01-1 Morphology after CCC



Figure F.33. Glass LAW-HPVR-02-1 Morphology after CCC



Figure F.34. Glass LAW-HPVR-03-1 Morphology after CCC

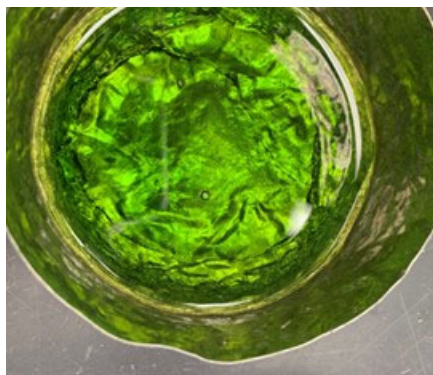


Figure F.35. Glass LAW-HPVR-04-1 Morphology after CCC



Figure F.36. Glass LAW-HPVR-05 Morphology after CCC



Figure F.37. Glass LAW-HPVR-06 Morphology after CCC



Figure F.38. Glass LAW-HPVR-07 Morphology after CCC

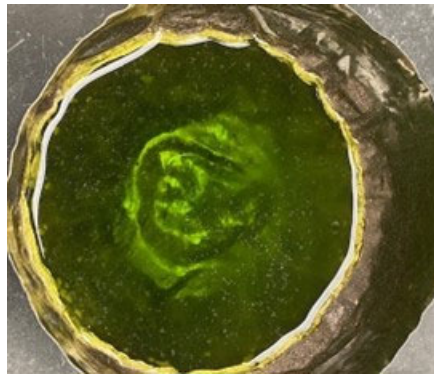


Figure F.39. Glass LAW-HPVR-08 Morphology after CCC



Figure F.40. Glass LAW-HPVR-09 Morphology after CCC



Figure F.41. Glass LAW-HPVR-10 Morphology after CCC



Figure F.42. Glass LAW-HPVR-11 Morphology after CCC



Figure F.43. Glass LAW-HPVR-12 Morphology after CCC



Figure F.44. Glass LAW-HPVR-13 Morphology after CCC



Figure F.45. Glass LAW-HPVR-14 Morphology after CCC. The quantity of the crystals was too low to be identified by XRD.



Figure F.46. Glass LAW-HPVR-15 Morphology after CCC

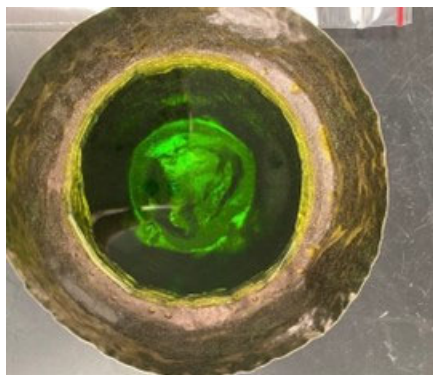


Figure F.47. Glass LAW-HPVR-16 Morphology after CCC



Figure F.48. Glass LAW-HPVR-17 Morphology after CCC

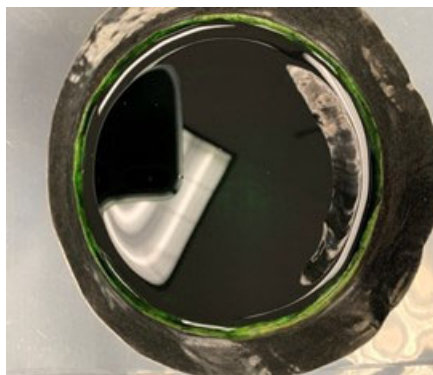


Figure F.49. Glass LAW-HPVR-18 Morphology after CCC

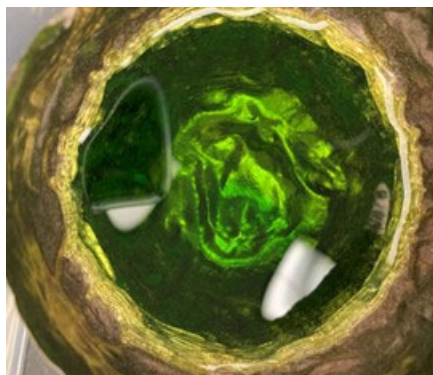


Figure F.50. Glass LAW-HPVR-19 Morphology after CCC



Figure F.51. Glass LAW-HPVR-20 Morphology after CCC

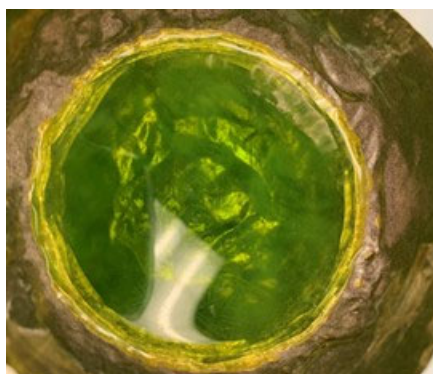


Figure F.52. Glass LAW-HPVR-21 Morphology after CCC



Figure F.53. Glass LAW-HPVR-22 Morphology after CCC



Figure F.54. Glass LAW-HPVR-23 Morphology after CCC



Figure F.55. Glass LAW-HPVR-24 Morphology after CCC



Figure F.56. Glass LAW-HPVR-25 Morphology after CCC

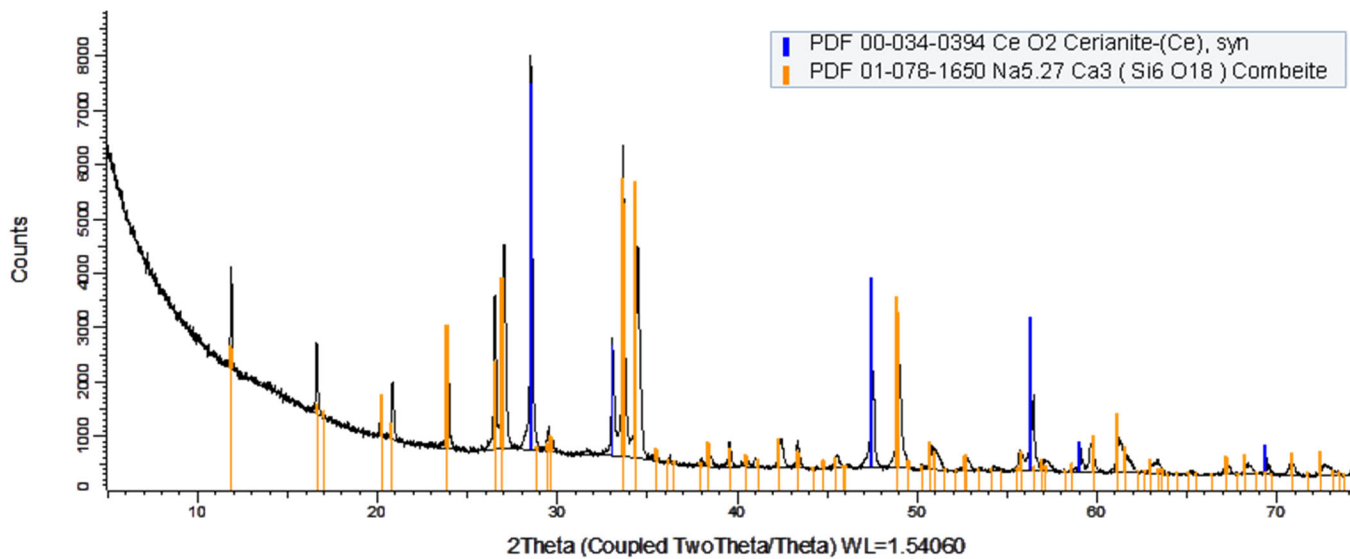


Figure F.57. XRD Pattern for Glass LAW-HPVR-25 after CCC



Figure F.58. Glass LAW-HPVR-26 Morphology after CCC

Appendix G – Crystal Fraction of Heat-Treated Glasses Photographs

This appendix contains photographs of the LAW Phase 5 glasses after they were heat treated at 950 °C for 24 hours (crystal fraction [CF] heat treatment). As indicated by these photographs, each glass showed a different response to heat treatment.

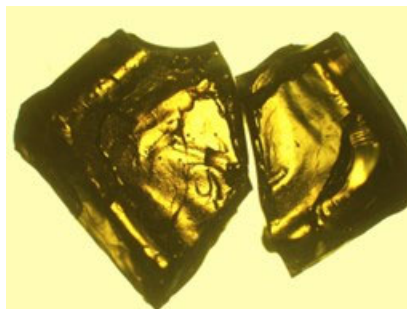


Figure G.1. Glass LP5-01 after CF Heat Treatment at 950 °C for 24 Hours

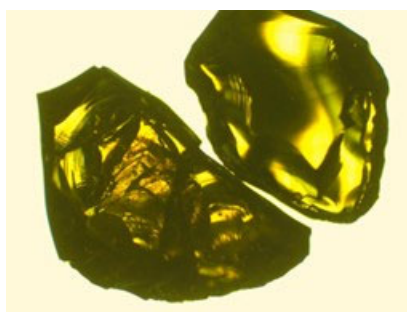


Figure G.2. Glass LP5-02 after CF Heat Treatment at 950 °C for 24 Hours

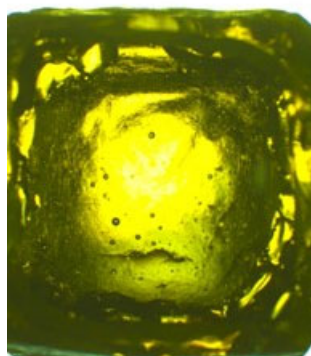


Figure G.3. Glass LP5-03 after CF Heat Treatment at 950 °C for 24 Hours



Figure G.4. Glass LP5-04 after CF Heat Treatment at 950 °C for 24 Hours

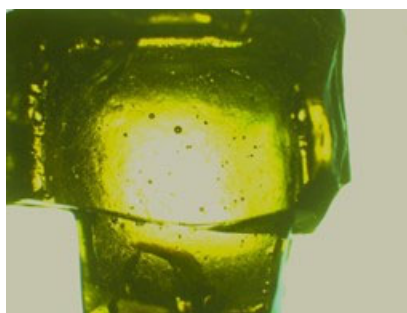


Figure G.5. Glass LP5-05 after CF Heat Treatment at 950 °C for 24 Hours



Figure G.6. Glass LP5-06-MOD1 after CF Heat Treatment at 950 °C for 24 Hours



Figure G.7. Glass LP5-07 after CF Heat Treatment at 950 °C for 24 Hours



Figure G.8. Glass LP5-08 after CF Heat Treatment at 950 °C for 24 Hours

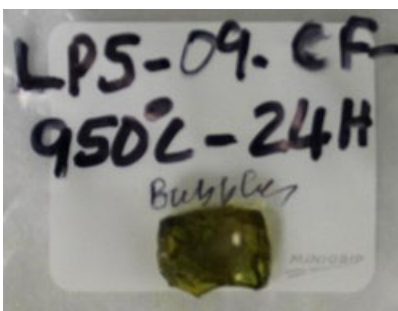


Figure G.9. Glass LP5-09 after CF Heat Treatment at 950 °C for 24 Hours

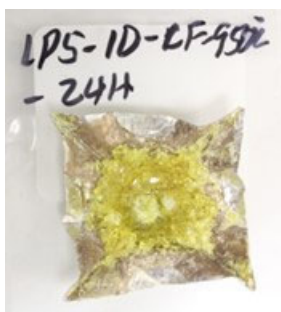


Figure G.10. Glass LP5-10 after CF Heat Treatment at 950 °C for 24 Hours

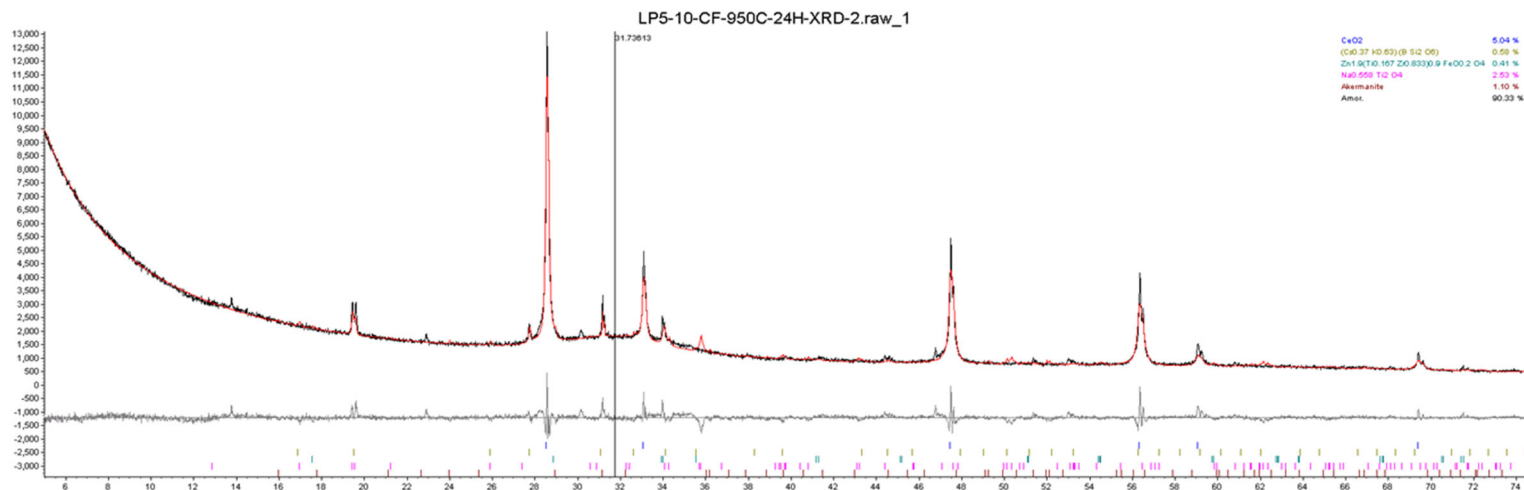


Figure G.11. XRD Pattern for Glass LP5-10 after CF Heat Treatment at 950 °C for 24 Hours



Figure G.12. Glass LP5-11 after CF Heat Treatment at 950 °C for 24 Hours



Figure G.13. Glass LP5-12-1 after CF Heat Treatment at 950 °C for 24 Hours

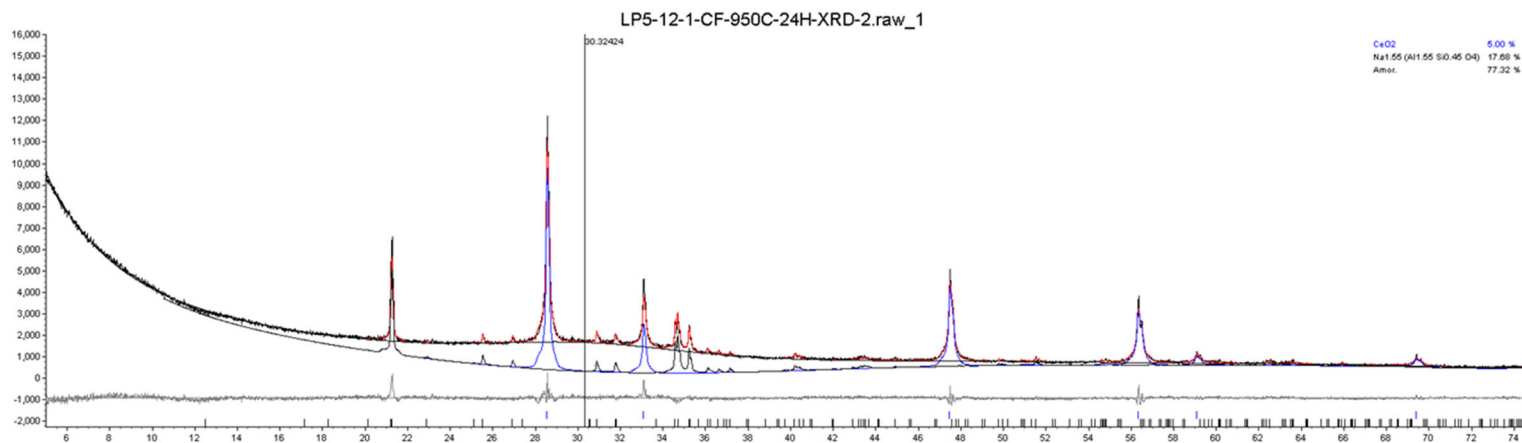


Figure G.14. XRD Pattern for Glass LP5-12-1 after CF Heat Treatment at 950 °C for 24 Hours



Figure G.15. Glass LP5-13 after CF Heat Treatment at 950 °C for 24 Hours

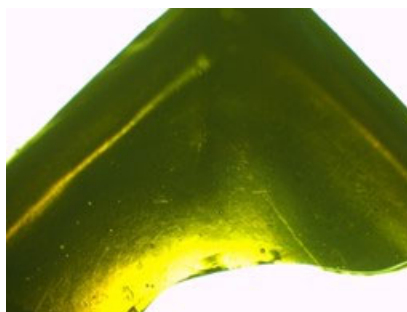


Figure G.16. Glass LP5-14 after CF Heat Treatment at 950 °C for 24 Hours



Figure G.17. Glass LP5-15 after CF Heat Treatment at 950 °C for 24 Hours



Figure G.18. Glass LP5-16-MOD1 after CF Heat Treatment at 950 °C for 24 Hours

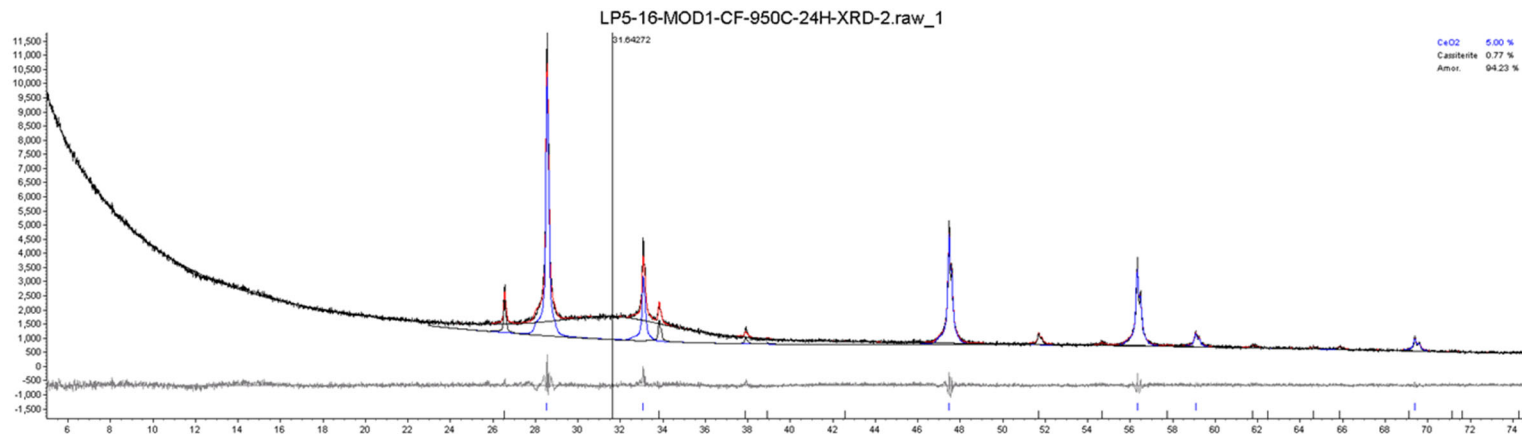


Figure G.19. XRD Pattern for Glass LP5-16-MOD1 after CF Heat Treatment at 950 °C for 24 Hours



Figure G.20. Glass LP5-17 after CF Heat Treatment at 950 °C for 24 Hours



Figure G.21. Glass LP5-18 after CF Heat Treatment at 950 °C for 24 Hours

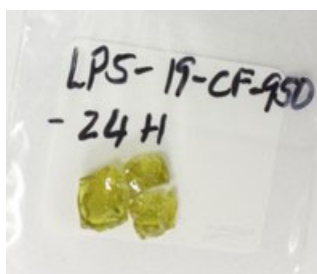


Figure G.22. Glass LP5-19 after CF Heat Treatment at 950 °C for 24 Hours



Figure G.23. Glass LP5-20 after CF Heat Treatment at 950 °C for 24 Hours



Figure G.24. Glass LP5-21 after CF Heat Treatment at 950 °C for 24 Hours



Figure G.25. Glass LP5-22 after CF Heat Treatment at 950 °C for 24 Hours



Figure G.26. Glass LP5-23 after CF Heat Treatment at 950 °C for 24 Hours



Figure G.27. Glass LP5-24 after CF Heat Treatment at 950 °C for 24 Hours



Figure G.28. Glass LP5-25 after CF Heat Treatment at 950 °C for 24 Hours

Appendix H – Viscosity Data

This appendix contains the measured viscosity data for each of the LAW Phase 5 glasses. The plots shown in this appendix are fitted to the Arrhenius equation:

$$\ln(\eta) = A + \frac{B}{T_K} \quad (\text{H.1})$$

where A and B are independent of temperature and temperature (T_K) is in K ($T(^{\circ}\text{C}) + 273.15$).

If the plots showed curvature, they would be better fit to the Vogel- Fulcher-Tamman (VFT) model:

$$\ln(\eta) = E + \frac{F}{T_k - T_0} \quad (\text{H.2})$$

where E , F , and T_0 are temperature independent and composition dependent coefficients and T_K is the temperature in Kelvin ($T(^{\circ}\text{C}) + 273.15$). The main intent of the figures and Arrhenius equation fits shown is to assess trends in the data and provide observations about whether there may be sufficient curvature in the data to consider VFT fits in the subsequent work that will decide between fitting the viscosity-temperature data to the Arrhenius or VFT equations. All the glasses in the LAW Phase 5 matrix appear to have very good fits to the Arrhenius equation and do not show a need for fitting to the VFT model.

H.1 Glass LP5G-01 Viscosity Data

Table H.1. Viscosity Data for Glass LP5-01

Measured Temp., °C	1/(T+273.15), K ⁻¹	Viscosity, Pa-s	ln η, Pa-s
1169	6.94E-04	0.52	-0.66
1074	7.42E-04	1.07	0.06
979	7.99E-04	2.83	1.04
1169	6.94E-04	0.54	-0.61
1226	6.67E-04	0.37	-1.00
1169	6.94E-04	0.55	-0.60

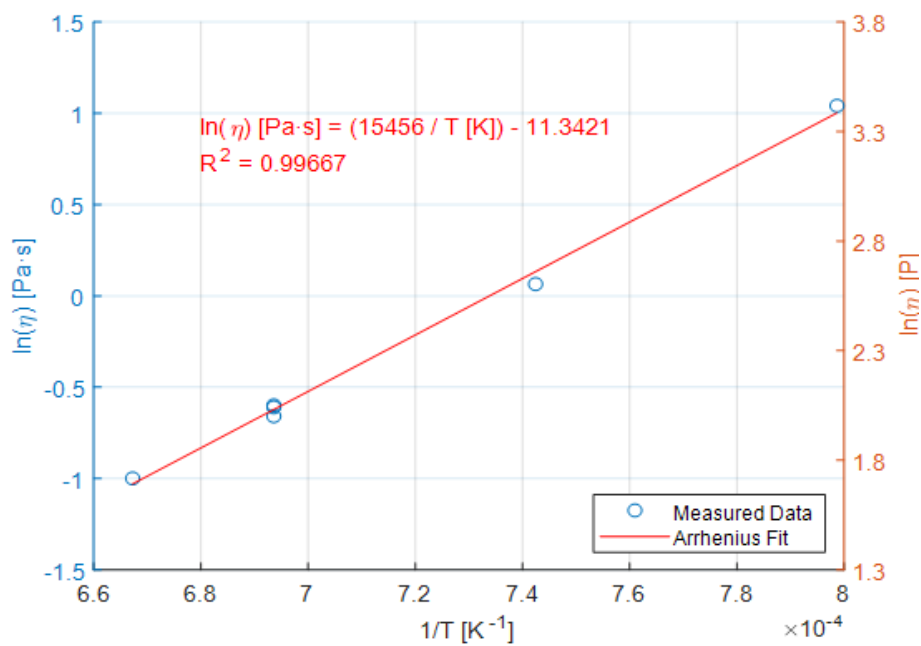


Figure H.1. Viscosity-Temperature Data and Arrhenius Equation Fit for Glass LP5-01

H.2 Glass LP5-02 Viscosity Data

Table H.2. Viscosity Data for Glass LP5-02

Measured Temp., °C	1/(T+273.15), K ⁻¹	Viscosity, Pa-s	ln η, Pa-s
1169	6.94E-04	0.56	-0.58
1074	7.42E-04	1.21	0.19
979	7.99E-04	3.24	1.17
1169	6.94E-04	0.58	-0.55
1226	6.67E-04	0.39	-0.95
1169	6.94E-04	0.57	-0.57

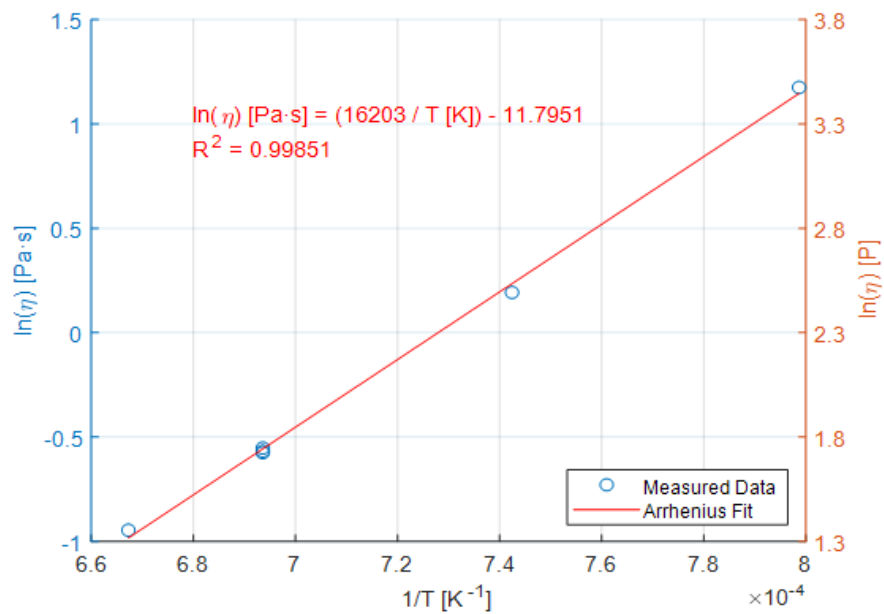


Figure H.2. Viscosity-Temperature Data and Arrhenius Equation Fit for Glass LP5-02

H.3 Glass LP5-03 Viscosity Data

Table H.3. Viscosity Data for Glass LP5-03

Measured Temp., °C	1/(T+273.15), K ⁻¹	Viscosity, Pa-s	ln η, Pa-s
1169	6.94E-04	0.88	-0.13
1074	7.42E-04	2.03	0.71
979	7.99E-04	5.78	1.75
1169	6.94E-04	0.86	-0.15
1235	6.63E-04	0.54	-0.61
1169	6.94E-04	0.85	-0.16

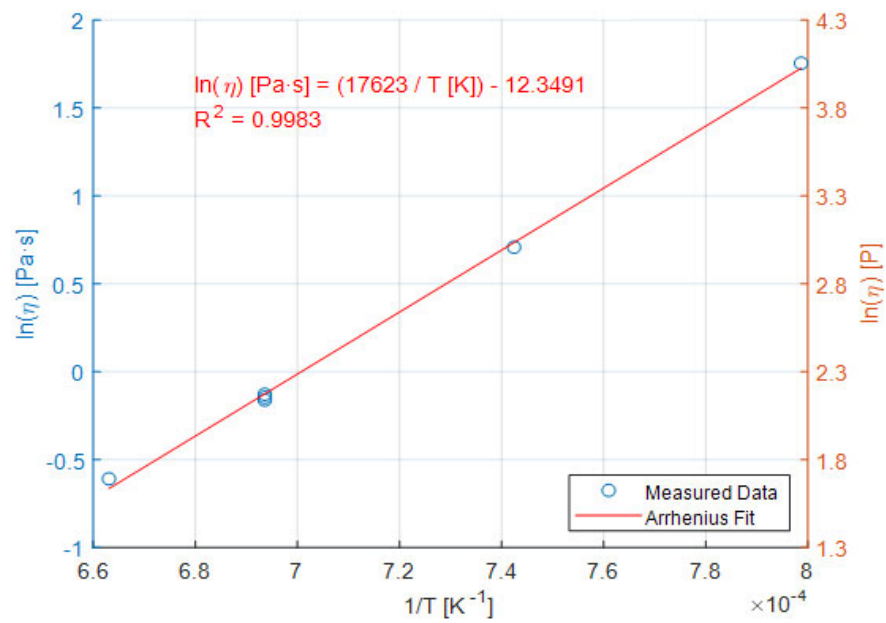


Figure H.3. Viscosity-Temperature Data and Arrhenius Equation Fit for Glass LP5-03

H.4 Glass LP5-04 Viscosity Data

Table H.4. Viscosity Data for Glass LP5-04

Measured Temp., °C	1/(T+273.15), K ⁻¹	Viscosity, Pa-s	ln η, Pa-s
1169	6.94E-04	0.54	-0.62
1074	7.42E-04	1.08	0.08
979	7.99E-04	2.67	0.98
1169	6.94E-04	0.52	-0.66
1235	6.63E-04	0.34	-1.08
1169	6.94E-04	0.51	-0.67

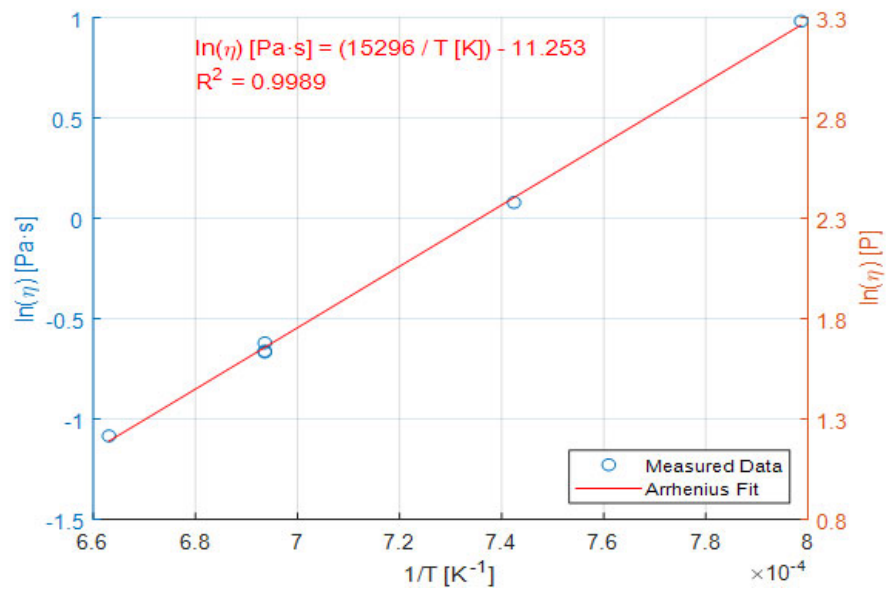


Figure H.4. Viscosity-Temperature Data and Arrhenius Equation Fit for Glass LP5-04

H.5 Glass LP5-05 Viscosity Data

Table H.5. Viscosity Data for Glass LP5-05

Measured Temp., °C	1/(T+273.15), K ⁻¹	Viscosity, Pa-s	ln η, Pa-s
1169	6.94E-04	0.75	-0.29
1074	7.42E-04	1.63	0.49
979	7.99E-04	4.43	1.49
1169	6.94E-04	0.75	-0.29
1226	6.67E-04	0.49	-0.70
1169	6.94E-04	0.74	-0.30

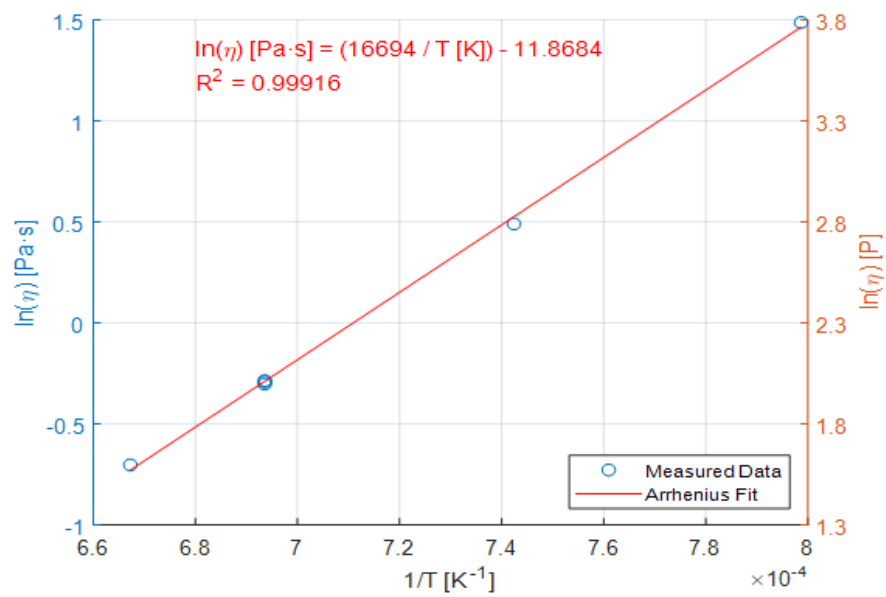


Figure H.5. Viscosity-Temperature Data and Arrhenius Equation Fit for Glass LP5-05

H.6 Glass LP5-06-MOD1 Viscosity Data

Table H.6. Viscosity Data for Glass LP5-06-MOD1

Measured Temp., °C	1/(T+273.15), K ⁻¹	Viscosity, Pa-s	ln η, Pa-s
1169	6.94E-04	3.10	1.13
1074	7.42E-04	7.69	2.04
979	7.99E-04	24.28	3.19
1169	6.94E-04	3.20	1.16
1233	6.64E-04	1.94	0.66
1169	6.94E-04	3.19	1.16

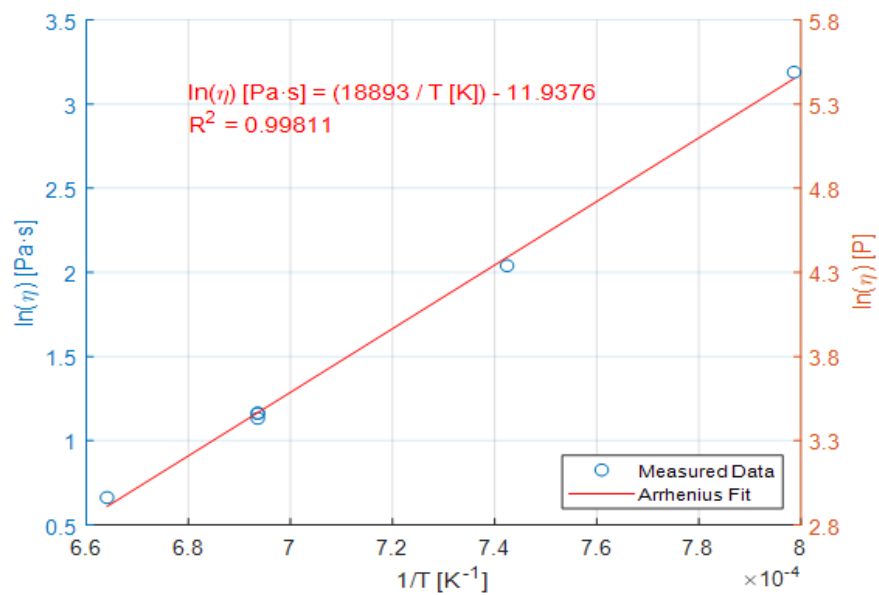


Figure H.6. Viscosity-Temperature Data and Arrhenius Equation Fit for Glass LP5-06-MOD1

H.7 Glass LP5-07 Viscosity Data

Table H.7. Viscosity Data for Glass LP5-07

Measured Temp., °C	1/(T+273.15), K ⁻¹	Viscosity, Pa-s	ln η, Pa-s
1169	6.94E-04	4.49	1.50
1074	7.42E-04	10.16	2.32
979	7.99E-04	27.24	3.30
1169	6.94E-04	4.50	1.50
1235	6.63E-04	2.70	0.99
1169	6.94E-04	4.47	1.50

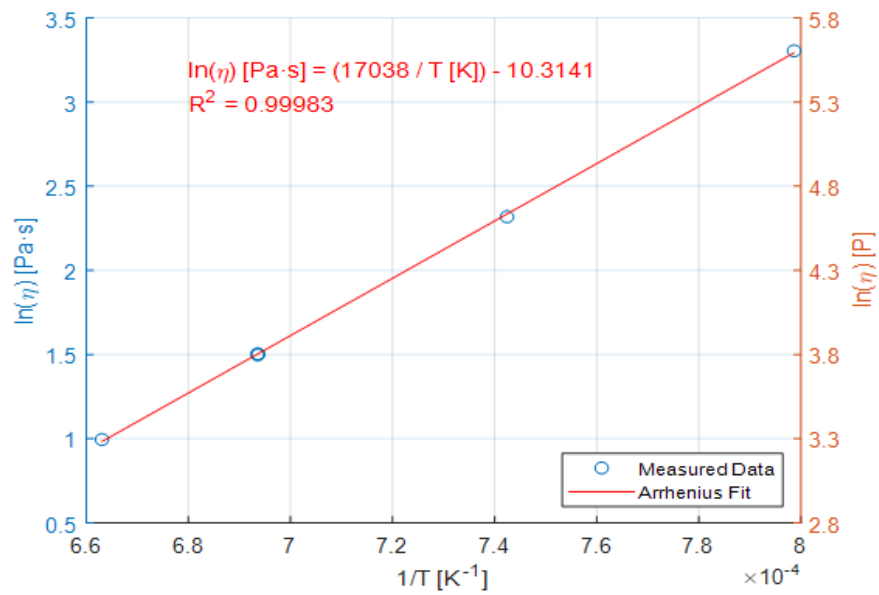


Figure H.7. Viscosity-Temperature Data and Arrhenius Equation Fit for Glass LP5-07

H.8 Glass LP5-08 Viscosity Data

Table H.8. Viscosity Data for Glass LP5-08

Measured Temp., °C	1/(T+273.15), K ⁻¹	Viscosity, Pa-s	ln η, Pa-s
1169	6.94E-04	3.30	1.19
1074	7.42E-04	7.34	1.99
979	7.99E-04	20.88	3.04
1169	6.94E-04	3.34	1.21
1226	6.67E-04	2.17	0.77
1169	6.94E-04	3.36	1.21

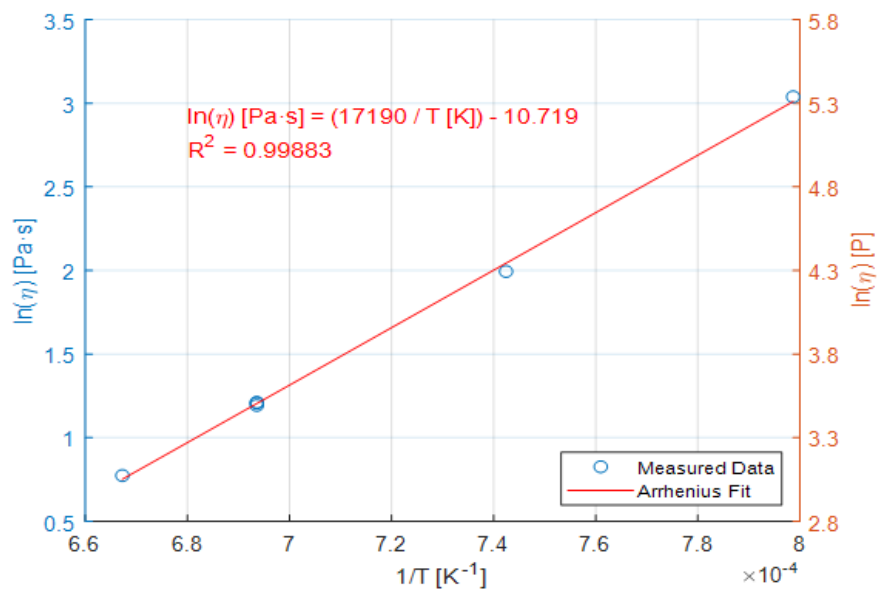


Figure H.8. Viscosity-Temperature Data and Arrhenius Equation Fit for Glass LP5-08

H.9 Glass LP5-09 Viscosity Data

Table H.9. Viscosity Data for Glass LP5-09

Measured Temp., °C	1/(T+273.15), K ⁻¹	Viscosity, Pa-s	ln η, Pa-s
1169	6.94E-04	1.88	0.63
1074	7.42E-04	4.35	1.47
979	7.99E-04	11.04	2.40
1169	6.94E-04	1.82	0.60
1231	6.65E-04	1.13	0.12
1169	6.94E-04	1.78	0.57

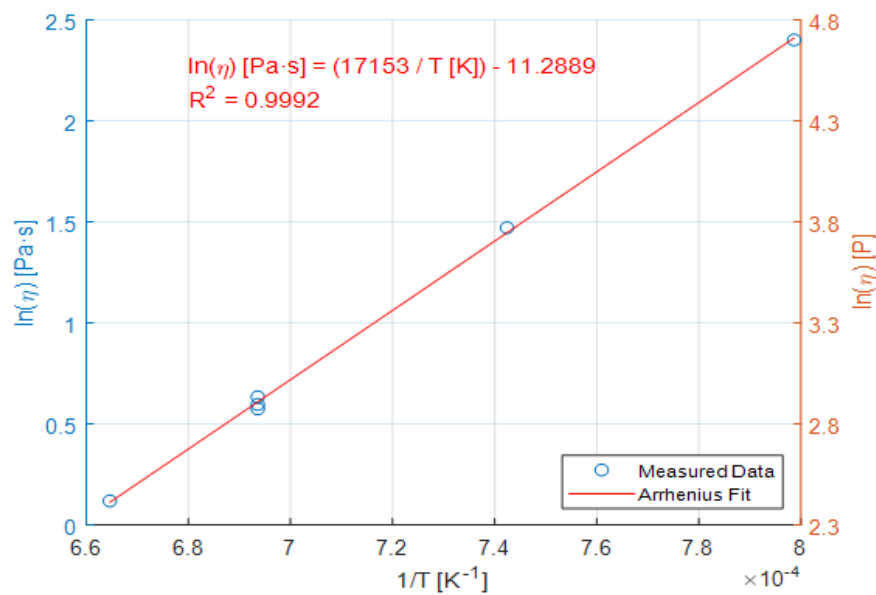


Figure H.9. Viscosity-Temperature Data and Arrhenius Equation Fit for Glass LP5-09

H.10 Glass LP5-10 Viscosity Data

Table H.10. Viscosity Data for Glass LP5-10

Measured Temp., °C	1/(T+273.15), K ⁻¹	Viscosity, Pa-s	ln η, Pa-s
1169	6.94E-04	1.56	0.44
1074	7.42E-04	3.75	1.32
979	7.99E-04	9.79	2.28
1169	6.94E-04	1.49	0.40
1232	6.65E-04	0.89	-0.11
1169	6.94E-04	1.45	0.37

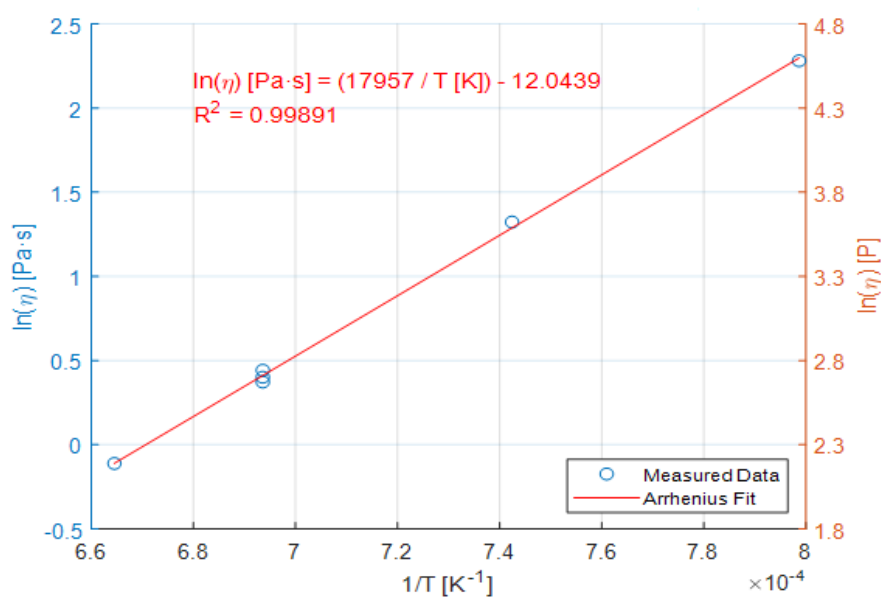


Figure H.10. Viscosity-Temperature Data and Arrhenius Equation Fit for Glass LP5-10

H.11 Glass LP5-11 Viscosity Data

Table H.11. Viscosity Data for Glass LP5-11

Measured Temp., °C	1/(T+273.15), K ⁻¹	Viscosity, Pa-s	ln η, Pa-s
1169	6.94E-04	1.57	0.45
1074	7.42E-04	3.30	1.19
979	7.99E-04	8.38	2.13
1169	6.94E-04	1.62	0.49
1235	6.63E-04	1.03	0.03
1169	6.94E-04	1.65	0.50

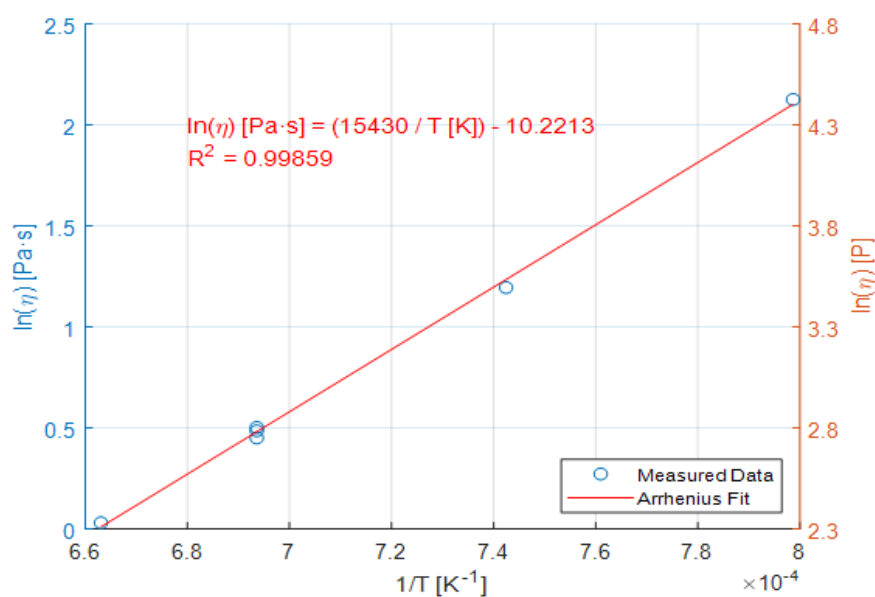


Figure H.11. Viscosity-Temperature Data and Arrhenius Equation Fit for Glass LP5-11

H.12 Glass LP5-12 Viscosity Data

Table H.12. Viscosity Data for Glass LP5-12-1

Measured Temp., °C	1/(T+273.15), K ⁻¹	Viscosity, Pa-s	ln η, Pa-s
1150	7.03E-04	7.06	1.95
1050	7.56E-04	21.40	3.06
950	8.18E-04	91.95	4.52
1150	7.03E-04	7.24	1.98
1220	6.70E-04	3.77	1.33
1150	7.03E-04	6.96	1.94

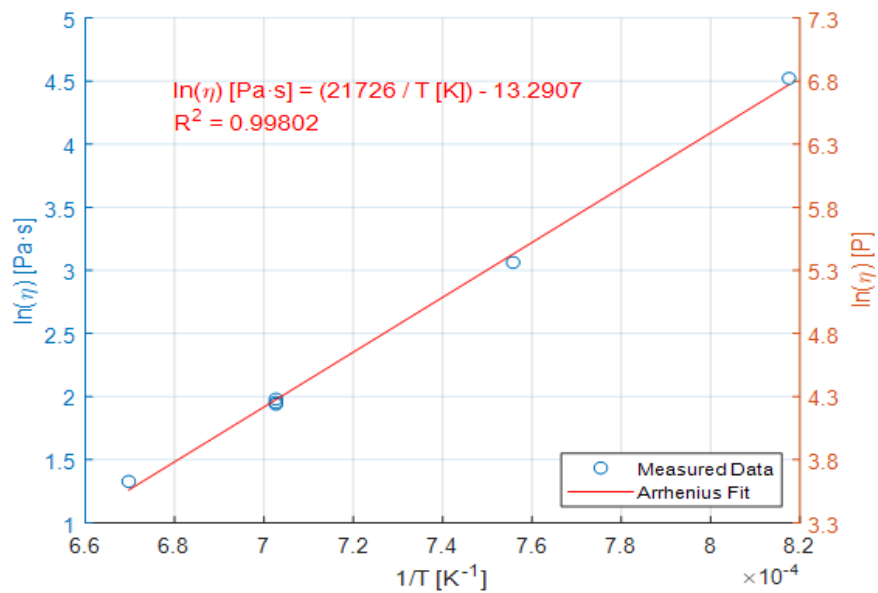


Figure H.12. Viscosity-Temperature Data and Arrhenius Equation Fit for Glass LP5-12-1

H.13 Glass LP5-13 Viscosity Data

Table H.13. Viscosity Data for Glass LP5-13

Measured Temp., °C	1/(T+273.15), K ⁻¹	Viscosity, Pa-s	ln η, Pa-s
1150	7.03E-04	1.02	0.02
1050	7.56E-04	2.24	0.81
950	8.18E-04	5.53	1.71
1150	7.03E-04	1.00	0.00
1229	6.66E-04	0.63	-0.47
1150	7.03E-04	1.03	0.03

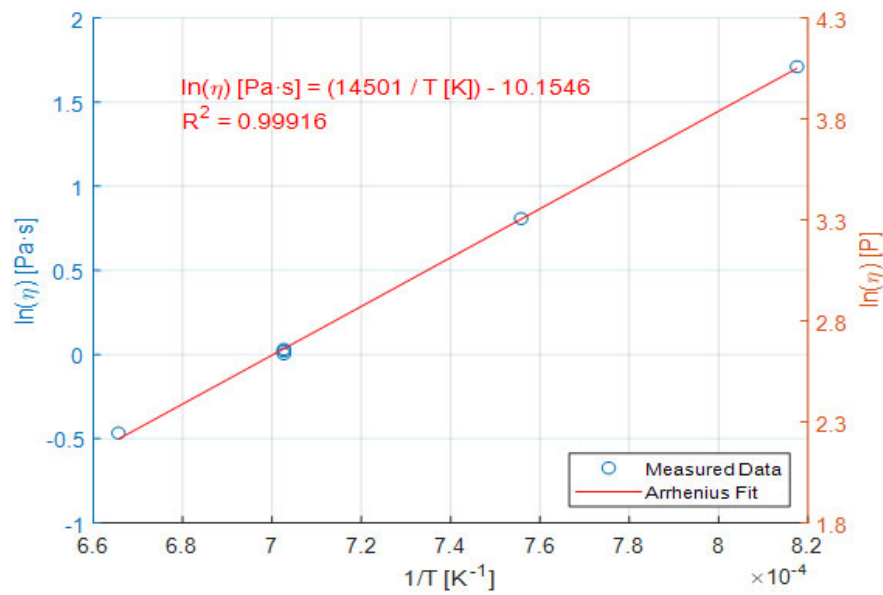


Figure H.13. Viscosity-Temperature Data and Arrhenius Equation Fit for Glass LP5-13

H.14 Glass LP5-14 Viscosity Data

Table H.14. Viscosity Data for Glass LP5-14

Measured Temp., °C	1/(T+273.15), K ⁻¹	Viscosity, Pa-s	ln η, Pa-s
1150	7.03E-04	2.39	0.87
1050	7.56E-04	6.58	1.88
950	8.18E-04	23.81	3.17
1150	7.03E-04	2.42	0.89
1220	6.70E-04	1.33	0.29
1150	7.03E-04	2.41	0.88

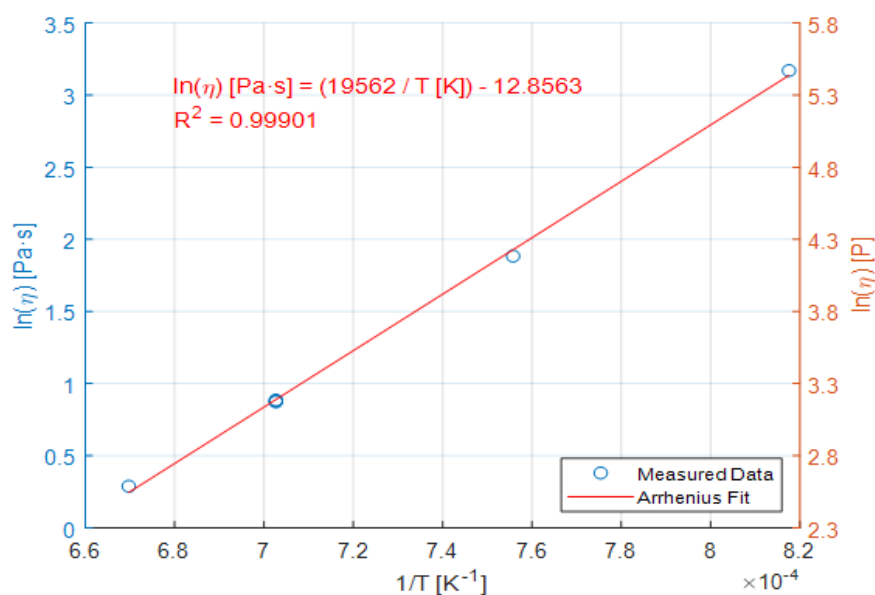


Figure H.14. Viscosity-Temperature Data and Arrhenius Equation Fit for Glass LP5-14

H.15 Glass LP5-15 Viscosity Data

Table H.15. Viscosity Data for Glass LP5-15

Measured Temp., °C	1/(T+273.15), K ⁻¹	Viscosity, Pa-s	ln η, Pa-s
1150	7.03E-04	5.05	1.62
1050	7.56E-04	13.62	2.61
950	8.18E-04	47.01	3.85
1150	7.03E-04	5.08	1.63
1230	6.65E-04	2.69	0.99
1150	7.03E-04	5.20	1.65

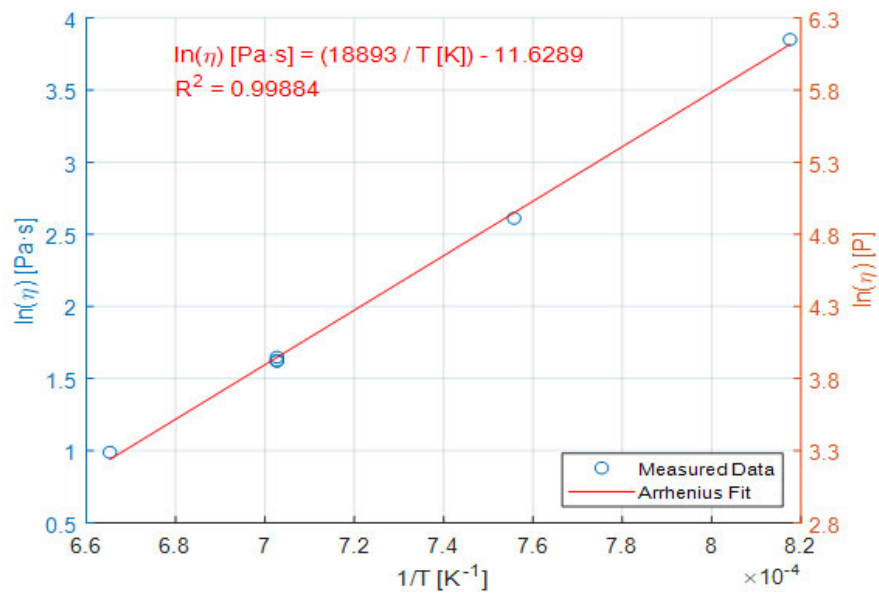


Figure H.15. Viscosity-Temperature Data and Arrhenius Equation Fit for Glass LP5-15

H.16 Glass LP5-16-MOD1 Viscosity Data

Table H.16. Viscosity Data for Glass LP5-16-MOD1

Measured Temp., °C	1/(T+273.15), K ⁻¹	Viscosity, Pa-s	ln η, Pa-s
1150	7.03E-04	1.71	0.54
1050	7.56E-04	4.78	1.56
950	8.18E-04	18.41	2.91
1150	7.03E-04	1.75	0.56
1230	6.65E-04	0.92	-0.09
1150	7.03E-04	1.71	0.54

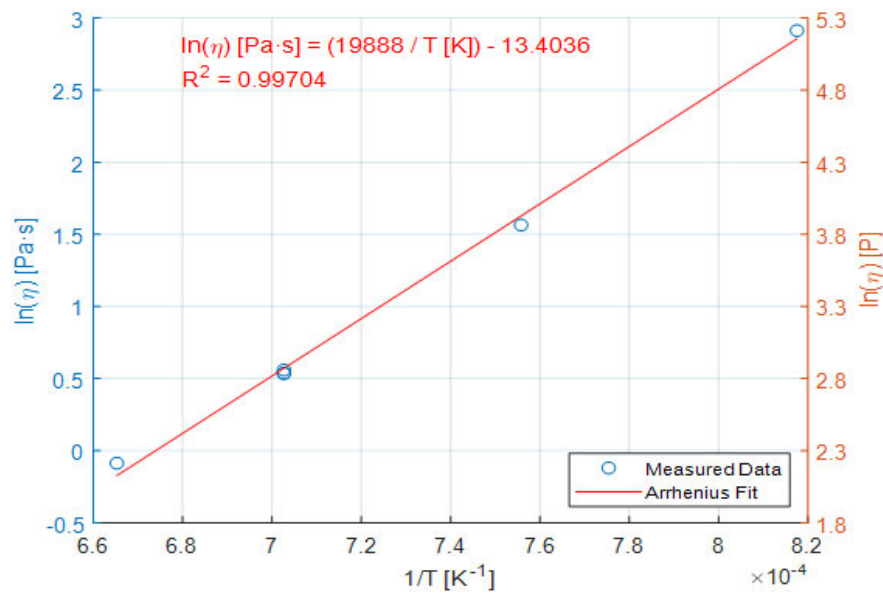


Figure H.16. Viscosity-Temperature Data and Arrhenius Equation Fit for Glass LP5-16-MOD1

H.17 Glass LP5-17 Viscosity Data

Table H.17. Viscosity Data for Glass LP5-17

Measured Temp., °C	1/(T+273.15), K ⁻¹	Viscosity, Pa-s	ln η, Pa-s
1150	7.03E-04	1.50	0.40
1050	7.56E-04	4.24	1.45
950	8.18E-04	16.17	2.78
1150	7.03E-04	1.50	0.40
1210	6.74E-04	0.86	-0.15
1150	7.03E-04	1.46	0.38

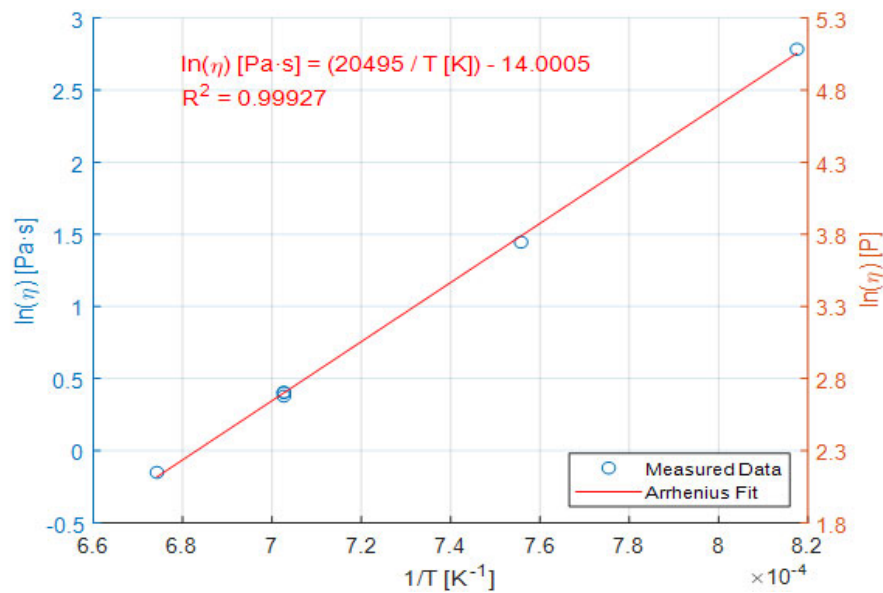


Figure H.17. Viscosity-Temperature Data and Arrhenius Equation Fit for Glass LP5-17

H.18 Glass LP5-18 Viscosity Data

Table H.18. Viscosity Data for Glass LP5-18

Measured Temp., °C	1/(T+273.15), K ⁻¹	Viscosity, Pa-s	ln η, Pa-s
1150	7.03E-04	2.13	0.76
1050	7.56E-04	4.77	1.56
950	8.18E-04	14.70	2.69
1150	7.03E-04	2.09	0.74
1210	6.74E-04	1.36	0.31
1150	7.03E-04	2.11	0.75

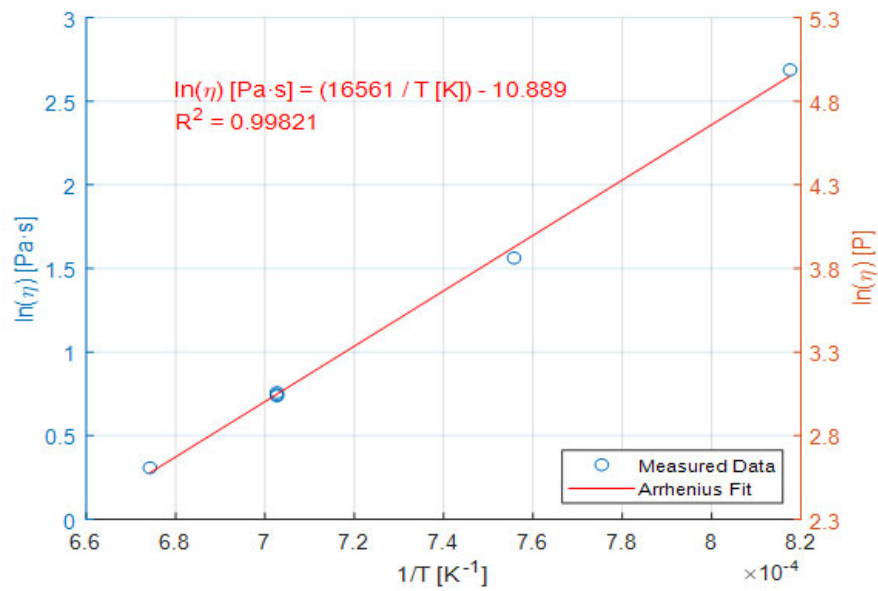


Figure H.18. Viscosity-Temperature Data and Arrhenius Equation Fit for Glass LP5-18

H.19 Glass LP5-19 Viscosity Data

Table H.19. Viscosity Data for Glass LP5-19

Measured Temp., °C	1/(T+273.15), K ⁻¹	Viscosity, Pa-s	ln η, Pa-s
1150	7.03E-04	0.81	-0.21
1050	7.56E-04	1.90	0.64
950	8.18E-04	5.67	1.74
1150	7.03E-04	0.83	-0.19
1220	6.70E-04	0.50	-0.70
1150	7.03E-04	0.81	-0.20

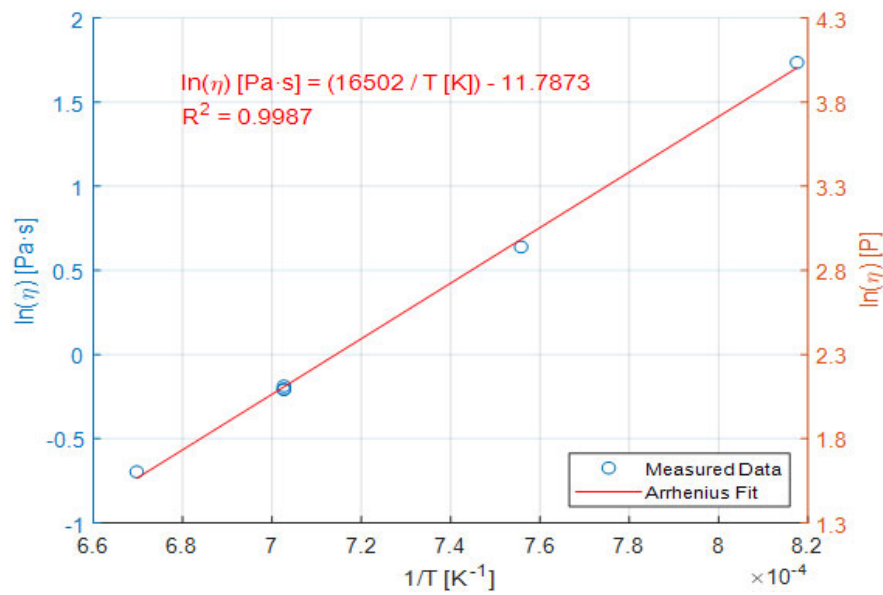


Figure H.19. Viscosity-Temperature Data and Arrhenius Equation Fit for Glass LP5-19

H.20 Glass LP5-20 Viscosity Data

Table H.20. Viscosity Data for Glass LP5-20

Measured Temp., °C	1/(T+273.15), K ⁻¹	Viscosity, Pa-s	ln η, Pa-s
1150	7.03E-04	1.36	0.30
1050	7.56E-04	3.31	1.20
950	8.18E-04	10.51	2.35
1150	7.03E-04	1.39	0.33
1220	6.70E-04	0.83	-0.18
1150	7.03E-04	1.38	0.32

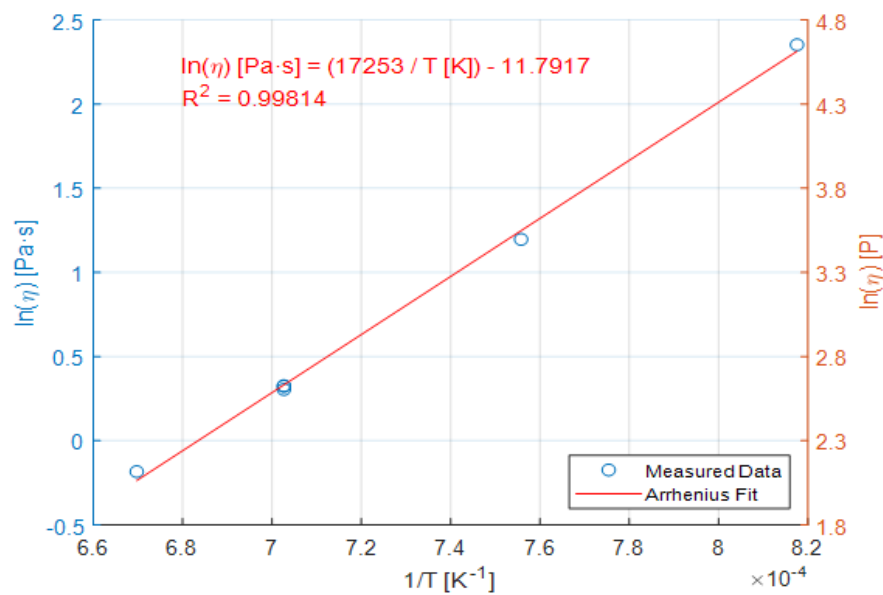


Figure H.20. Viscosity-Temperature Data and Arrhenius Equation Fit for Glass LP5-20

H.21 Glass LP5-21 Viscosity Data

Table H.21. Viscosity Data for Glass LP5-21

Measured Temp., °C	1/(T+273.15), K ⁻¹	Viscosity, Pa-s	ln η, Pa-s
1150	7.03E-04	1.02	0.02
1050	7.56E-04	2.24	0.81
950	8.18E-04	6.29	1.84
1150	7.03E-04	1.03	0.03
1220	6.70E-04	0.64	-0.44
1150	7.03E-04	1.01	0.01

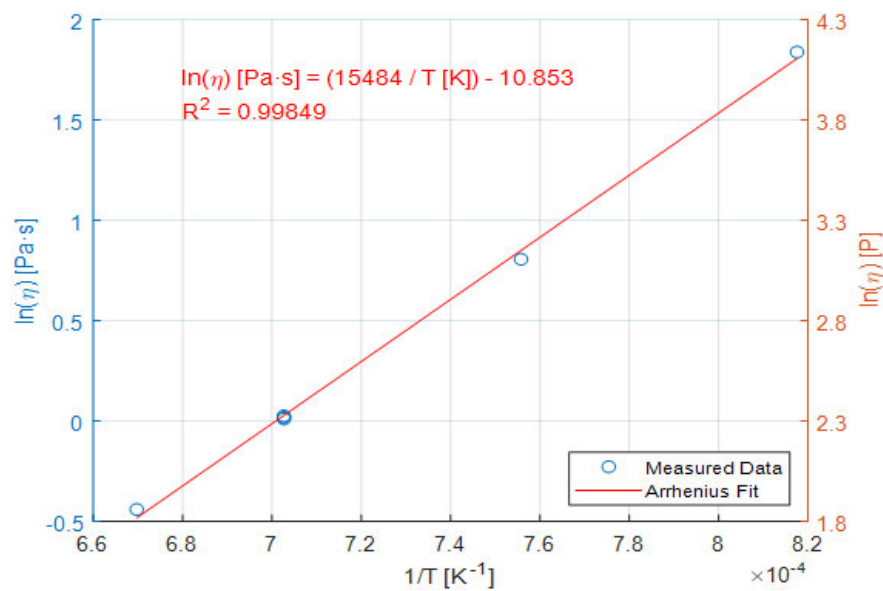


Figure H.21. Viscosity-Temperature Data and Arrhenius Equation Fit for Glass LP5-21

H.22 Glass LP5-22 Viscosity Data

Table H.22. Viscosity Data for Glass LP5-22

Measured Temp., °C	1/(T+273.15), K ⁻¹	Viscosity, Pa-s	ln η, Pa-s
1150	7.03E-04	3.54	1.26
1050	7.56E-04	8.55	2.15
950	8.18E-04	27.83	3.33
1150	7.03E-04	3.56	1.27
1220	6.70E-04	2.24	0.80
1150	7.03E-04	3.52	1.26

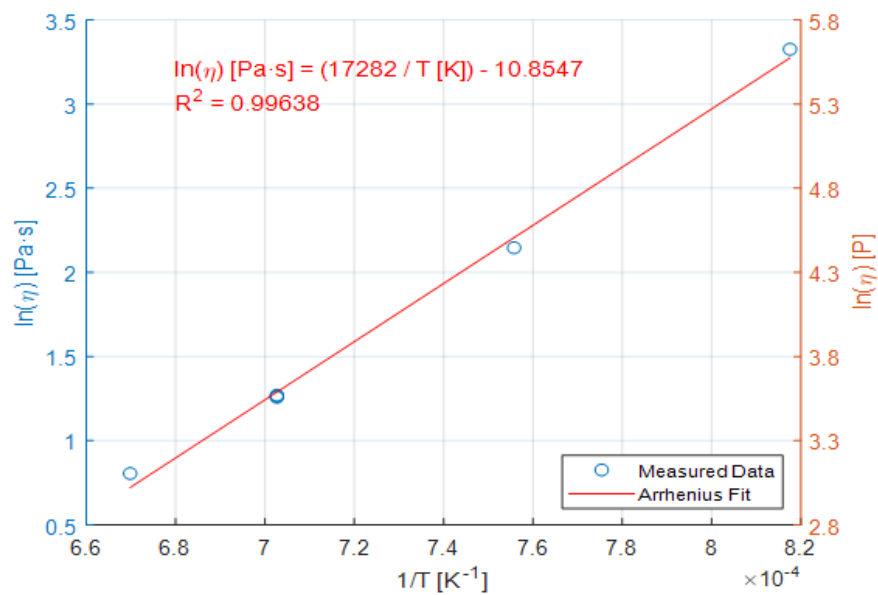


Figure H.22. Viscosity-Temperature Data and Arrhenius Equation Fit for Glass LP5-22

H.23 Glass LP5-23 Viscosity Data

Table H.23. Viscosity Data for Glass LP5-23

Measured Temp., °C	1/(T+273.15), K ⁻¹	Viscosity, Pa-s	ln η, Pa-s
1150	7.03E-04	4.60	1.53
1050	7.56E-04	11.28	2.42
950	8.18E-04	34.94	3.55
1150	7.03E-04	4.46	1.50
1216	6.71E-04	2.78	1.02
1150	7.03E-04	4.42	1.49

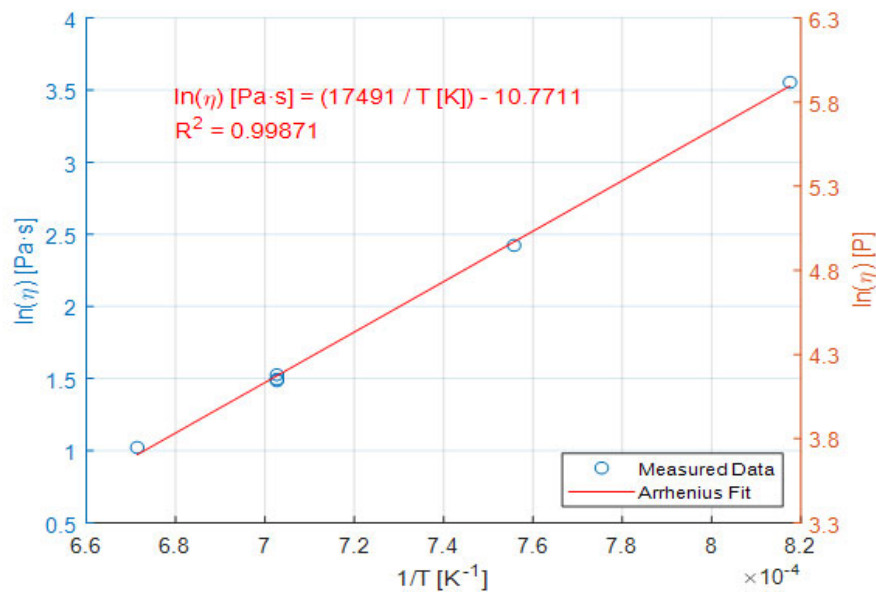


Figure H.23. Viscosity-Temperature Data and Arrhenius Equation Fit for Glass LP5-23

H.24 Glass LP5-24 Viscosity Data

Table H.24. Viscosity Data for Glass LP5-24

Measured Temp., °C	1/(T+273.15), K ⁻¹	Viscosity, Pa-s	ln η, Pa-s
1150	7.03E-04	5.26	1.66
1050	7.56E-04	16.74	2.82
950	8.18E-04	54.31	3.99
1150	7.03E-04	5.05	1.62
1210	6.74E-04	2.93	1.08
1150	7.03E-04	5.04	1.62

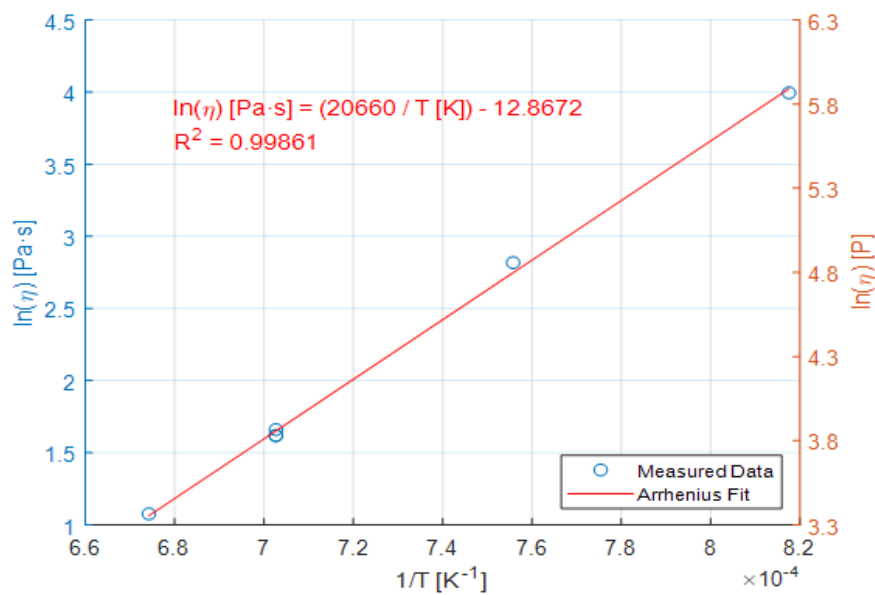


Figure H.24. Viscosity-Temperature Data and Arrhenius Equation Fit for Glass LP5-24

H.25 Glass LP5-25 Viscosity Data

Table H.25. Viscosity Data for Glass LP5-25

Measured Temp., °C	1/(T+273.15), K ⁻¹	Viscosity, Pa-s	ln η, Pa-s
1150	7.03E-04	4.45	1.49
1050	7.56E-04	11.59	2.45
950	8.18E-04	40.78	3.71
1150	7.03E-04	4.54	1.51
1203	6.78E-04	2.89	1.06
1150	7.03E-04	4.39	1.48

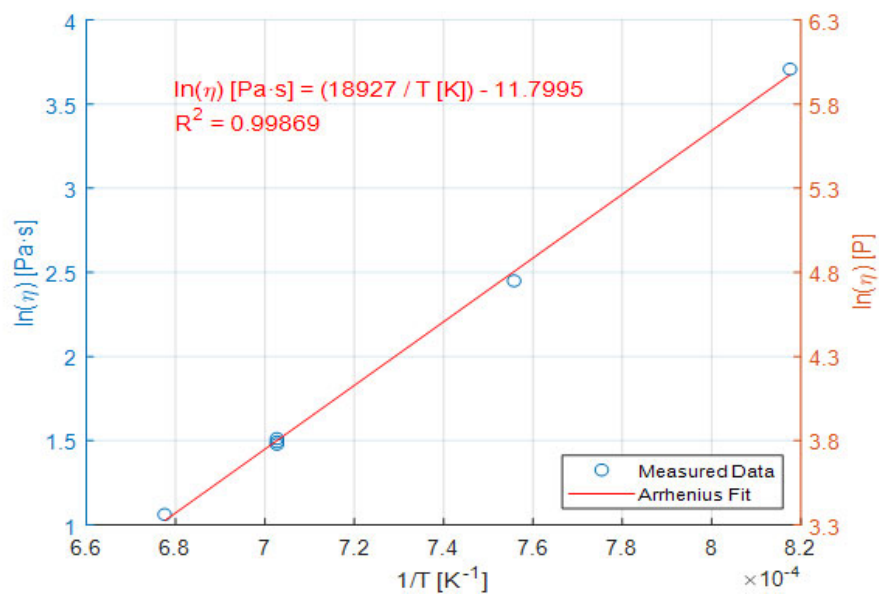


Figure H.25. Viscosity-Temperature Data and Arrhenius Equation Fit for Glass LP5-25

Appendix I – Electrical Conductivity Data

This appendix contains the measured electrical conductivity data for each of the glasses in the LAW Phase 5 matrix.

The plots shown in this appendix are fitted to the Arrhenius equation, which is shown below:

$$\ln(\varepsilon) = A + B/T_K \quad (I.1)$$

where A and B are independent of temperature and temperature (T_K) is in K ($T(^{\circ}\text{C}) + 273.15$).

However, some of the plots showed curvature and would be better fit to the Vogel-Fulcher-Tamman (VFT) model.

The main intent of the figures and Arrhenius equation fits shown in this appendix is to assess trends in the data and provide observations about whether there may be sufficient curvature in the data to consider VFT fits in the subsequent work that will decide between fitting the data to the Arrhenius or VFT equations for the electrical conductivity-temperature data for each glass that is being made.

I.1 Glass LP5-01 Electrical Conductivity Data

Table I.1. Electrical Conductivity Data for Glass LP5-01

Temperature, °C	Conductivity, S/m	$1/(T+273.15), K^{-1}$	$\ln \epsilon$ (S/m)
979	35.86	7.99E-04	3.58
979	43.21	7.99E-04	3.77
1074	96.88	7.42E-04	4.57
1074	84.15	7.42E-04	4.43
1169	98.27	6.94E-04	4.59
1216	135.81	6.72E-04	4.91
1216	135.73	6.72E-04	4.91

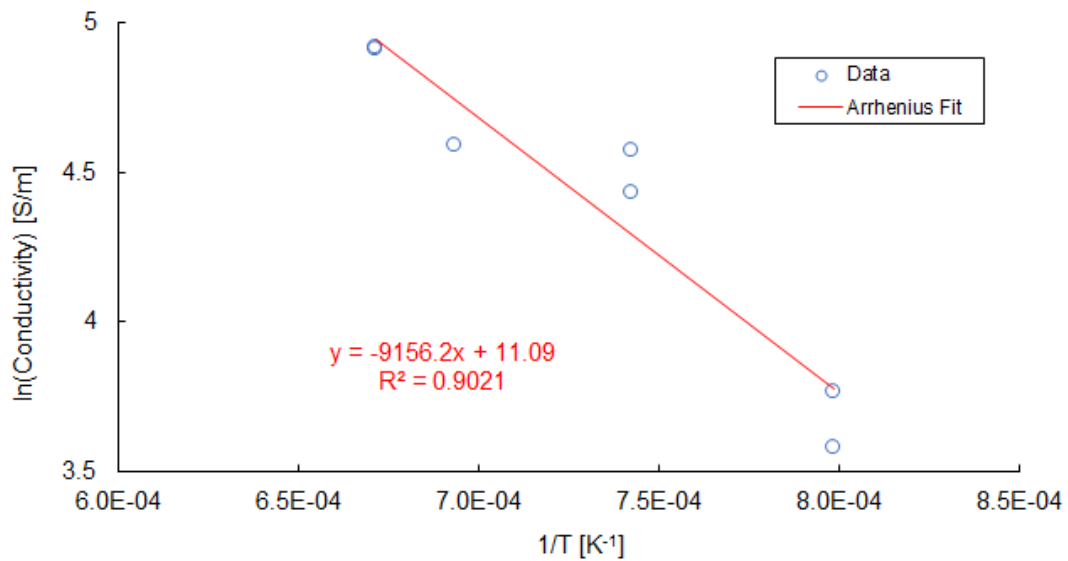


Figure I.1. Electrical Conductivity-Temperature Data and Arrhenius Equation Fit for Glass LP5-01

I.2 Glass LP5-02 Electrical Conductivity Data

Table I.2. Electrical Conductivity Data for Glass LP5-02

Temperature, °C	Conductivity, S/m	1/(T+273.15), K ⁻¹	ln(ε, S/m)
979	86.15	7.99E-04	4.46
979	86.01	7.99E-04	4.45
1074	119.80	7.42E-04	4.79
1074	119.64	7.42E-04	4.78
1169	152.71	6.94E-04	5.03
1169	152.65	6.94E-04	5.03
1216	166.73	6.72E-04	5.12

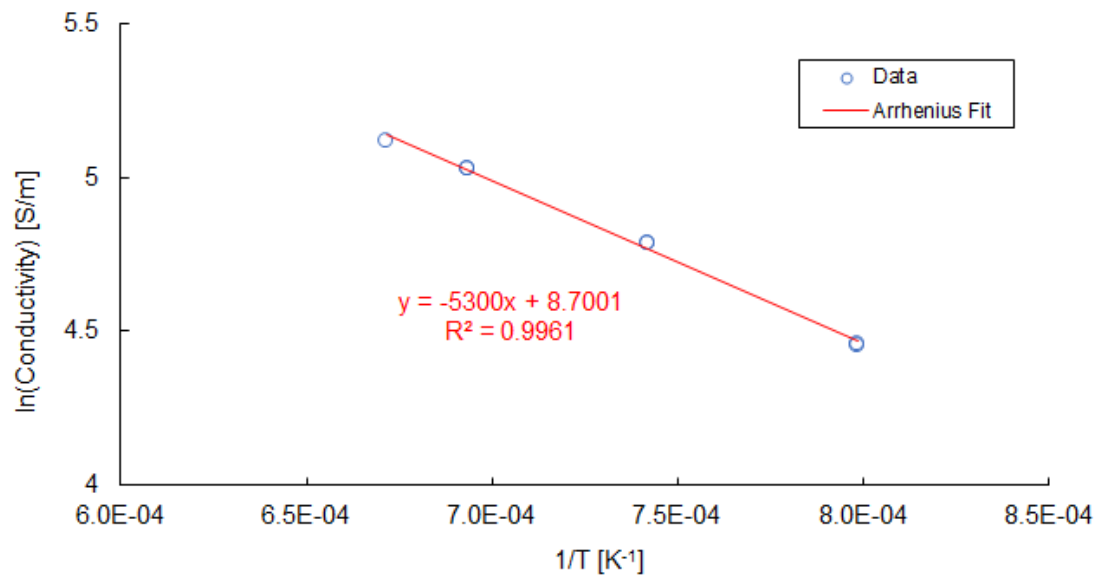


Figure I.2. Electrical Conductivity-Temperature Data and Arrhenius Equation Fit for Glass LP5-02

I.3 Glass LP5-03 Electrical Conductivity Data

Table I.3. Electrical Conductivity Data for Glass LP5-03

Temperature, °C	Conductivity, S/m	1/(T+273.15), K ⁻¹	ln(ε, S/m)
979	52.71	7.99E-04	3.96
979	52.58	7.99E-04	3.96
1074	72.71	7.42E-04	4.29
1074	72.59	7.42E-04	4.28
1169	93.55	6.94E-04	4.54
1169	93.23	6.94E-04	4.54
1216	103.54	6.72E-04	4.64

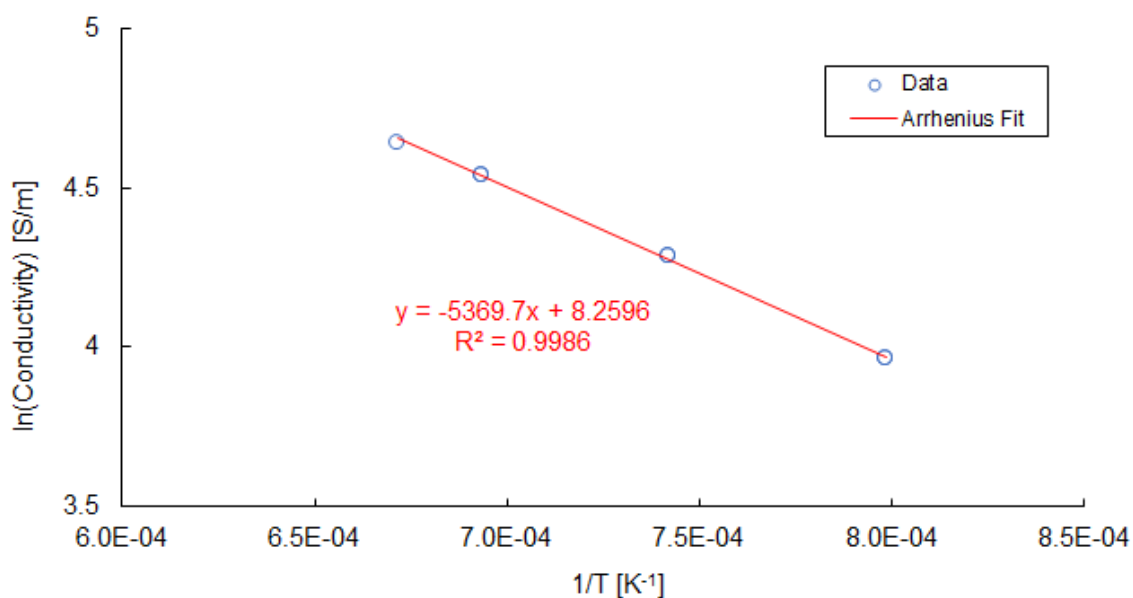


Figure I.3. Electrical Conductivity-Temperature Data and Arrhenius Equation Fit for Glass LP5-03

I.4 Glass LP5-04 Electrical Conductivity Data

Table I.4. Electrical Conductivity Data for Glass LP5-04

Temperature, °C	Conductivity, S/m	1/(T+273.15), K ⁻¹	ln(ε, S/m)
979	63.16	7.99E-04	4.15
979	63.00	7.99E-04	4.14
1074	89.43	7.42E-04	4.49
1074	89.60	7.42E-04	4.50
1169	118.66	6.94E-04	4.78
1169	118.64	6.94E-04	4.78
1216	133.30	6.72E-04	4.89
1216	133.74	6.72E-04	4.90

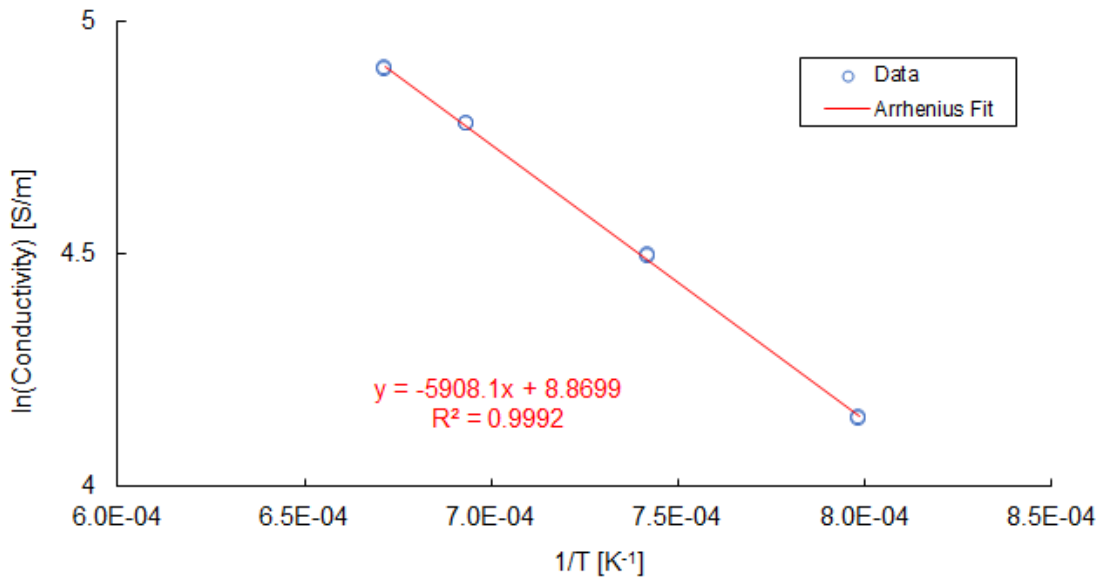


Figure I.4. Electrical Conductivity-Temperature Data and Arrhenius Equation Fit for Glass LP5-04

I.5 Glass LP5-05 Electrical Conductivity Data

Table I.5. Electrical Conductivity Data for Glass LP5-05

Temperature, °C	Conductivity, S/m	1/(T+273.15), K ⁻¹	ln(ϵ , S/m)
979	40.15	7.99E-04	3.69
979	32.87	7.99E-04	3.49
1074	39.91	7.42E-04	3.69
1074	42.60	7.42E-04	3.75
1169	50.01	6.94E-04	3.91
1169	80.16	6.94E-04	4.38
1216	85.14	6.72E-04	4.44

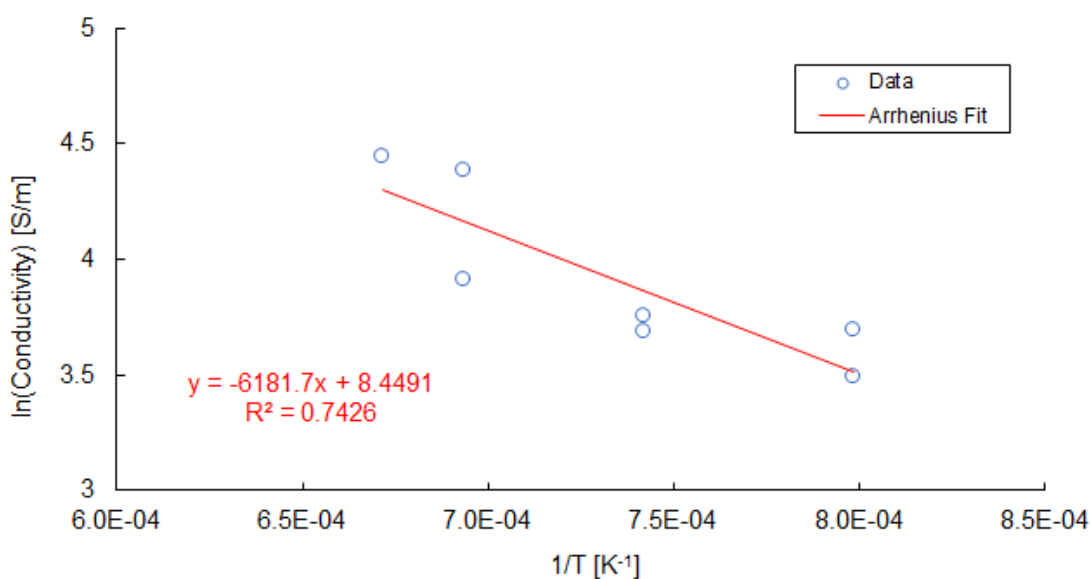


Figure I.5. Electrical Conductivity-Temperature Data and Arrhenius Equation Fit for Glass LP5-05

I.6 Glass LP5-06-MOD1 Electrical Conductivity Data

Table I.6. Electrical Conductivity Data for Glass LP5-06-MOD1

Temperature, °C	Conductivity, S/m	1/(T+273.15), K ⁻¹	ln(ε, S/m)
979	59.30	7.99E-04	4.08
979	59.17	7.99E-04	4.08
1074	83.66	7.42E-04	4.43
1074	83.42	7.42E-04	4.42
1169	109.33	6.94E-04	4.69
1216	122.02	6.72E-04	4.80

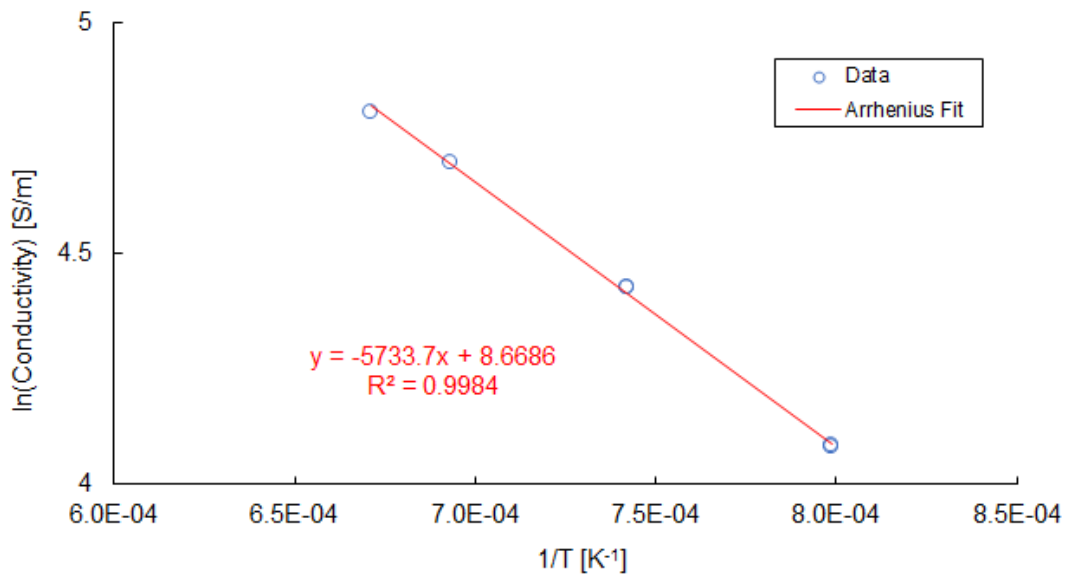


Figure I.6. Electrical Conductivity -Temperature Data and Arrhenius Equation Fit for Glass LP5-06-MOD1

I.7 Glass LP5-07 Electrical Conductivity Data

Table I.7. Electrical Conductivity Data for Glass LP5-07

Temperature, °C	Conductivity, S/m	1/(T+273.15), K ⁻¹	ln(ε, S/m)
979	59.29	7.99E-04	4.08
979	59.03	7.99E-04	4.08
1074	78.97	7.42E-04	4.37
1074	78.88	7.42E-04	4.37
1169	97.75	6.94E-04	4.58
1169	97.74	6.94E-04	4.58
1216	106.26	6.72E-04	4.67

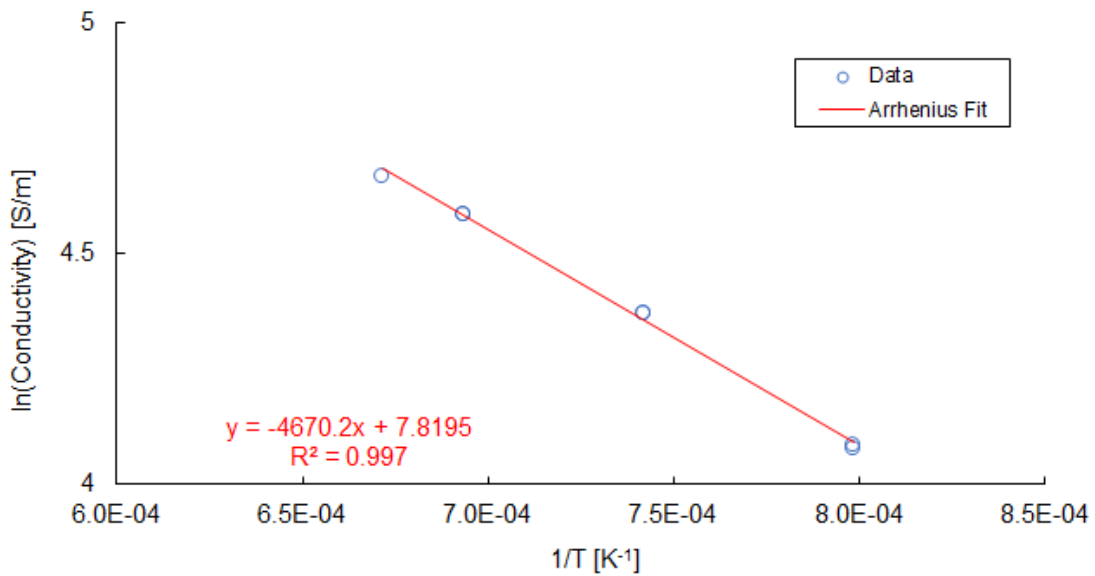


Figure I.7. Electrical Conductivity-Temperature Data and Arrhenius Equation Fit for Glass LP5-07

I.8 Glass LP5-08 Electrical Conductivity Data

Table I.8. Electrical Conductivity Data for Glass LP5-08

Temperature, °C	Conductivity, S/m	1/(T+273.15), K ⁻¹	ln(ε, S/m)
979	77.66	7.99E-04	4.35
979	77.53	7.99E-04	4.35
1074	104.95	7.42E-04	4.65
1074	104.80	7.42E-04	4.65
1169	132.56	6.94E-04	4.89
1169	132.46	6.94E-04	4.89
1216	141.23	6.72E-04	4.95
1216	146.89	6.72E-04	4.99

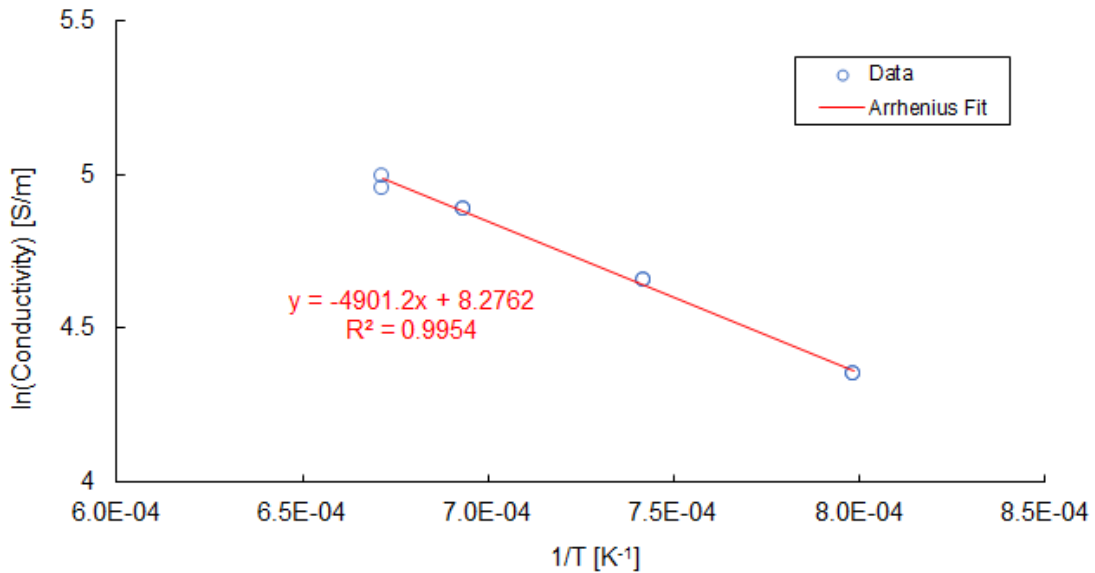


Figure I.8. Electrical Conductivity-Temperature Data and Arrhenius Equation Fit for Glass LP5-08

I.9 Glass LP5-09 Electrical Conductivity Data

Table I.9. Electrical Conductivity Data for Glass LP5-09

Temperature, °C	Conductivity, S/m	1/(T+273.15), K ⁻¹	ln(ε, S/m)
979	66.50	7.99E-04	4.20
979	66.39	7.99E-04	4.20
1074	89.26	7.42E-04	4.49
1074	89.17	7.42E-04	4.49
1169	111.12	6.94E-04	4.71
1169	111.18	6.94E-04	4.71
1216	121.30	6.72E-04	4.80
1216	109.26	6.72E-04	4.69

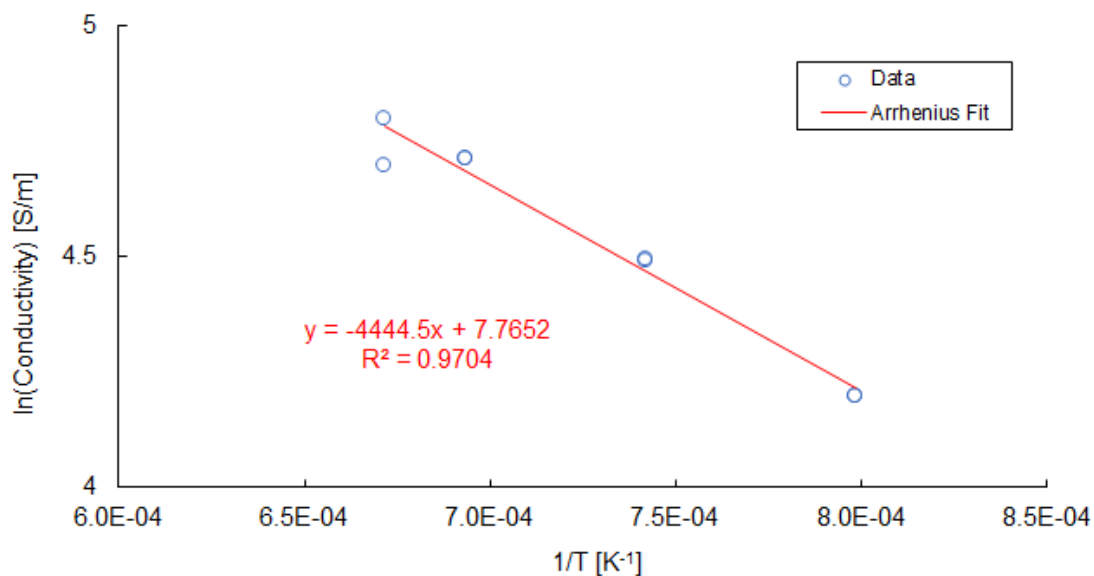


Figure I.9. Electrical Conductivity-Temperature Data and Arrhenius Equation Fit for Glass LP5-09

I.10 Glass LP5-10 Electrical Conductivity Data

Table I.10. Electrical Conductivity Data for Glass LP5-10

Temperature, °C	Conductivity, S/m	1/(T+273.15), K ⁻¹	ln(ϵ , S/m)
979	83.92	7.99E-04	4.43
979	82.52	7.99E-04	4.41
1074	115.55	7.42E-04	4.75
1074	114.54	7.42E-04	4.74
1169	146.50	6.94E-04	4.99
1169	146.88	6.94E-04	4.99
1216	161.89	6.72E-04	5.09
1216	139.88	6.72E-04	4.94

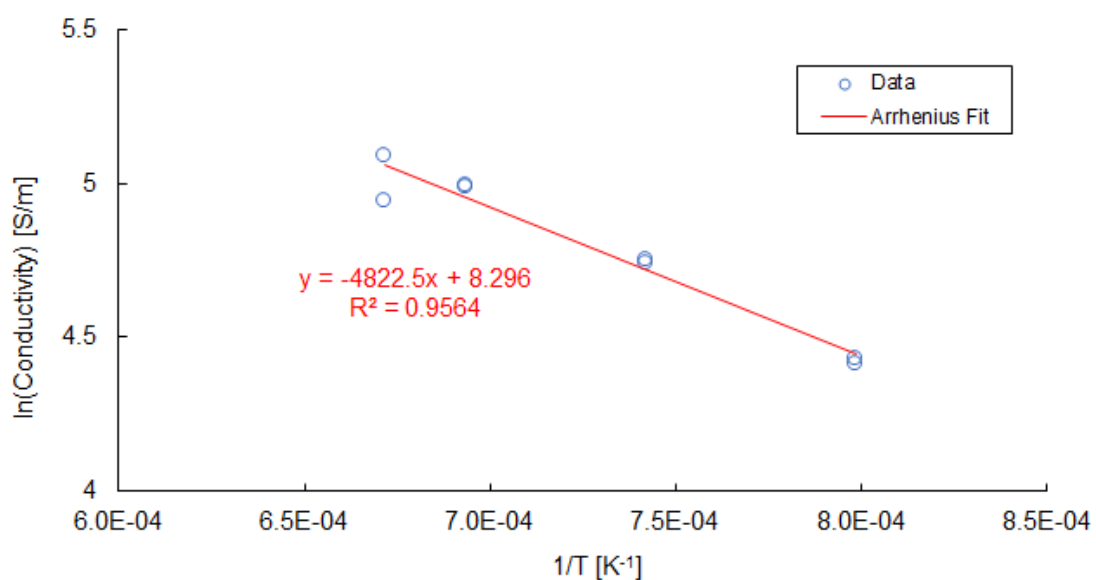


Figure I.10. Electrical Conductivity-Temperature Data and Arrhenius Equation Fit of Glass LP5-10

I.11 Glass LP5-11 Electrical Conductivity Data

Table I.11. Electrical Conductivity Data for Glass LP5-11

Temperature, °C	Conductivity, S/m	1/(T+273.15), K ⁻¹	ln(ε, S/m)
979	49.36	7.99E-04	3.90
979	66.15	7.99E-04	4.19
1074	83.80	7.42E-04	4.43
1074	83.15	7.42E-04	4.42
1169	120.36	6.94E-04	4.79
1169	108.17	6.94E-04	4.68
1216	129.17	6.72E-04	4.86
1216	127.01	6.72E-04	4.84

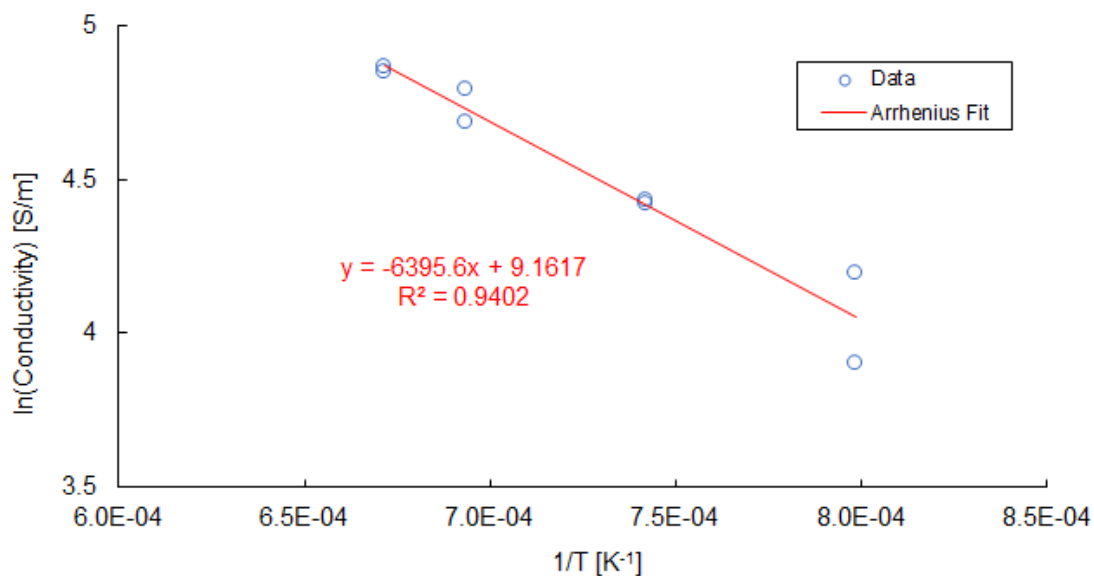


Figure I.11. Electrical Conductivity-Temperature Data and Arrhenius Equation Fit for Glass LP5-11

I.12 Glass LP5-12-1 Electrical Conductivity Data

Table I.12. Electrical Conductivity Data for Glass LP5-12-1

Temperature, °C	Conductivity, S/m	1/(T+273.15), K ⁻¹	ln(ε, S/m)
950	22.78	8.18E-04	3.13
950	22.96	8.18E-04	3.13
1050	31.11	7.56E-04	3.44
1050	30.91	7.56E-04	3.43
1150	46.50	7.03E-04	3.84
1150	66.64	7.03E-04	4.20
1200	80.16	6.79E-04	4.38
1200	74.93	6.79E-04	4.32

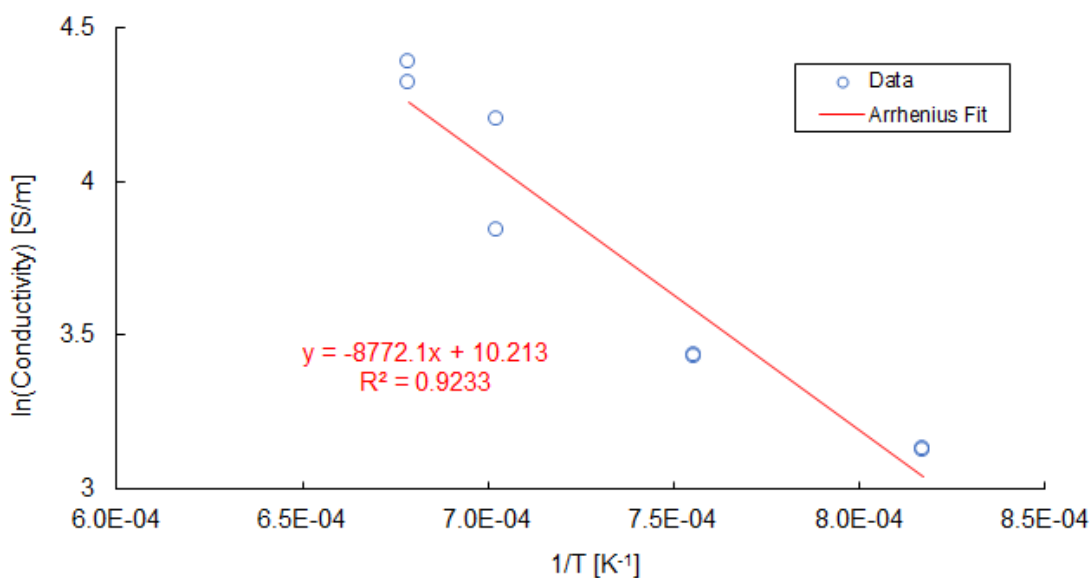


Figure I.12. Electrical Conductivity-Temperature Data and Arrhenius Equation Fit for Glass LP5-12-1

I.13 Glass LP5-13 Electrical Conductivity Data

Table I.13. Electrical Conductivity Data for Glass LP5-13

Temperature, °C	Conductivity, S/m	1/(T+273.15), K ⁻¹	ln(ε, S/m)
950	47.06	8.18E-04	3.85
950	42.46	8.18E-04	3.75
1050	91.04	7.56E-04	4.51
1050	53.75	7.56E-04	3.98
1150	115.58	7.03E-04	4.75
1150	111.76	7.03E-04	4.72
1200	127.17	6.79E-04	4.85
1200	142.95	6.79E-04	4.96

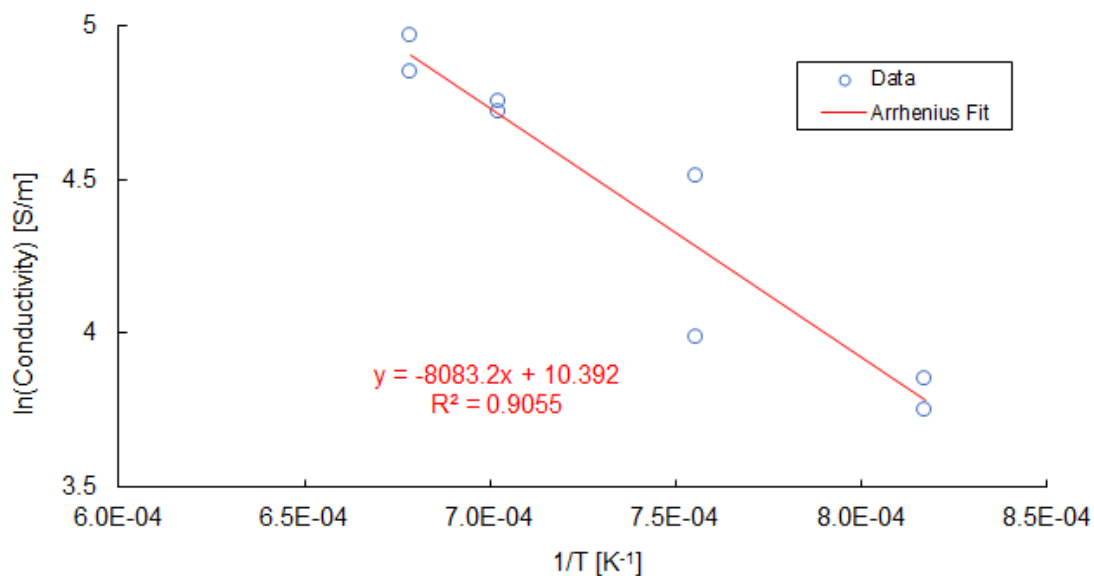


Figure I.13. Electrical Conductivity-Temperature Data and Arrhenius Equation Fit for Glass LP5-13

I.14 Glass LP5-14 Electrical Conductivity Data

Table I.14. Electrical Conductivity Data for Glass LP5-14

Temperature, °C	Conductivity, S/m	1/(T+273.15), K ⁻¹	ln(σ, S/m)
950	30.31	8.18E-04	3.41
950	29.71	8.18E-04	3.39
1050	35.38	7.56E-04	3.57
1050	42.49	7.56E-04	3.75
1150	43.21	7.03E-04	3.77
1150	72.14	7.03E-04	4.28
1200	96.22	6.79E-04	4.57
1200	96.83	6.79E-04	4.57

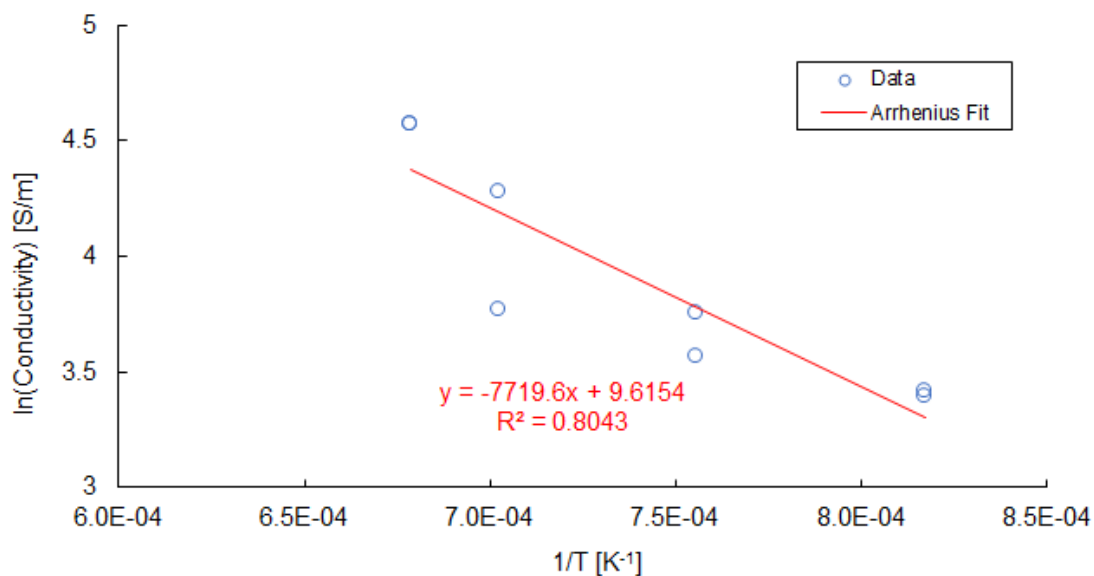


Figure I.14. Electrical Conductivity-Temperature Data and Arrhenius Equation Fit for Glass LP5-14

I.15 Glass LP5-15 Electrical Conductivity Data

Table I.15. Electrical Conductivity Data for Glass LP5-15

Temperature, °C	Conductivity, S/m	1/(T+273.15), K ⁻¹	ln(ε, S/m)
950	29.35	8.18E-04	3.38
950	29.71	8.18E-04	3.39
1050	40.88	7.56E-04	3.71
1050	40.81	7.56E-04	3.71
1150	62.24	7.03E-04	4.13
1150	58.97	7.03E-04	4.08
1200	110.51	6.79E-04	4.71

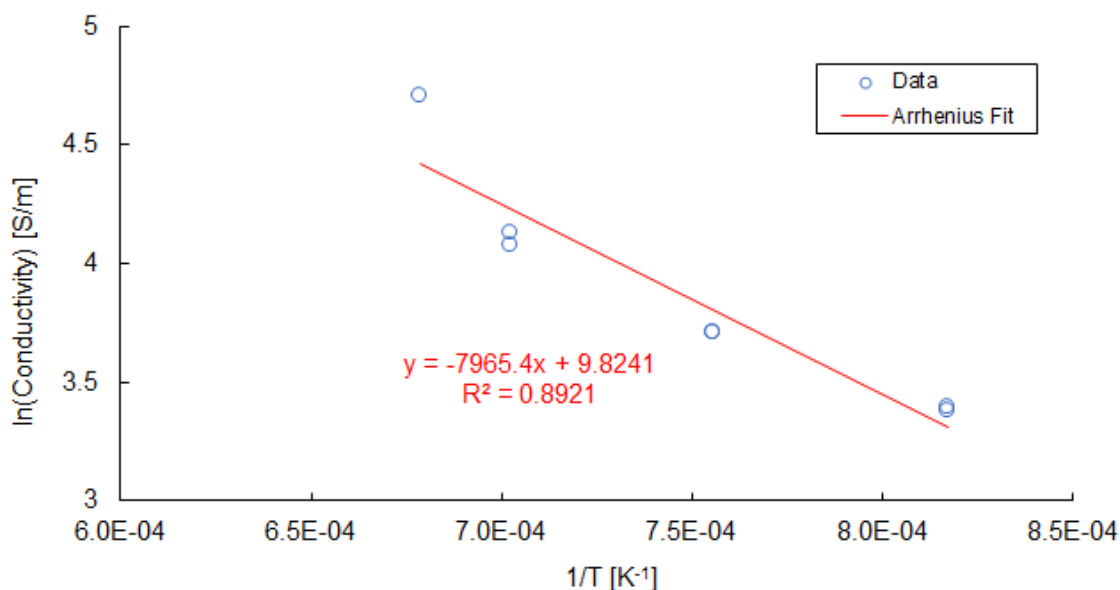


Figure I.15. Electrical Conductivity-Temperature Data and Arrhenius Equation Fit for Glass LP5-15

I.16 Glass LP5-16-MOD1 Electrical Conductivity Data

Table I.16. Electrical Conductivity Data for Glass LP5-16-MOD1

Temperature, °C	Conductivity, S/m	1/(T+273.15), K ⁻¹	ln(ε, S/m)
950	44.56	8.18E-04	3.80
950	44.27	8.18E-04	3.79
1050	37.24	7.56E-04	3.62
1050	43.42	7.56E-04	3.77
1150	48.58	7.03E-04	3.88
1150	73.29	7.03E-04	4.29
1200	82.49	6.79E-04	4.41
1200	88.80	6.79E-04	4.49

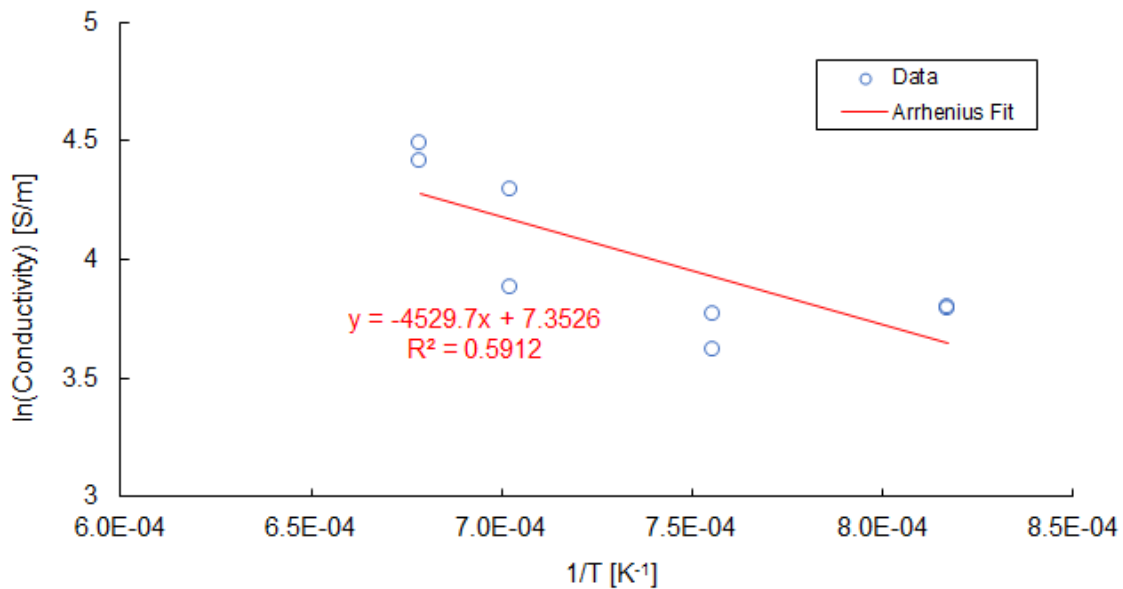


Figure I.16. Electrical Conductivity-Temperature Data and Arrhenius Equation Fit for Glass LP5-16-MOD1

I.17 Glass LP5-17 Electrical Conductivity Data

Table I.17. Electrical Conductivity Data for Glass LP5-17

Temperature, °C	Conductivity, S/m	1/(T+273.15), K ⁻¹	ln(σ, S/m)
950	37.97	8.18E-04	3.64
950	37.58	8.18E-04	3.63
1050	62.79	7.56E-04	4.14
1050	62.35	7.56E-04	4.13
1150	87.47	7.03E-04	4.47
1150	87.71	7.03E-04	4.47
1200	100.81	6.79E-04	4.61
1200	101.14	6.79E-04	4.62

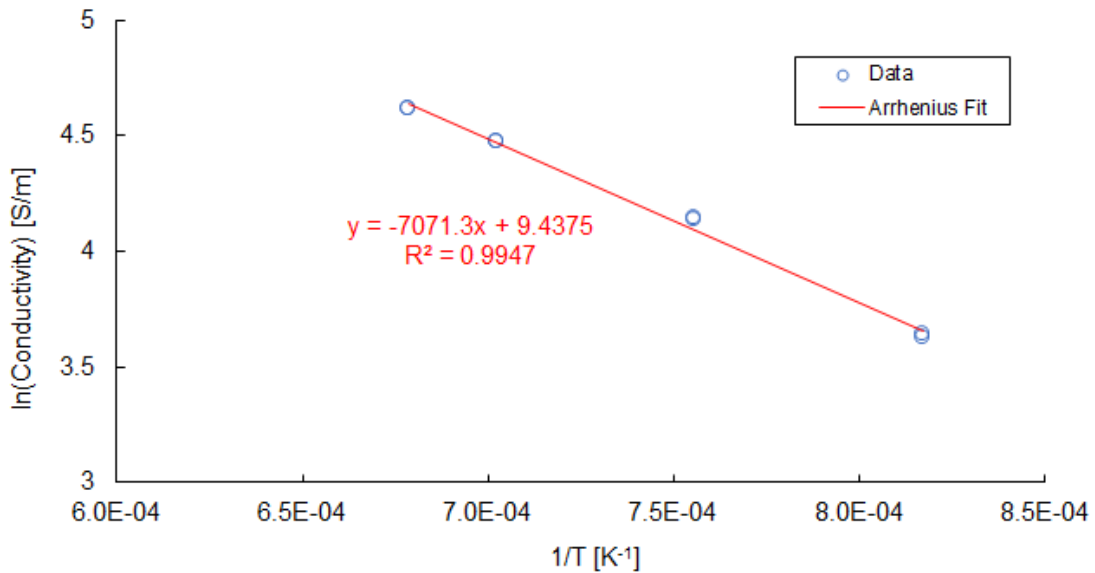


Figure I.17. Electrical Conductivity-Temperature Data and Arrhenius Equation Fit for Glass LP5-17

I.18 Glass LP5-18 Electrical Conductivity Data

Table I.18. Electrical Conductivity Data for Glass LP5-18

Temperature, °C	Conductivity, S/m	1/(T+273.15), K ⁻¹	ln(σ , S/m)
950	54.63	8.18E-04	4.00
950	61.92	8.18E-04	4.13
1050	72.53	7.56E-04	4.28
1050	72.82	7.56E-04	4.29
1150	105.47	7.03E-04	4.66
1150	104.96	7.03E-04	4.65
1200	115.07	6.79E-04	4.75
1200	115.38	6.79E-04	4.75

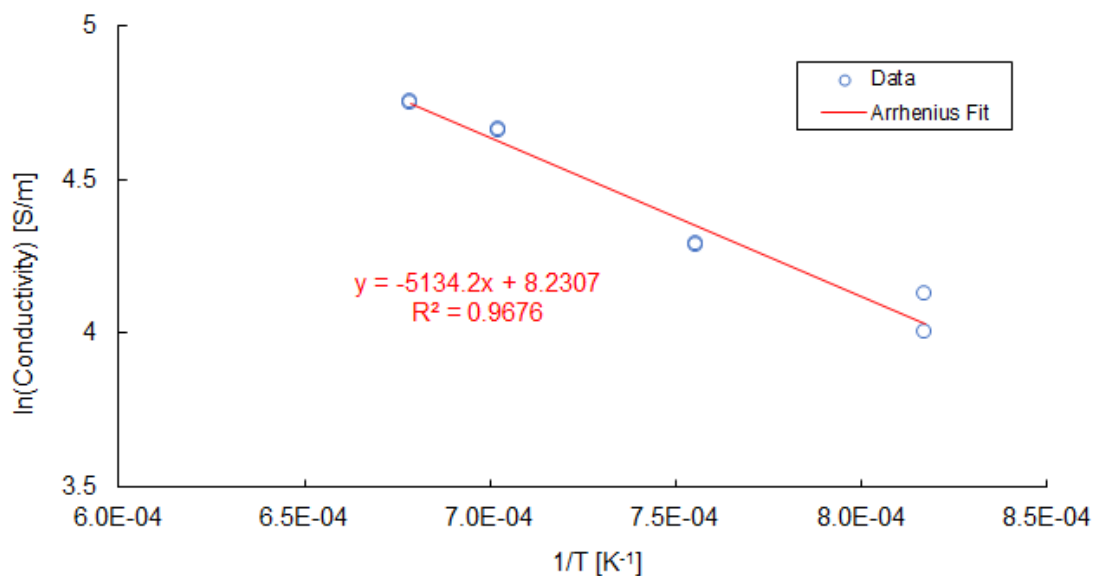


Figure I.18. Electrical Conductivity-Temperature Data and Arrhenius Equation Fit for Glass LP5-18

I.19 Glass LP5-19 Electrical Conductivity Data

Table I.19. Electrical Conductivity Data for Glass LP5-19

Temperature, °C	Conductivity, S/m	1/(T+273.15), K ⁻¹	ln(σ , S/m)
950	51.63	8.18E-04	3.94
950	39.58	8.18E-04	3.68
1050	77.67	7.56E-04	4.35
1050	75.74	7.56E-04	4.33
1150	105.85	7.03E-04	4.66
1150	103.35	7.03E-04	4.64
1200	120.16	6.79E-04	4.79
1200	119.23	6.79E-04	4.78

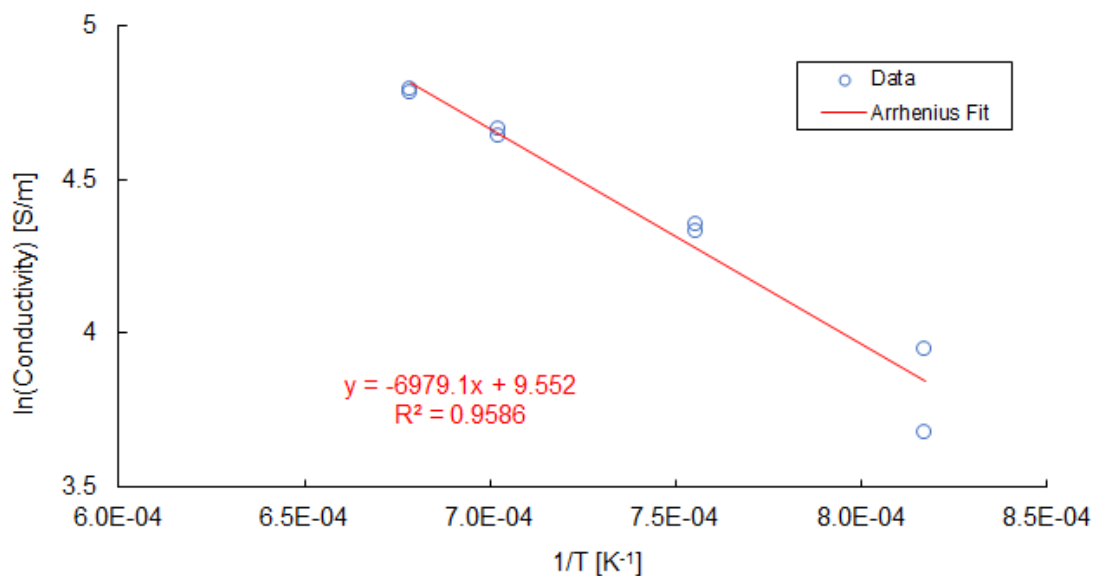


Figure I.19. Electrical Conductivity-Temperature Data and Arrhenius Equation Fit for Glass LP5-19

I.20 Glass LP5-20 Electrical Conductivity Data

Table I.20. Electrical Conductivity Data for Glass LP5-20

Temperature, °C	Conductivity, S/m	1/(T+273.15), K ⁻¹	ln(σ , S/m)
950	46.18	8.18E-04	3.83
950	40.60	8.18E-04	3.70
1050	53.16	7.56E-04	3.97
1050	62.36	7.56E-04	4.13
1150	49.54	7.03E-04	3.90
1150	75.01	7.03E-04	4.32
1200	91.22	6.79E-04	4.51
1200	90.90	6.79E-04	4.51

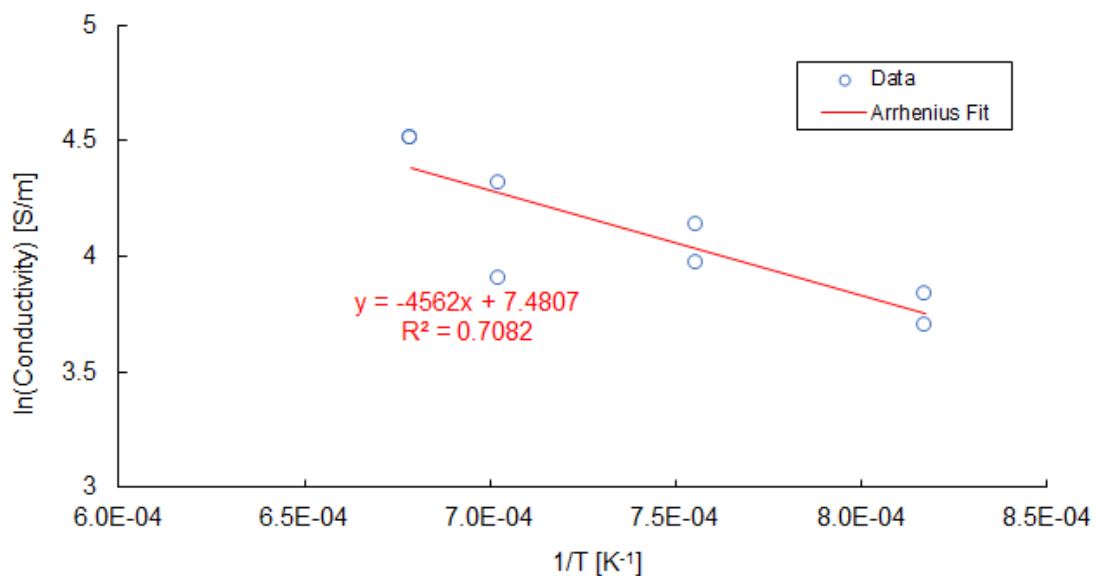


Figure I.20. Electrical Conductivity-Temperature Data and Arrhenius Equation Fit for Glass LP5-20

I.21 Glass LP5-21 Electrical Conductivity Data

Table I.21. Electrical Conductivity Data for Glass LP5-21

Temperature, °C	Conductivity, S/m	1/(T+273.15), K ⁻¹	ln(σ, S/m)
950	51.26	8.18E-04	3.94
950	53.45	8.18E-04	3.98
1050	78.99	7.56E-04	4.37
1050	78.73	7.56E-04	4.37
1150	102.73	7.03E-04	4.63
1150	103.46	7.03E-04	4.64
1200	104.17	6.79E-04	4.65
1200	103.30	6.79E-04	4.64

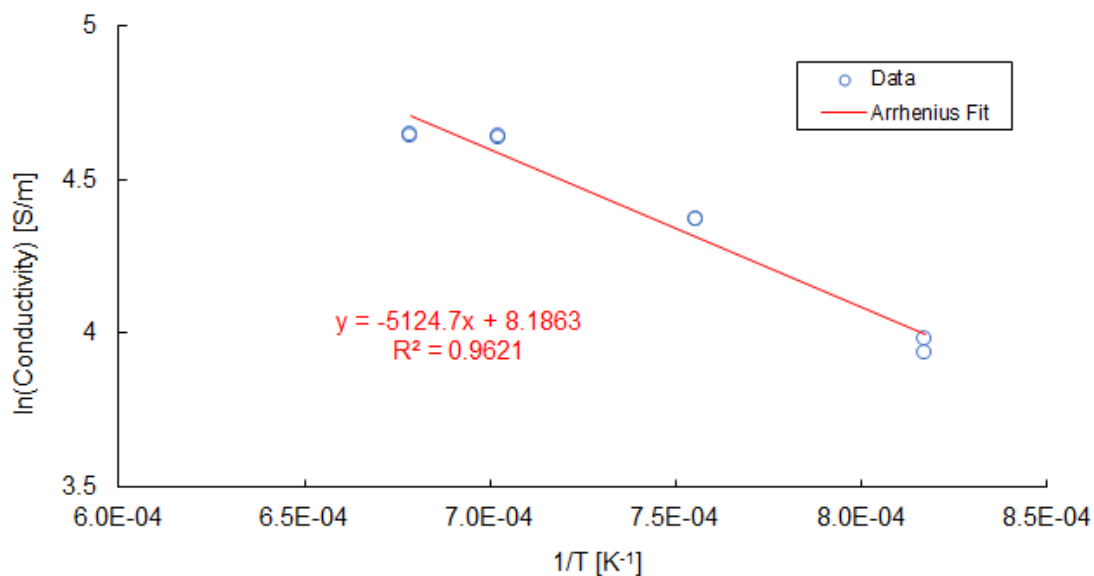


Figure I.21. Electrical Conductivity-Temperature Data and Arrhenius Equation Fit for Glass LP5-21

I.22 Glass LP5-22 Electrical Conductivity Data

Table I.22. Electrical Conductivity Data for Glass LP5-22

Temperature, °C	Conductivity, S/m	1/(T+273.15), K ⁻¹	ln(σ, S/m)
950	53.52	8.18E-04	3.98
950	53.21	8.18E-04	3.97
1050	56.46	7.56E-04	4.03
1050	54.82	7.56E-04	4.00
1150	90.84	7.03E-04	4.51
1150	89.52	7.03E-04	4.49
1200	114.55	6.79E-04	4.74
1200	101.60	6.79E-04	4.62

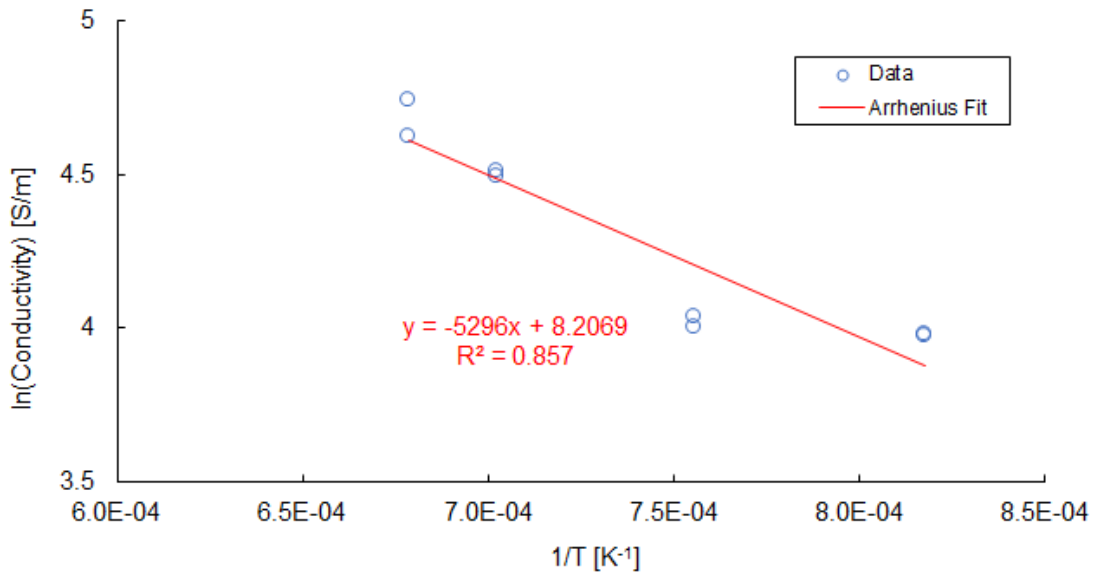


Figure I.22. Electrical Conductivity-Temperature Data and Arrhenius Equation Fit for Glass LP5-22

I.23 Glass LP5-23 Electrical Conductivity Data

Table I.23. Electrical Conductivity Data for Glass LP5-23

Temperature, °C	Conductivity, S/m	1/(T+273.15), K ⁻¹	ln(σ, S/m)
950	44.71	8.18E-04	3.80
950	44.44	8.18E-04	3.79
1050	47.76	7.56E-04	3.87
1050	60.90	7.56E-04	4.11
1150	85.09	7.03E-04	4.44
1150	85.21	7.03E-04	4.45
1200	94.09	6.79E-04	4.54
1200	94.13	6.79E-04	4.54

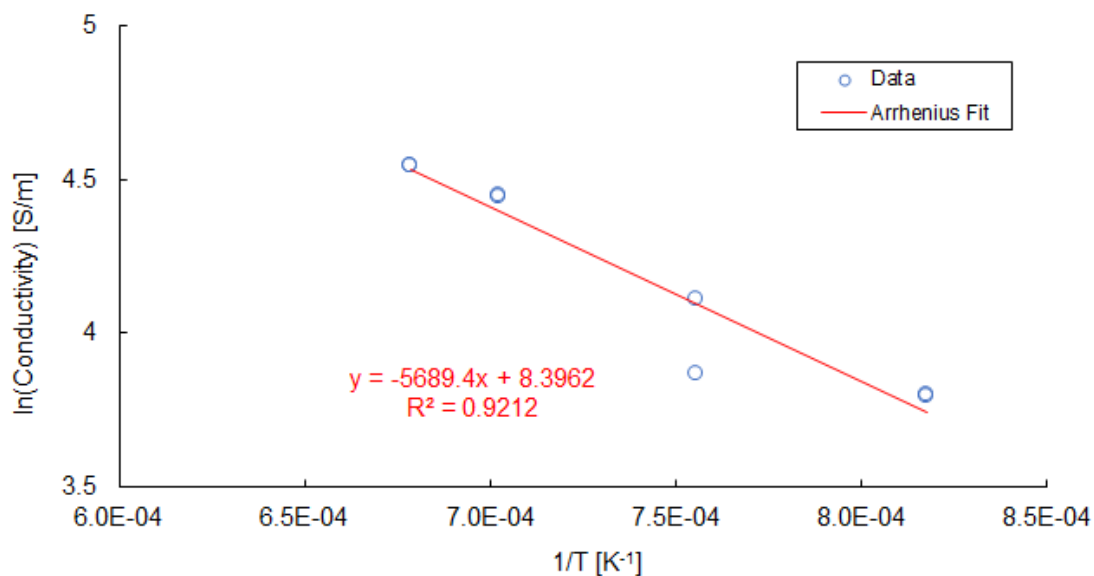


Figure I.23. Electrical Conductivity-Temperature Data and Arrhenius Equation Fit for Glass LP5-23

I.24 Glass LP5-24 Electrical Conductivity Data

Table I.24. Electrical Conductivity Data for Glass LP5-24

Temperature, °C	Conductivity, S/m	1/(T+273.15), K ⁻¹	ln(σ, S/m)
950	22.89	8.18E-04	3.13
950	20.62	8.18E-04	3.03
1050	64.48	7.56E-04	4.17
1050	32.77	7.56E-04	3.49
1150	81.95	7.03E-04	4.41
1150	86.07	7.03E-04	4.46
1200	97.94	6.79E-04	4.58
1200	87.92	6.79E-04	4.48

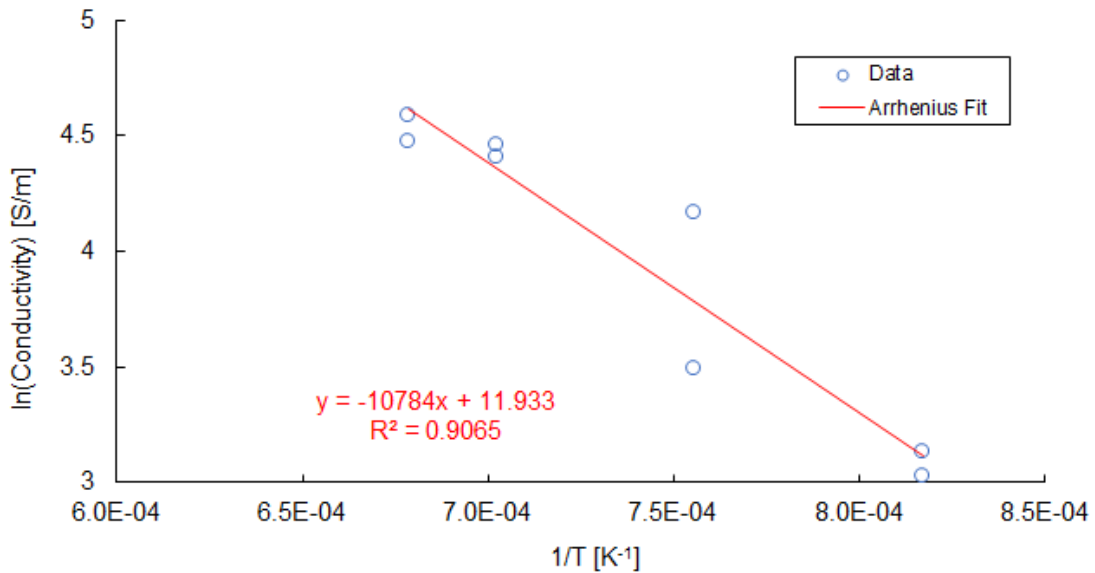


Figure I.24. Electrical Conductivity-Temperature Data and Arrhenius Equation Fit for Glass LP5-24

I.25 Glass LP5-25 Electrical Conductivity Data

Table I.25. Electrical Conductivity Data for Glass LP5-25

Temperature, °C	Conductivity, S/m	1/(T+273.15), K ⁻¹	ln(σ, S/m)
950	12.10	8.18E-04	2.49
950	11.96	8.18E-04	2.48
1050	18.78	7.56E-04	2.93
1050	21.14	7.56E-04	3.05
1150	25.71	7.03E-04	3.25
1150	28.44	7.03E-04	3.35
1200	48.27	6.79E-04	3.88

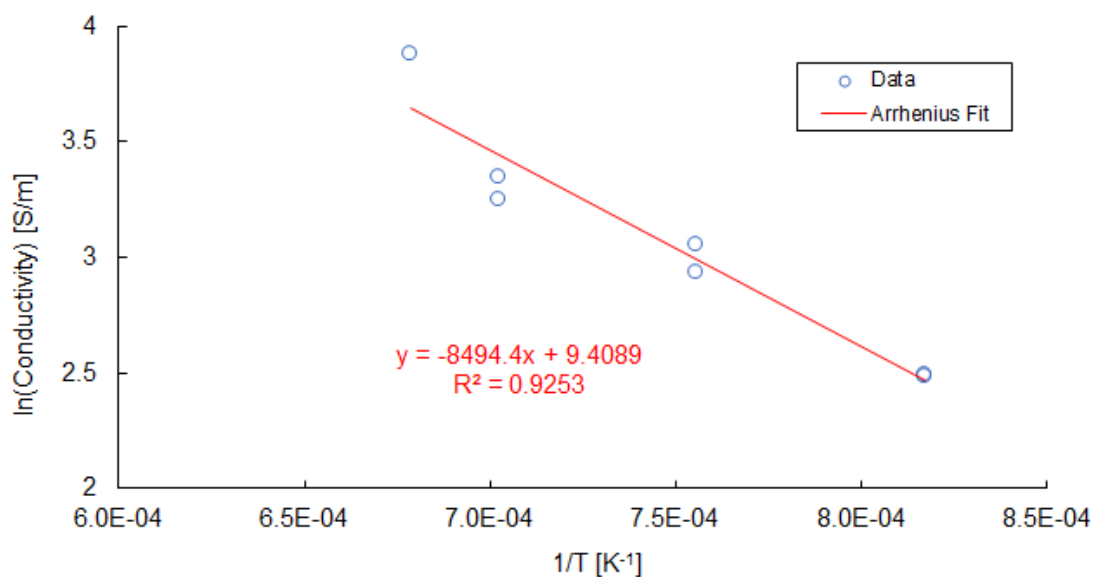


Figure I.25. Electrical Conductivity-Temperature Data and Arrhenius Equation Fit for Glass LP5-25

Pacific Northwest National Laboratory

902 Battelle Boulevard
P.O. Box 999
Richland, WA 99354
1-888-375-PNNL (7665)

www.pnnl.gov